

Inter–Agency Space Debris Coordination Committee



International 24-Hour LEO Space Debris Measurement Campaign 2015

IADC Action Item 33.1

Working Group 1

Participating Members:

NASA: Joseph Hamilton

NASA/Study Lead

ESA: Klemens Letsch
Delphine Cerutti-Maori

ESA/Study Lead
ESA/Study Member

Table of Contents

1.	Introduction	1
1.1	Summary	2
2.	Pencil-Beam Radars	3
2.1	HUSIR	4
2.2	Goldstone	8
2.3	TIRA (Fraunhofer FHR)	11
3.	Phased Array Radars.....	19
3.1	Cobra Dane.	19
4.	On-orbit Fragmentations.....	23
5.	Conclusion.....	25
6.	References	26
7.	Definitions and Acronyms.....	27
8.	Appendices	29
	Appendix A – TIRA Radar.....	29
A.1	Experiment Setup.....	29
A.2	Data Processing	30
A.3	Detection List	32
A.4	References	52
	Appendix B – HUSIR Radar	53
B.1	Experiment Setup.....	53
B.2	Data Processing	54
B.3	Campaign Parameters	55
B.4	Detection List	55
B.5	References	62

Appendix C – Goldstone Radar	63
C.1 Experiment Setup.....	63
C.2 Campaign Parameters	65
C.3 Detection List	65
C.4 References	66
Appendix D – Cobra Dane Radar	67
D.1 Experiment Setup.....	67
D.2 Data Collection	68
C.3 Detection List	68
Appendix E – NASA’s Size Estimation Model.....	76
Appendix F – World Map of Participating Radar Locations.....	80

Tables

1.1	Summary of the Radars Participating in the 2015 Campaign, the Number of Hours Observed, and the Beam Park Configuration.....	2
4-1.	List of Known On-orbit Fragmentations for the Time Period 17 November 2008 through 8 December 2015.	24
4-2	List of Anomalous Events for the Time Period 17 November 2008 through 8 December 2015.....	24
A-1.	Instrument Parameters used by the TIRA Radar for the 2015 Campaign.....	29
A-2.	Campaign Parameters for the TIRA Radar for the 2015 Campaign	29
A-3.	TIRA Detection Results of S-BPE-115 on DOY 15342.....	33
B-1.	Instrument Parameters used by the Haystack Radar for the 2015 Campaign	53
B-3.	Campaign Parameters for the HUSIR Radar for the 2015 Campaign	55
B-4.	HUSIR Detection List for the 2015 Campaign.....	55
C-1.	Instrument Parameters used by the Goldstone Radar for the 2015 Campaign	63
C-2.	Campaign Parameters for the Goldstone Radar for the 2015 Campaign	65
C-3.	Goldstone Detection List for the 2015 Campaign	65
D-1.	Instrument Parameters for the Cobra Dane Radar used during the 2015 Campaign	67
D-2.	Campaign Parameters for the Cobra Dane Radar used during the 2015 Campaign	68
D-3.	Cobra Dane Detection List for the 2015 Campaign.....	68
E-1.	The NASA SEM Curve $x=g(z)$ in the Mie Resonance Region.....	78

Figures

2.1	MIT's Lincoln Space Surveillance Complex (LSSC). HUSIR is in the large radome at upper left.....	4
2.2	Distribution of altitude vs. Doppler-inclination for HUSIR detections in the 2015 campaign.	5
2.3	Detection rate vs. size distribution for all objects detected by HUSIR in the 2015 campaign.	6
2.4	Detection rate vs. inclination distribution for all objects detected by HUSIR in the 2015 campaign.	7
2.5	Detection rate vs. altitude distribution for all objects detected by HUSIR in the 2015 campaign.	7
2.6	Deep Space Station 14 (DSS-14) "Mars" located at the Goldstone Deep Space Communications Complex.	8
2.7	Distribution of altitude vs. Doppler-inclination for Goldstone detections in the 2015 campaign.	9
2.8	Size distribution for all objects detected by Goldstone in the 2015 campaign.	10
2.9	The TIRA Radar is located inside a 47.5-meter radome.....	11
2.10	Detection rate versus object diameter for all objects detected by TIRA in the 2015 campaign.	12
2.11	Detection rate versus object RCS for all objects detected by TIRA in the 2015 campaign.	13
2.12	Detection rate versus range rate for all objects detected by TIRA in the 2015 campaign.	14
2.13	Detection rate versus Doppler inclination for TIRA detections in the 2015 campaign.	15
2.14	Detection rate versus altitude for all objects detected by TIRA in the 2015 campaign.	15
2.15	Altitude versus range rate for all objects detected by TIRA in the 2015 campaign.	16

2.16	Altitude versus Doppler inclination for TIRA detections in the 2015 campaign.	17
2.17	Object diameter versus altitude for all objects detected by TIRA in the 2015 campaign.	18
2.18	Object diameter versus range rate for all objects detected by TIRA in the 2015 campaign.	18
3.1	Cobra Dane phased array radar in Shemya, Alaska.	19
3.2	Size distribution for all TAGGED and UNASSO detections by Cobra Dane in the 2015 campaign.	20
3.3	Distribution of altitude vs. TLE inclination for TAGGED and UNASSO targets detected by Cobra Dane in the 2015 campaign.	21
3.4	Distribution of TLE eccentricity vs. TLE inclination for TAGGED and UNASSO targets detected by Cobra Dane in the 2015 campaign.	21
3.5	Distribution of TLE perigee altitude vs. TLE eccentricity for TAGGED and UNASSO targets detected by Cobra Dane in the 2015 campaign.	22

A-1.	Processing flow chart.	30
A-2.	TIRA’s L-band far field radiation pattern (one-way).	31
B-1.	An overview of the data collection and analysis.....	54
C-1.	Block diagram of the Goldstone Orbital Debris Radar (ODR) bi-static configuration.	64
E-1.	Results of RCS-to-Physical size measurements on 39 “representative” debris objects over the frequency range 2.0 - 18 GHz (15 - 1.67 cm wavelength).	77
F-1.	Map of radar locations for 2015 campaign.	80

This page intentionally left blank

1. Introduction

The Inter-Agency Space Debris Coordination Committee (IADC) provides the organizational framework for sponsoring periodic international measurement campaigns of the space debris environment. The IADC has conducted two types of campaigns: high altitude campaigns designed to measure the debris environment at near-geostationary altitudes using mostly optical telescopes, and low altitude campaigns using primarily radars. One of the goals of the low altitude campaigns is to collect data for 24 contiguous hours. In this way, all orbit planes can be sampled. Multiple sensors are used, each with its own strengths and weaknesses, to provide a more complete understanding of the environment. Comparing results between sensors also provides a better understanding of the potential biases resulting from any one sensor. Conducting the campaigns at roughly regular intervals over a long period also allows researchers to examine trends and growth of the environment over time. For this reason, low altitude campaigns are anticipated at 2-year intervals [6]. This is the eighth IADC low altitude campaign conducted. The first campaign was conducted in 1996 and two campaigns were conducted in 1999. The 2002 campaign was delayed until January 2003 because of scheduling conflicts, and the fifth, sixth, and seventh campaigns were conducted in 2004, 2008, and 2013 respectively. The eighth campaign was conducted on 8 December 2015.

This report covers the results obtained from the low altitude campaign conducted in 2015. The Objectives of Action Item 33.3, “International 24-Hour LEO Space Debris Measurement Campaign 2015” included:

- Update statistical characterization of the dynamic low Earth orbit (LEO) debris population
- Compare data collected over a common collection period
- Encourage participation by organizations that may not have contributed in past campaigns
- Concentrate on altitudes less than 2000 km

The LEO debris population is dynamic. It changes over time because of particle loss caused by atmospheric drag and reentry and by normal space traffic, and by sudden injection of particles from explosions and collisions. The concept of conducting a LEO campaign every 2 years was adopted by Working Group 1 in 2002. The 2-year schedule does not preclude member agencies from more frequent or continuous measurements. However, comparison of data collected during a common collection period is needed periodically.

The strategy of routinely measuring the LEO environment has been validated by events in 2007 and 2009. Significant on-orbit fragmentations occurred during those years. The 2008 campaign provided a good baseline to compare against later campaigns, which will show the effects on the environment from these major events.

Three of the five radars that participated in the 2008 24-hour campaign also participated in the 2015 campaign. The European Incoherent Scatter Scientific Association (EISCAT) Svalbard Radar (ESR) was not funded for participation in the 2015 campaign and the Haystack Auxiliary Radar (HAX) is operating at a reduced power level. However, the TIRA system of the Fraunhofer Research Institute for High Frequency Physics and Radar Techniques (FHR), Haystack Ultrawideband Satellite Imaging Radar (HUSIR), and Cobra Dane radars participated in both the 2008 and 2015 campaigns. Additionally, the Goldstone radar participated in the 2015 24-hour campaign, and its results are also included in this report. This report will concentrate on the results collected in 2015.

1.1 Summary

The 24-Hour LEO Space Debris Measurement Campaign 2015 was conducted on 8 December 2015. The following table is a summary of radars, observation hours, and beam park configurations. Due to the different staring configuration from previous campaigns, a comparison against historical data will not be included in this report.

**Table 1-1 – Summary of the Radars Participating in the 2015 Campaign,
the Number of Hours Observed, and the Beam Park Configuration**

Radar Name:	Observation Hours (approx.):	Staring Configuration:
HUSIR	19.2	Az: 180°, El: 20° (20S)
Goldstone	6	Az: 180°, El: 25° (25S)
Cobra Dane	13	Az: 319°, El: 20°-60° (fan beam)
TIRA	24	Az: 165°, El: 10°

2. Pencil Beam Radars

Three pencil-beam radars were used during the 2015 24-hour campaign: the TIRA radar, sponsored by the European Space Agency (ESA) and operated by Fraunhofer FHR; the HUSIR radar, sponsored by NASA and operated by the Massachusetts Institute of Technology's Lincoln Laboratory (MIT/LL); and the Goldstone radar, sponsored by NASA and operated by the Jet Propulsion Laboratory.

Each of the pencil-beam radars was operated in a staring mode. In this mode, the radar was pointed at a fixed azimuth and elevation and recorded data on objects as they passed through the narrow beam of the radar.

The orbital inclination of an object detected by a monopulse radar operating in the staring mode can be measured from the time history of the position of the object through the beam determined from the open loop monopulse azimuth and elevation voltage ratios. The direction and angular velocity, along with the range, range rate, and time, are transformed into the classic orbital elements, including inclination. However, the narrow field-of-view of the radars provides a very small arc of the orbit and a relatively small amount of measurement noise quickly degrades the velocity determination, making the derived values of inclination and eccentricity invalid. Inclination can also be estimated from range rate information if circular orbits are assumed. Inclination derived by this method will be referred to as Doppler inclination. The Doppler is the frequency shift from the transmitted signal to the received signal caused by the line-of-sight relative motion of the target, or range rate.

If the assumption of a circular orbit is used, the line-of-sight velocity can be related to the orbital inclination of the object for an antenna beam that is not pointed vertically. An error is introduced, of course, if the orbit is non-circular (i.e., $ecc \neq 0$). However, the error is not significant for modest eccentricities ($ecc < 0.1$). In practice, the Doppler inclination has proved more accurate than determining inclination from the monopulse signals as the object passes through the main lobe of the radar beam.

2.1 HUSIR



**Figure 2.1. MIT's Lincoln Space Surveillance Complex (LSSC).
HUSIR is in the large radome at upper left.**

2.1.1 Background

The Haystack Ultrawideband Satellite Imaging Radar (HUSIR, formerly known as Haystack Observatory) is a Cassegrain reflector antenna located in Westford, Massachusetts, USA (42.62° N. latitude, 71.49° W. longitude). It is operated by the Massachusetts Institute of Technology's Lincoln Laboratories as part of their Lincoln Space Surveillance Complex. It is a monopulse tracking radar capable of operating at X-band and W-band frequencies; however, for the purposes of orbital debris measurements it is operated in a beam park mode at X-band using a low pulse repetition frequency (PRF), fixed-frequency waveform. HUSIR and HAX are the primary source of radar observations for the NASA Orbital Debris Program Office (ODPO) contributing approximately 1000 hours of observation time per year.

2.1.2 HUSIR Upgrade

In 2013 MIT/LL completed a major upgrade to the Haystack Observatory adding a millimeter-wave W-Band radar capability, in addition to the X-Band system. This included a whole new Cassegrain antenna, a new back-structure for improved pointing precision, new signal processing, new waveform generator, and additional hardware components [7]. Currently the ODPO does not make use of the W-band capabilities due to the proportionately small beamwidth creating a much smaller observation volume that is not ideal for statistically sampling the LEO debris environment [2].

2.1.3 24-Hour Campaign Measurements

During the 2015 24-Hour LEO Space Debris Measurement Campaign, HUSIR obtained approximately 19.2 hours of observations over a 24-hour period. Starting at 12:16 GMT on 8 December 2015, the radar pointed at an elevation of 20° above the horizon and due south. This pointing geometry has the benefit of observing debris in lower inclination orbits than our standard 75° elevation, due east staring mode; however, this geometry results in decreased sensitivity to smaller debris objects due to increased slant ranges and atmospheric effects. Over the campaign observation period, HUSIR obtained 251 detections.

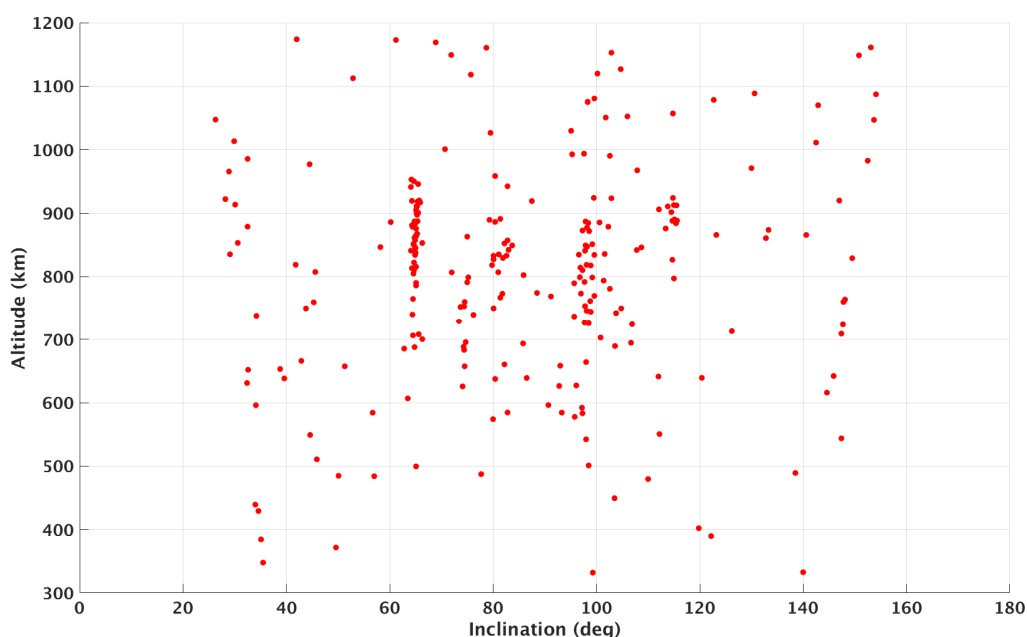


Figure 2.2. Distribution of altitude vs. Doppler-inclination for HUSIR detections in the 2015 campaign.

Figure 2.2 illustrates the population of debris at approximately 65° inclination and ranging from 700 km to 1000 km in altitude. It is believed that this debris population is dominated by a stable population of Sodium-Potassium (NaK) spheres from Radar Ocean Reconnaissance Satellites (RORSAT) [3]. The small cluster at 120° inclination and 900 km altitude is believed also to be part of the NaK population but mirrored about the 90° midpoint due to an ambiguity in calculating Doppler inclinations. There is also a substantial population of debris in sun-synchronous orbit at approximately 98° inclination and ranging from altitudes of 700 km to 900 km. This population is due to a combination of the popularity of sun-synchronous orbits and the 2007 Fengyun-1C (FY-1C) anti-satellite test (ASAT).

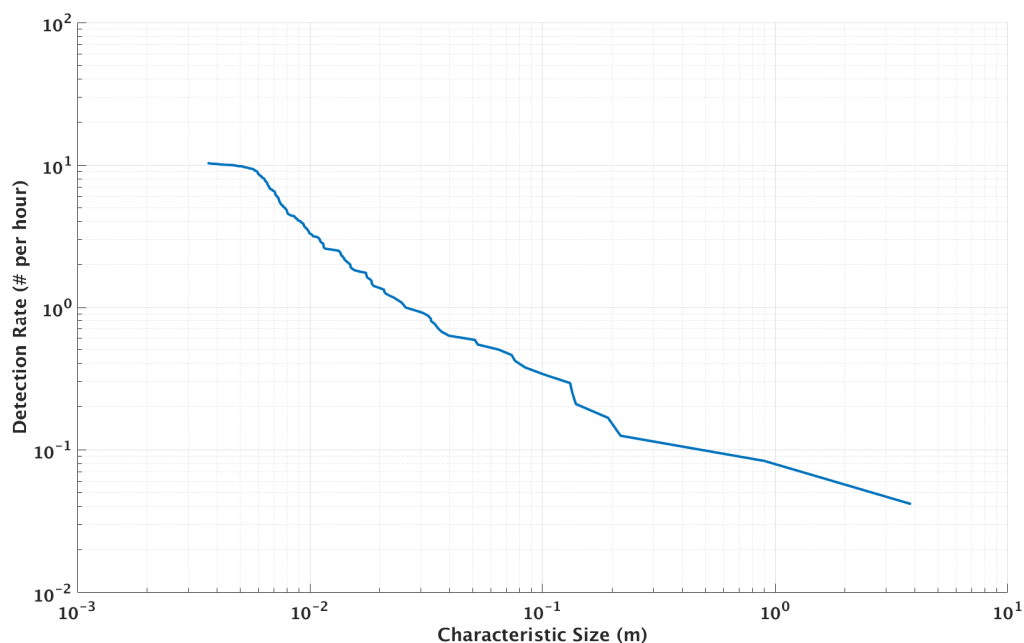


Figure 2.3. Detection rate vs. size distribution for all objects detected by HUSIR in the 2015 campaign.

Due to the south-staring orientation of this campaign, we see a decreased detection rate of centimeter- and millimeter-sized debris compared to previously reported figures. We begin to see significant granularity in the distribution above 10 cm, however, 14 of the 70 detections above 10 cm could be correlated to known cataloged objects.

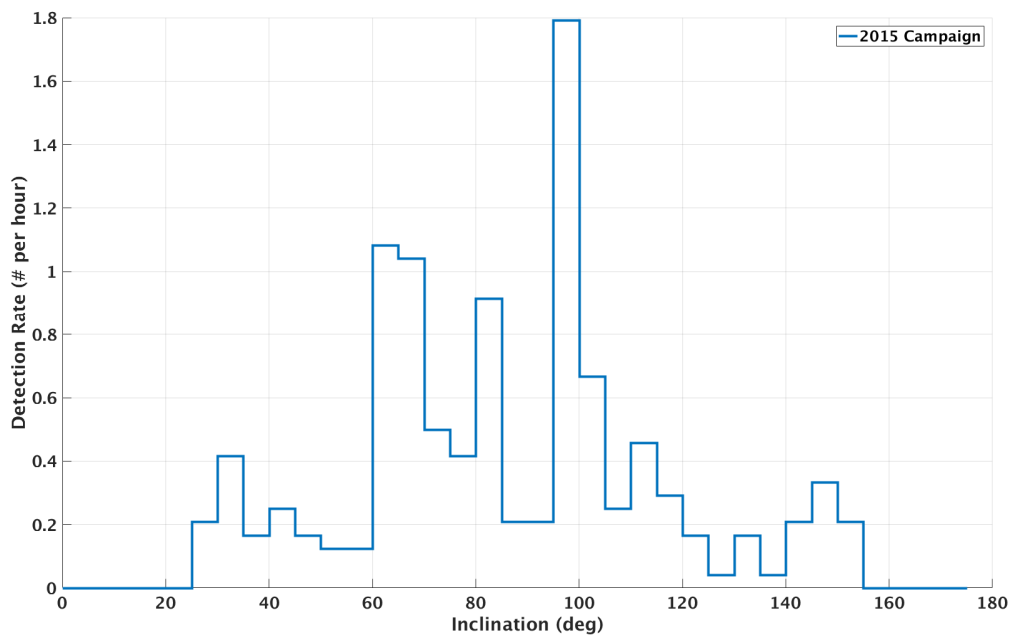


Figure 2.4. Detection rate vs. inclination distribution for all objects detected by HUSIR in the 2015 campaign.

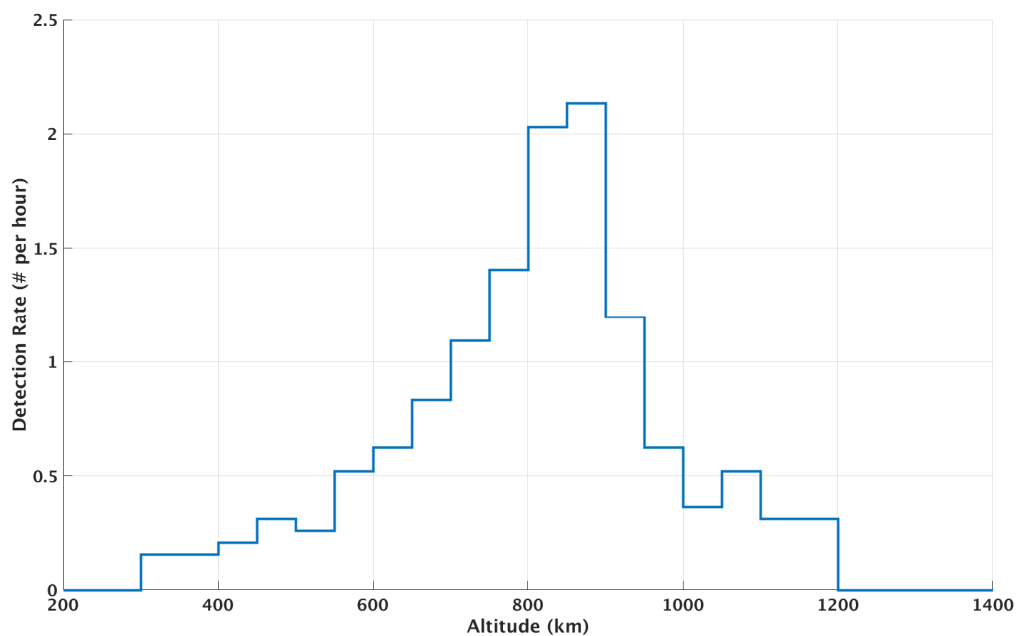


Figure 2.5. Detection rate vs. altitude distribution for all objects detected by HUSIR in the 2015 campaign.

The above figures of detection rate vs. altitude and detection rate vs. inclination provide an alternate perspective of Figure 2.2 by binning all of the detections in 50 km altitude bins and 10-degree inclination bins. The three highest peaks in Figure 2.4 are, from left to right, indicative of the stable NaK sphere population near 65° inclination, the Iridium-33 debris cloud near 86° inclination, and the FY-1C ASAT test debris cloud near 98° inclination.

2.2 Goldstone



Figure 2.6. Deep Space Station 14 (DSS-14) “Mars” located at the Goldstone Deep Space Communications Complex.

2.2.1 Background

The Goldstone Solar System Radar is a Cassegrain reflector antenna located near Barstow, California, USA (35.43° N. latitude, 116.89° W. longitude). It is operated by the NASA Jet Propulsion Laboratory as part of the Goldstone Deep Space Communications Complex. The radar primarily performs planetary research while operating in a monostatic mode. For orbital debris measurements

Goldstone operates in a bi-static configuration at X-band utilizing DSS-14 “Mars” for transmit and DSS-15 “Uranus” for receive. A bi-static configuration is necessary because the transmit and receive (T/R) switch was designed for relatively slow operation with very distant targets far beyond LEO. This arrangement places a sensitivity limit on Goldstone detection performance, limiting the minimum detectable size object in near Earth orbit to approximately 1 mm diameter. Due to this sensitivity to such small objects, Goldstone plays a key role in observing the millimeter orbital debris environment for NASA. Currently Goldstone does not have monopulse capabilities like HUSIR and TIRA. Until recently (late 2016), Goldstone also only reported principal polarization (PP) detections. Due to the importance of the primary mission supporting the Deep Space Network, Goldstone has a very busy schedule and observing time is limited [5].

2.2.2 24-Hour Campaign Measurements

During the 2015 24-Hour LEO Space Debris Measurement Campaign, Goldstone obtained approximately 6 hours of observations. Starting at 02:51 GMT on 8 December 2015 the radar pointed at an elevation of 25° above the horizon and due south. Over the 6-hour observation period Goldstone obtained 37 detections.

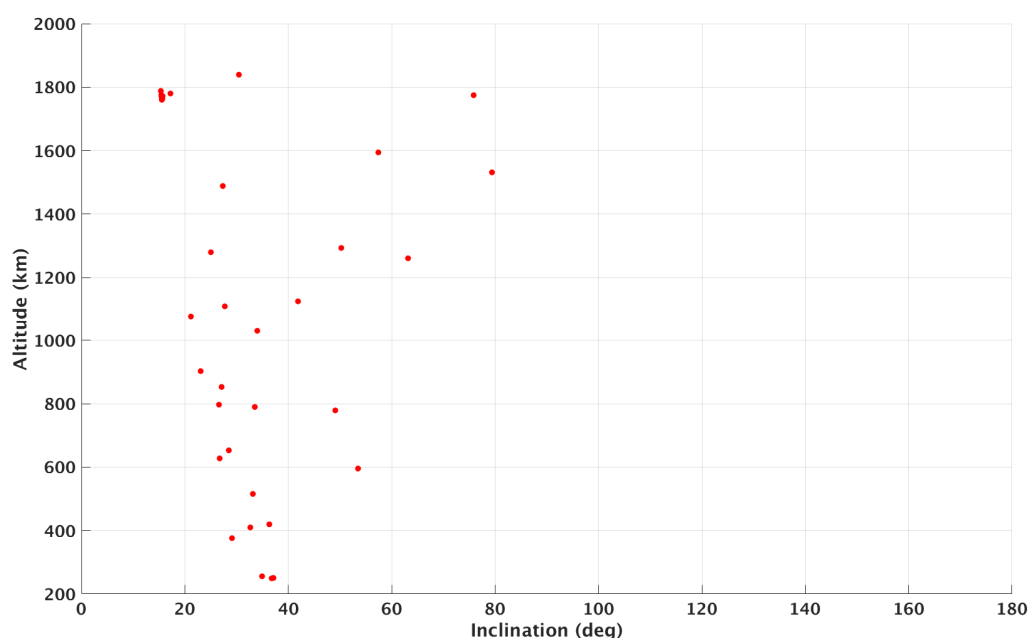


Figure 2.7. Distribution of altitude vs. Doppler-inclination for Goldstone detections in the 2015 campaign.

Figure 2.7 does not show any substantial clouds or notable debris populations. The cluster of detections at approximately 1800 km and 15° inclination is of interest; however, we were unable to correlate them to any cataloged objects or known events. Our current analysis indicates these detections may be debris in highly eccentric geosynchronous transfer orbits.

Note: There is an ambiguity in calculating Doppler inclinations because we only have one component of the velocity along the radar line of sight; therefore, we cannot distinguish between a low inclination object and a high inclination, retrograde object. We have chosen the low inclination solution

in the above plot but we cannot rule out the possibility that some of these objects are in high inclination, retrograde orbits.

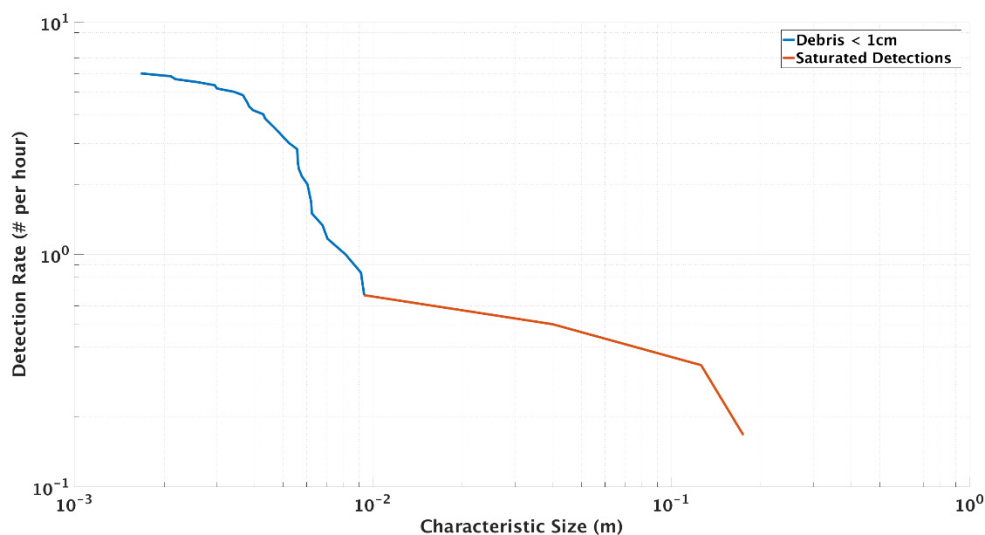


Figure 2.8. Size distribution for all objects detected by Goldstone in the 2015 campaign.

Due to its primary mission of communicating with deep space satellites and performing radar measurements of terrestrial bodies in the solar system, the Goldstone radar is an incredibly sensitive system. As a result, the receiver hardware can easily be saturated by strong signals from larger pieces of debris in LEO. In Figure 2.8, we believe that any detections over 1 cm are likely to saturate the receiver hardware and the resulting measurements are not to be trusted. These detections have been included only for completeness.

2.3 TIRA

TIRA is an English acronym for a particular radar asset at the Fraunhofer FHR complex, the "Tracking and Imaging Radar."



Figure 2.9. The TIRA Radar is located inside a 47.5-meter radome.

2.3.1 Background

The TIRA system is located in Wachtberg near Bonn, Germany (50.62° N. latitude, 7.13° E. longitude). It is operated by Fraunhofer FHR. TIRA is a monopulse tracking radar, employing a 34-meter parabolic dish antenna, a significant factor that results in its very sensitive detection capability. It is capable of operating at both L-band and Ku-band frequencies for high precision target tracking and high-resolution target imaging, respectively. For orbital debris collection, it primarily operates in a beam park mode at L-band. Historically the TIRA system has performed beam park experiments in both monostatic and bistatic mode in cooperation with Radiotelescope Effelsberg.

2.3.2 24-Hour Campaign Measurements

During the 2015 24-Hour LEO Space Debris Measurement Campaign, TIRA obtained approximately 24 hours of observations. Starting at 12:00 GMT on 8 December 2015, the radar pointed at an elevation of 10° above the horizon and south-southeast (165° azimuth). Over the observation period TIRA obtained the following results:

- Number of detected objects before screening: **624**
- Number of detected objects after screening: **472**
- Number of correlated catalogue objects: **164**
- Number of uncorrelated large objects: **8**

(Characteristic length >100 cm)

Cumulative Plots

Figs. 2.10 and 2.11 present the cumulative detection rate versus object diameter and object RCS, respectively. The green line in Figs. 2.10 and 2.11 indicates the change of scattering regime between geometric scattering and resonance scattering.

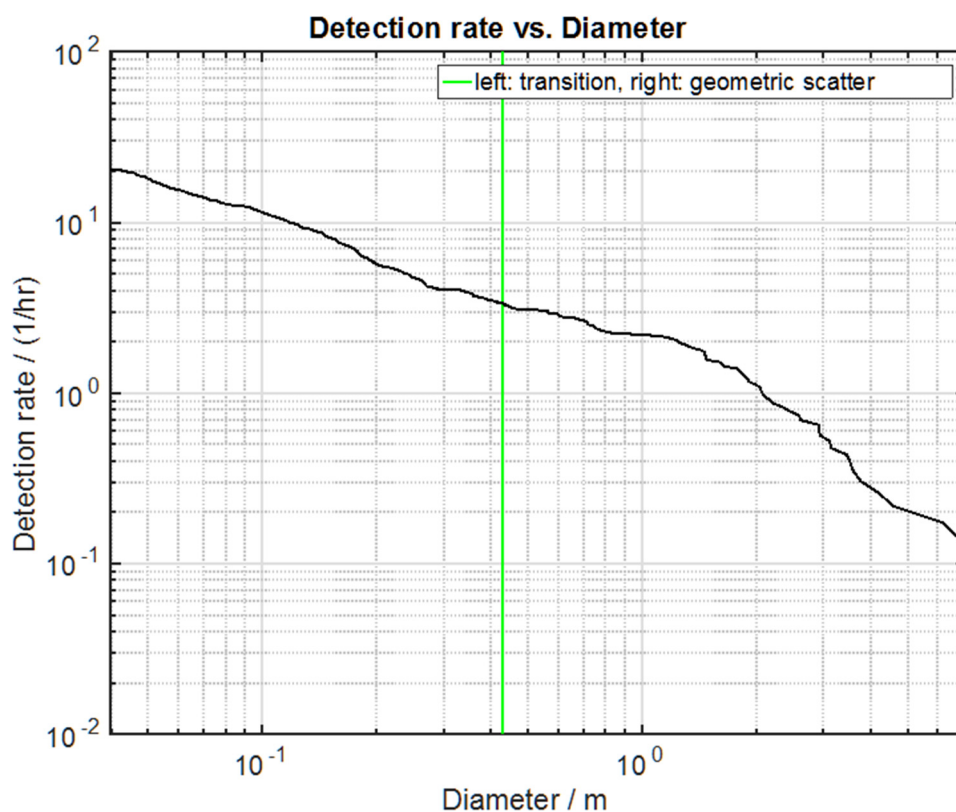


Figure 2.10. Detection rate versus object diameter for all objects detected by TIRA in the 2015 campaign.

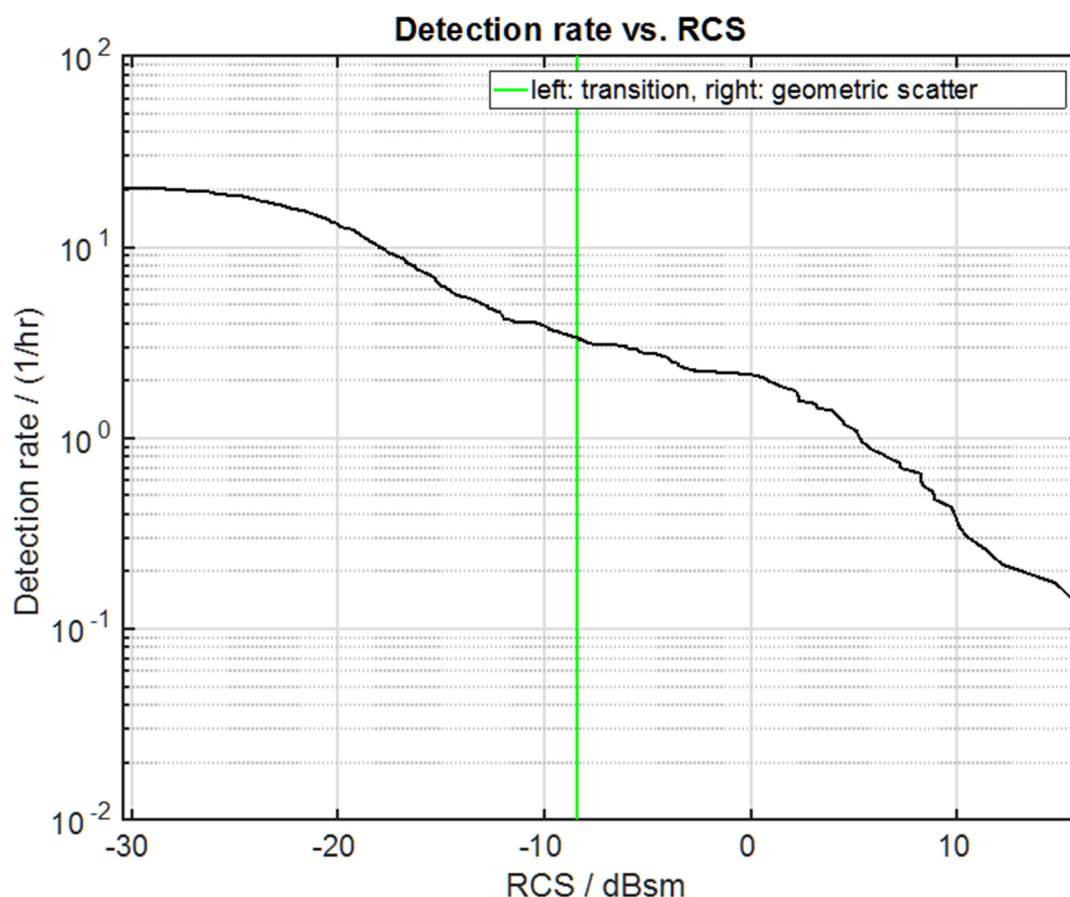


Figure 2.11. Detection rate versus object RCS for all objects detected by TIRA in the 2015 campaign.

Histograms

Fig. 2.12 shows the detection rate versus range rate of all detected objects. A large number of detections occur around the radial velocity 0 m/s. As evidenced in Fig. 2.18, the debris are small with diameters lower than 20 cm and most of them are smaller than 10 cm. Since these detections are uniformly distributed over all the altitudes between 400 km up to 1100 km (not shown in this report), they cannot correspond to ionosphere reflections (in this case, their altitudes would be concentrated around 400 km). The origin of these detections and whether these detections are true or caused by a system/processing artifact are still unclear at the time of writing this report. Therefore, the detections around the radial velocity 0 m/s should be either kept or discarded from the detection list of TIRA depending on the results achieved by the other radar sensors.

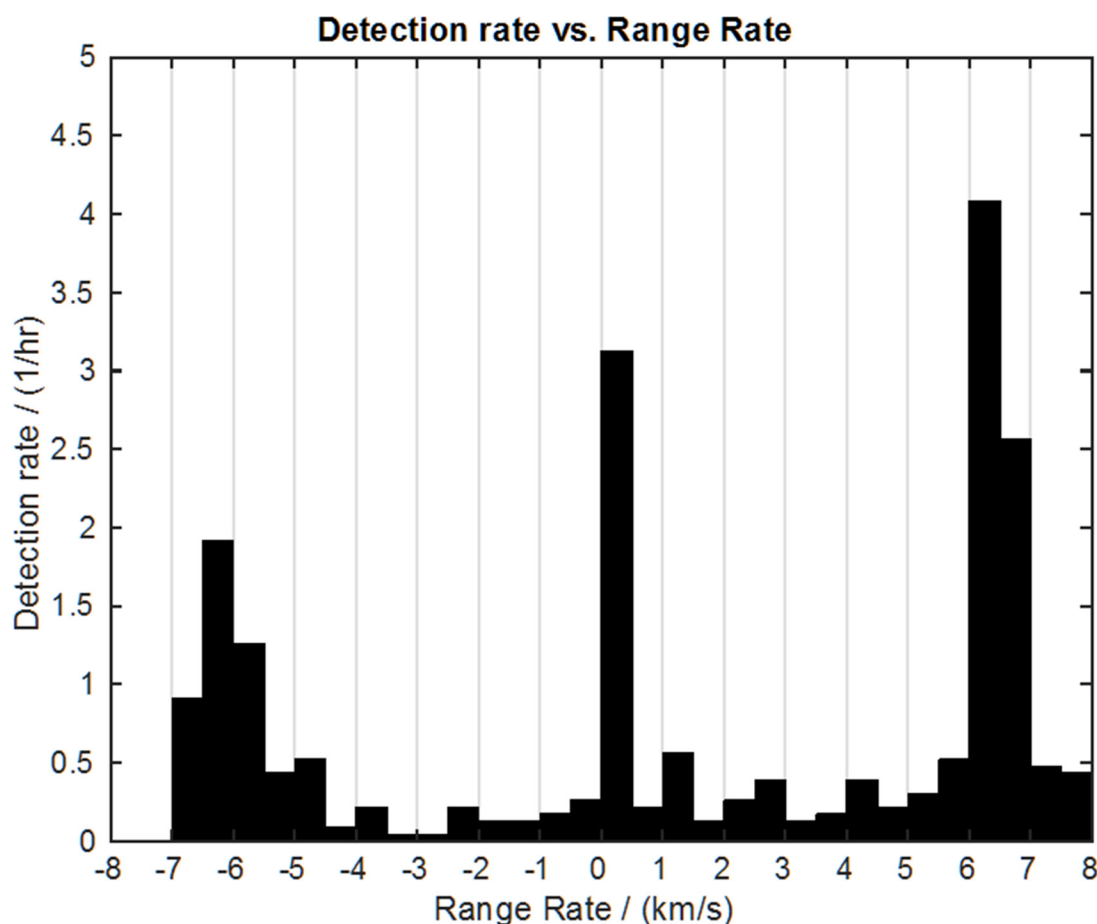


Figure 2.12. Detection rate versus range rate for all objects detected by TIRA in the 2015 campaign.

The selection of the Doppler inclination from the range rate in Fig. 2.13 was done from the crossing direction of the object through the antenna beam. Since the detected debris are usually small (low RCS objects), they can only be detected after signal integration over several pulses. The estimation of their crossing direction through the beam is based, however, on the monopulse ratios, which are computed for each single pulse independently. Since the SNR per pulse is usually small, the estimation accuracy of the elevation and azimuth angles is low. Therefore the estimation of the crossing direction and thus of the Doppler inclination can be inaccurate. Alternatively, instead of trying to estimate the Doppler inclination from the radar data, the Doppler inclination of objects with range rate within the interval $[-5,5]$ km/s can be assigned to the lower value of the two Doppler inclination solutions, as could be shown by simulations performed with Program for Radar and Optical Observation Forecasting (PROOF) 2009©. In this case, in the detection list of TIRA, the lower of the two Doppler inclination solutions has to be selected.

Finally, Fig. 2.14 presents the detection rate versus altitude of all detected objects.

Note: For a South-staring antenna pointing, the calculation of the Doppler inclination from an object's estimated range rate does not provide a unique solution any longer but two solutions.

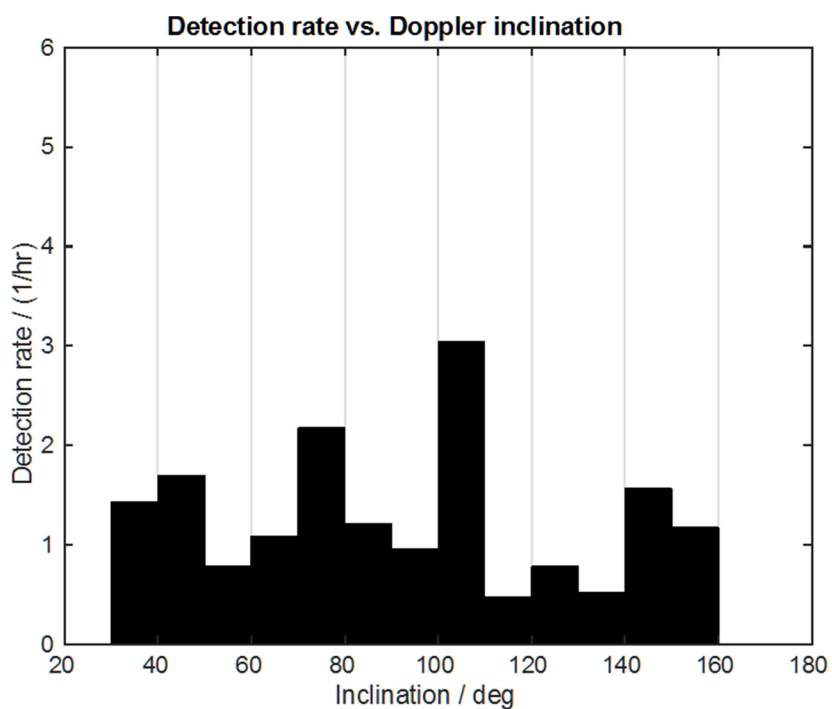


Figure 2.13. Detection rate versus Doppler inclination for TIRA detections in the 2015 campaign.

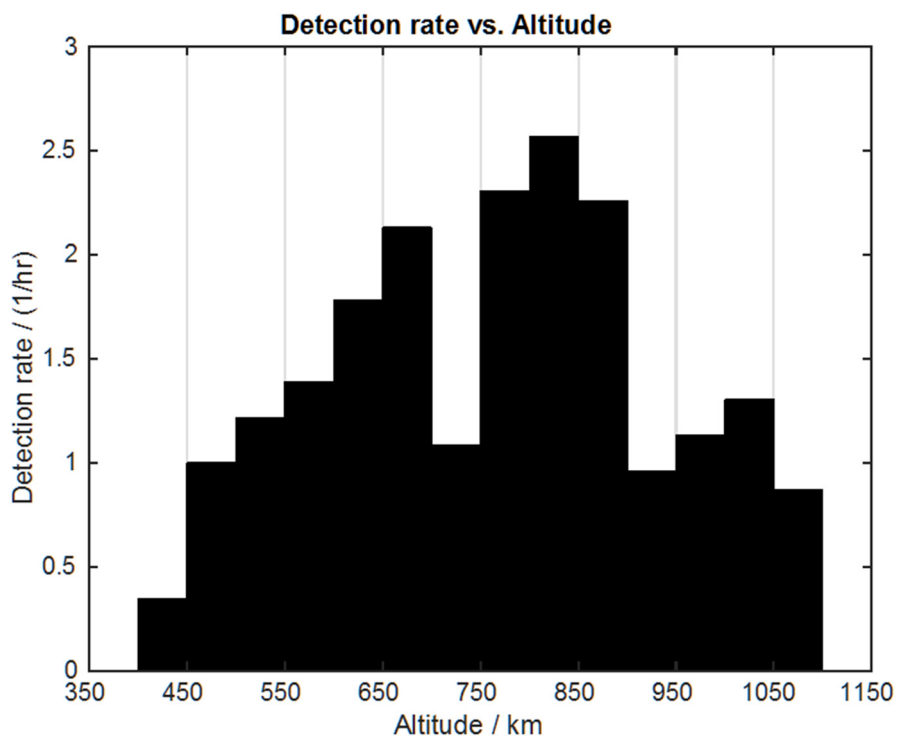


Figure 2.14. Detection rate versus altitude for all objects detected by TIRA in the 2015 campaign.

Scatter Plots

Fig. 2.15 to 2.18 show different parameter representations of the detected debris in the form of scatter plots in order to better understand the origin of these debris. Fig. 2.15 and 2.16 reveal the distribution of the debris altitude versus range rate and Doppler inclination, respectively. The color bar evidences lines of equal range rate (Fig. 2.15) or Doppler inclination (Fig. 2.16). The dashed lines show the Doppler inclination boundaries.

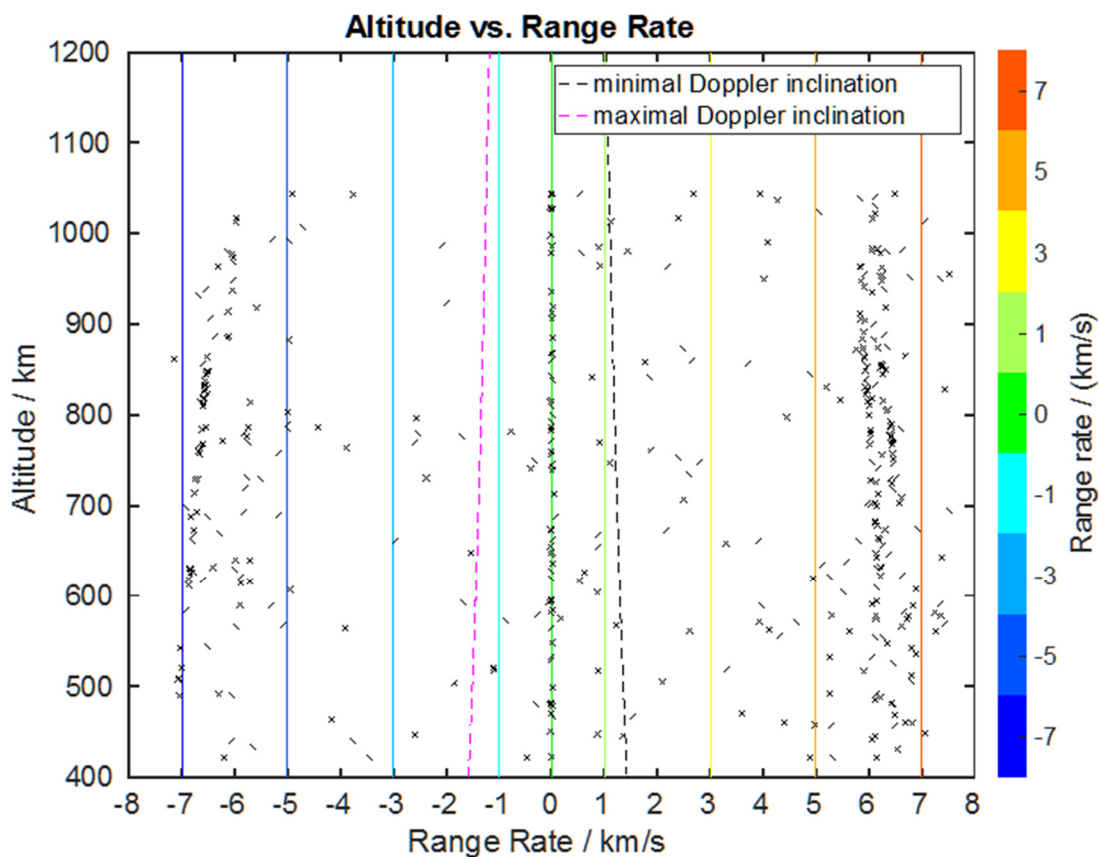


Figure 2.15. Altitude versus range rate for all objects detected by TIRA in the 2015 campaign.

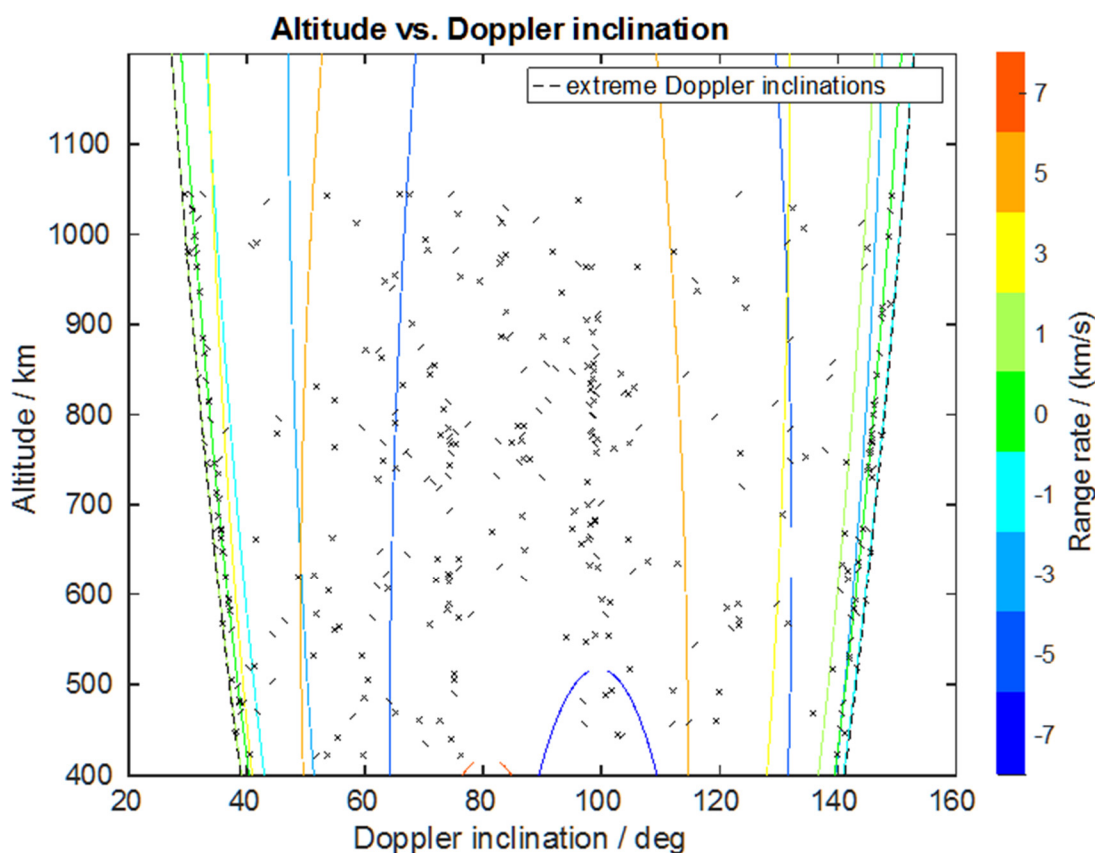


Figure 2.16. Altitude versus Doppler inclination for TIRA detections in the 2015 campaign.

In Fig. 2.17, the colored lines indicate the theoretical detection thresholds (diameter versus altitude) for different integration lengths. One can observe a very good fit between achieved detections and theoretical thresholds, indicating that the theoretical sensitivity of TIRA corresponds to the experimentally achieved sensitivity.

Fig. 2.18 investigates the relationship between object diameter and range rate.

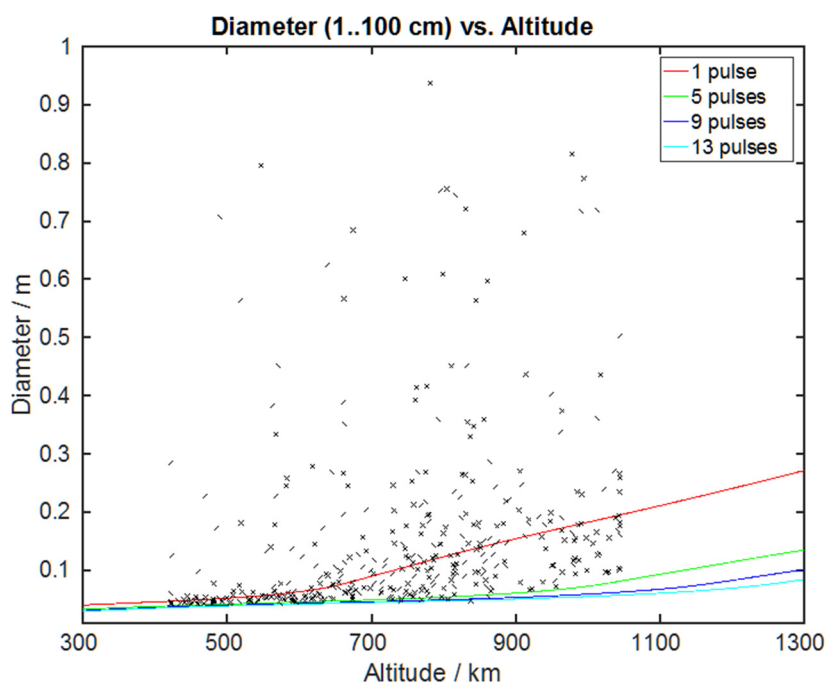


Figure 2.17. Object diameter versus altitude for all objects detected by TIRA in the 2015 campaign.

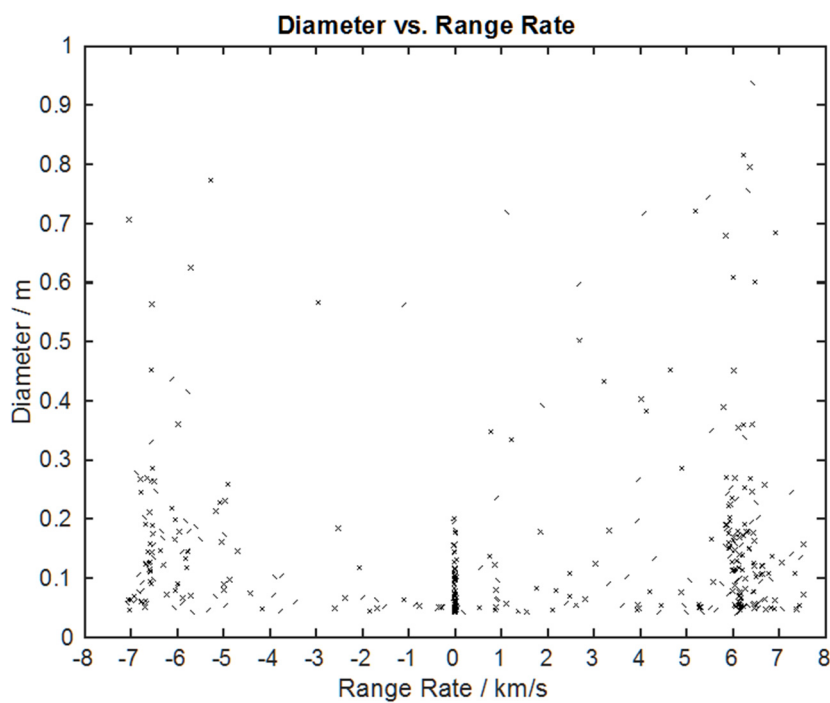


Figure 2.18. Object diameter versus range rate for all objects detected by TIRA in the 2015 campaign.

3. Phased Array Radar

3.1 Cobra Dane (AN/FPS-108)



Figure 3.1. Cobra Dane phased array radar in Shemya, Alaska.

3.1.1 Background

The AN/FPS-108 Cobra Dane radar is an electronically scanned radar installation at Eareckson Air Station, located on the island of Shemya, Alaska (52.7° N. latitude, 174.1° E. longitude). It is a single face, phased array radar with a 29 m- (95 ft.) diameter antenna aligned at an azimuth of 319°. Cobra Dane operates in the 1215–1400 MHz frequency region, i.e., L-band. Phased array radars have the benefit of being able to electronically steer and point their beam without having to move the antenna physically. Due to Cobra Dane's primary mission supporting the U.S. Department of Defense, some of the parameters associated with the operation of the radar are not available to the general public.

3.1.2 24-Hour Campaign Measurements

For the 24-hour campaign, Cobra Dane obtained approximately 13 hours of observations. The radar started taking data at 19:38 GMT on 8 December 2015. For this campaign, the antenna beam is rapidly moved in a long, narrow vertical pattern to create a virtual fan beam, or fence. Each individual beam position in the fence is revisited often enough that orbiting objects cannot travel the width of the fence between revisits. The fence is therefore referred to as a “leak-proof” fence. When an object is detected in the fence, some of the radar’s resources can be used to track the object while maintaining the fence. To maintain the leak-proof fence, only uncorrelated detections (objects not in the United States Space Command (USSPACECOM) catalog or analysts objects) were tracked [6]. During the 13-hour observation period Cobra Dane obtained 142 detections that correlated with objects in the catalog (TAGGED), 389 detections not associated with a cataloged object but of sufficient quality to determine an element set (UNASSO), and 3065 detections not associated with a cataloged object and having no element set derived from the detection (UCT_UNASSO).

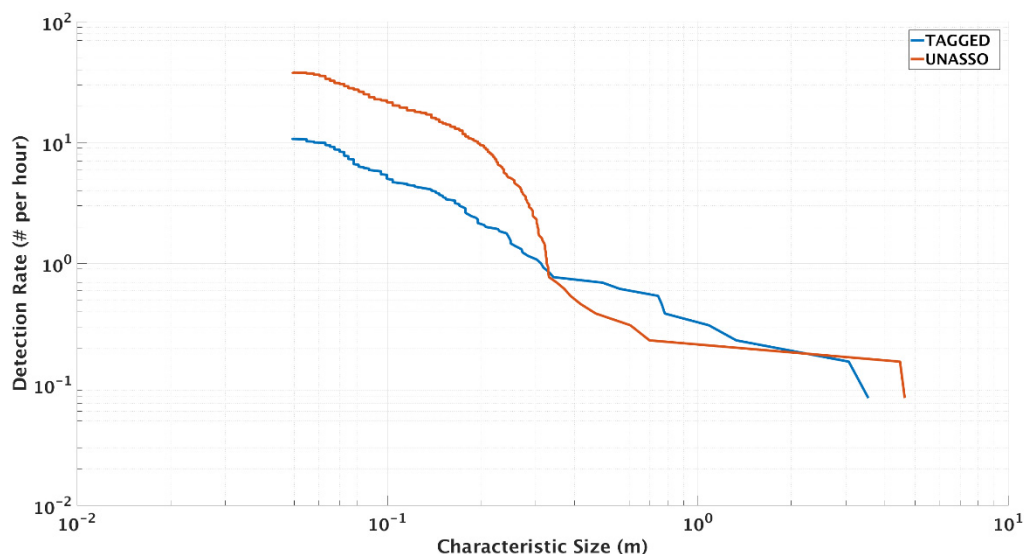


Figure 3.2. Size distribution for all TAGGED and UNASSO detections by Cobra Dane in the 2015 campaign.

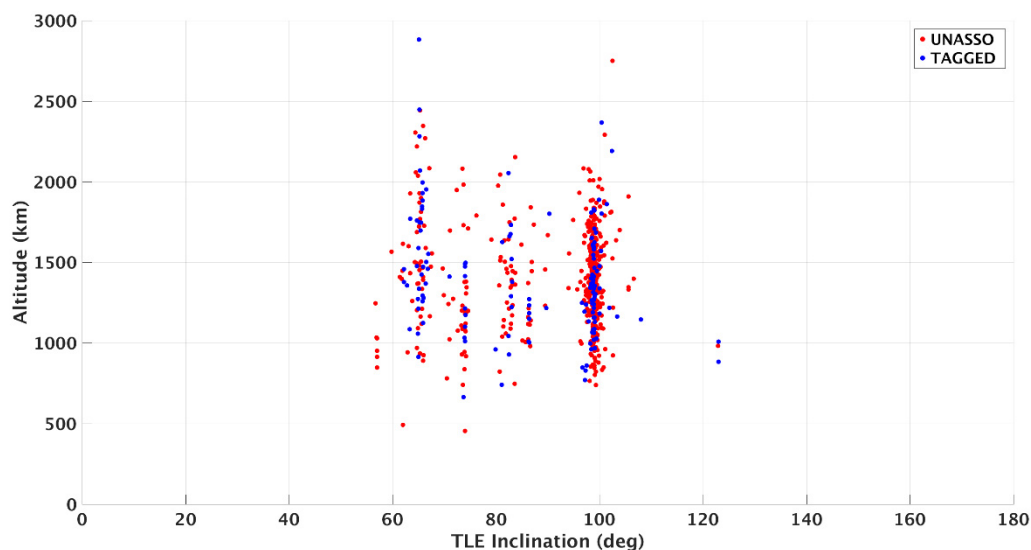


Figure 3.3. Distribution of altitude vs. TLE inclination for TAGGED and UNASSO targets detected by Cobra Dane in the 2015 campaign.

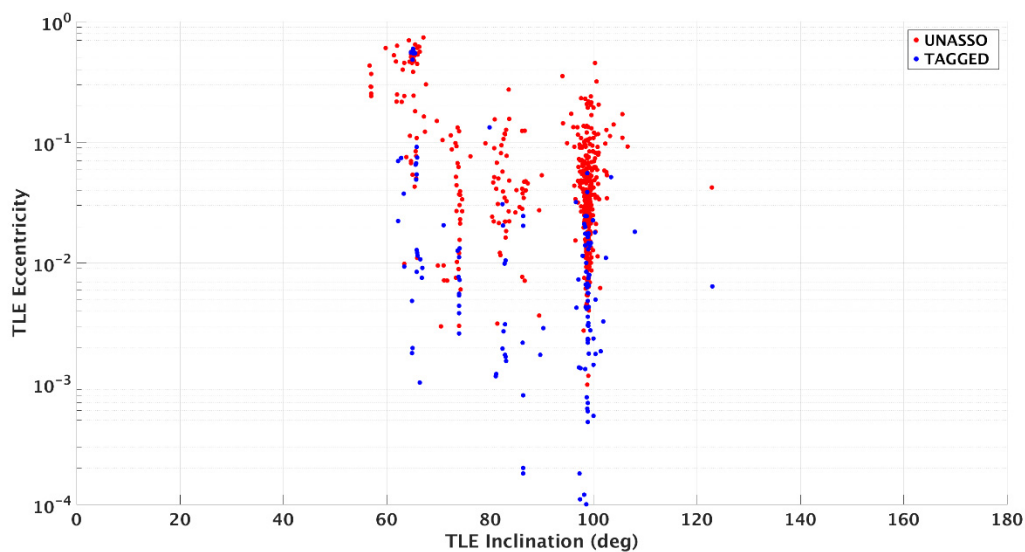


Figure 3.4. Distribution of TLE eccentricity vs. TLE inclination for TAGGED and UNASSO targets detected by Cobra Dane in the 2015 campaign.

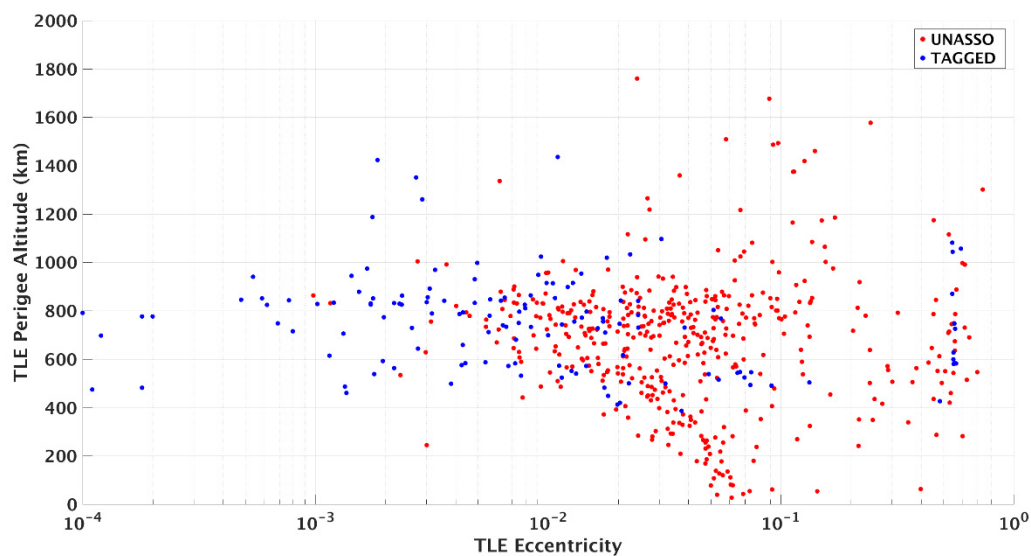


Figure 3.5. Distribution of TLE perigee altitude vs. TLE eccentricity for TAGGED and UNASSO targets detected by Cobra Dane in the 2015 campaign.

4. On-orbit Fragmentations

In addition to the normal space traffic from launches and natural orbital decay there have been 27 on-orbit fragmentations and 10 anomalous events since the 2008 24-Hour Campaign in which NASA participated. A list of the fragmentations is provided in Table 4-1 and a list of the anomalous events is provided in Table 4-2 [1, 2].

The most significant event since the 2008 campaign was the collision of the inactive satellite Cosmos-2251 with Iridium-33 on 10 February 2009. The collision occurred at an altitude of 789 km above Siberia. Both satellites were in nearly circular orbits with inclinations of 74° and 86.4° respectively.

Table 4-1 – List of Known On-orbit Fragmentations for the Time Period 17 November 2008 through 8 December 2015

SATELLITE NAME	INTERNATIONAL DESIGNATOR	US SATELLITE NUMBER	SATELLITE OWNER	SATELLITE TYPE	SATELLITE MASS (KG)	LAUNCH DATE	BREAKUP DATE	APOGEE (KM)	PERIGEE (KM)	CLINATION (DEG)	ASSESSED CAUSE	ADDITIONAL INFORMATION
COSMOS 2251	1993-036A	22675	RF	PAYLOAD	900	16-Jun-93	10-Feb-09	800	775	74.0	COLLISION, ACCIDENTAL	COLLIDED WITH IRIIDIUM 33
IRIDIUM 33	1997-051C	24946	USA	PAYLOAD	560	14-Sep-97	10-Feb-09	780	775	86.4	COLLISION, ACCIDENTAL	COLLIDED WITH COSMOS 2251
COSMOS 2139-41 ULLAGE MOTOR	1991-025F	21220	USSR	OP. DEBRIS	55	4-Apr-91	8-Mar-09	18535	465	64.9	PROPULSION	PROTON-K BLOCK DM SOZ
COSMOS 192	1967-116A	3047	USSR	PAYLOAD	750	23-Nov-67	30-Aug-09	715	710	74.0	UNKNOWN	
YAOGAN 1	2006-015A	29092	PRC	PAYLOAD	2720	26-Apr-06	4-Feb-10	630	625	97.9	UNKNOWN	
CHINASAT 6A R/B	2010-042B	37151	PRC	ROCKET BODY	3062	4-Sep-10	4-Sep-10	41894	194	25.2	UNKNOWN	CZ-3 FINAL STAGE
AMC 14 BRIZ-M R/B	2008-011B	32709	RF	ROCKET BODY	2500	14-Mar-08	13-Oct-10	26565	645	48.9	PROPULSION	PROTON-K BRIZ-M STAGE
BEIDOU G4 R/B	2010-057B	37211	PRC	ROCKET BODY	3060	1-Nov-10	1-Nov-10	35780	160	20.5	UNKNOWN	CZ-3C FINAL STAGE
IGS 4A/4B R/B DEBRIS	2007-005E	30590	JAPAN	OP. DEBRIS	UNK	24-Feb-07	23-Dec-10	440	430	97.3	UNKNOWN	H-IIA DEBRIS
COSMOS 2434-36 ULLAGE MOTOR	2007-065G	32399	RF	OP. DEBRIS	55	25-Dec-07	18-Aug-11	18965	540	65.0	PROPULSION	PROTON-K BLOCK DM SOZ
COSMOS 2079-81 ULLAGE MOTOR	1990-045F	20630	USSR	OP. DEBRIS	55	19-May-90	17-Nov-11	18620	420	65.0	PROPULSION	PROTON-K BLOCK DM SOZ
NIGCOMSAT 1R R/B	2011-077B	38015	PRC	ROCKET BODY	3060	19-Dec-11	~21-Dec-11	41715	230	24.3	UNKNOWN	CZ-3B FINAL STAGE
BEIDOU G5 R/B	2012-008B	38092	PRC	ROCKET BODY	3060	24-Feb-12	26-Feb-12	35950	150	20.7	UNKNOWN	CZ-3C FINAL STAGE
TELKOM 3 / EXPRESS MD2 BRIZ-M R/B	2012-044C	38746	RF	ROCKET BODY	2600	6-Aug-12	16-Oct-12	5010	265	49.9	PROPULSION	PROTON-K BRIZ-M STAGE
DMSP 5D-2 F9 (USA 29)	1988-006A	18822	USA	PAYLOAD	468	3-Feb-88	14-17 Dec-12	810	800	98.8	UNKNOWN	
CASSIOPE R/B	2013-055B	39266	USA	ROCKET BODY	3500	29-Sep-13	29-Sep-13	1490	320	81.0	PROPULSION	FALCON 9 SECOND STAGE
ARGOS/ORSTED/SUNSAT R/B	1999-008D	25637	USA	ROCKET BODY	921	23-Feb-99	28-Apr-14	840	635	96.5	UNKNOWN	DELTA 2 SECOND STAGE
COSMOS 2428	2007-029A	31792	RF	PAYLOAD	3250?	29-Jun-07	10-May-14	860	845	71.0	UNKNOWN	
COSMOS 2442-44 ULLAGE MOTOR	2008-046H	33385	RF	OP. DEBRIS	55	25-Sep-08	20-May-14	18720	865	65.0	PROPULSION	PROTON-K BLOCK DM SOZ
OPS 0757 (TACSAT) R/B	1969-013B	3692	USA	ROCKET BODY	1874	9-Feb-69	4-Jun-14	37130	35970	8.7	UNKNOWN	TITAN TRANSTAGE
COSMOS 2294-96 ULLAGE MOTOR	1994-076G	23402	RF	OP. DEBRIS	55	20-Nov-94	7-Jun-14	18990	420	65.0	PROPULSION	PROTON-K BLOCK DM SOZ
COSMOS 2459-61 ULLAGE MOTOR	2010-007G	36406	RF	OP. DEBRIS	55	1-Mar-10	9-Jul-14	18750	770	65.0	PROPULSION	PROTON-K BLOCK DM SOZ
COSMOS 2431-33 ULLAGE MOTOR	2007-052F	32280	RF	OP. DEBRIS	55	26-Oct-07	13-Aug-14	18790	730	65.0	PROPULSION	PROTON-K BLOCK DM SOZ
USA 109 (DMSP 5D-2 F13)	1995-015A	23533	USA	PAYLOAD	850	24-Mar-95	3-Feb-15	840	840	98.8	BATTERY	Operational at event time
PROGRESS-M 27M R/B	2015-024B	40620	RF	ROCKET BODY	2355	28-Apr-15	28-Apr-15	181	169	51.7	UNKNOWN	Soyuz 2.1a (3); separation with PROGRESS M-27M
SL-23 DEBRIS	2011-037B	37756	RF	OP. DEBRIS	375	18-Jul-11	3/4-Aug-15	3649	428	51.4	UNKNOWN	Fregat-SB SBB propellant tank
NOAA 16	2000-055A	26536	USA	PAYLOAD	1475	21-Sep-00	25-Nov-15	858	842	98.9	UNKNOWN	

Table 4-2 – List of Anomalous Events for the Time Period 17 November 2008 through 8 December 2015

SATELLITE NAME	INTERNATIONAL DESIGNATOR	US SATELLITE NUMBER	LAUNCH DATE	FIRST EVENT DATE	KNOWN EVENTS	APOGEE (KM)	PERIGEE (KM)	INCLINATION (DEG)
COSMOS 1818	1987-011A	17369	1-Feb-87	4-Jul-08	1	800	775	65.0
COSMOS 1417 R/B	1982-102B	13618	19-Oct-82	Early-09	1	1000	955	83.0
NOAA 11	1988-089A	19531	24-Sep-88	24-Nov-10	1	850	835	98.8
NOAA 12	1991-032A	21263	14-May-91	2-Oct-11	1	815	800	98.7
NOAA 14	1994-089A	23455	30-Dec-94	Jul-12	1	860	850	98.8
BLITS	2009-049G	35871	17-Sep-09	22-Jan-13	1	825	815	98.6
COSMOS 1867	1987-060A	18187	10-Jul-87	21-Mar to 4-Apr-14	1	800	775	65.0
IRIDIUM 47	1997-082C	25106	20-Dec-97	7-Jun-14	1	781	778	86.4
HAIYANG 2A	2011-043A	37781	15-Aug-11	6/7-Jul-14	2	965	965	99.0
IRIDIUM 91	2002-005A	27372	11-Feb-02	30-Nov-14	1	781	777	86.4

5.0 Conclusion

The IADC 24-hour campaigns have proven to be a useful tool for surveying the LEO debris environment, as well as a beneficial exercise in international cooperation and coordination in the debris community. The 2015 campaign provided an interesting insight into lower inclination debris populations that have not been substantially surveyed in recent years. Since the 2008 campaign, there have been significant events in LEO that have greatly altered the debris environment such as the Iridium-Cosmos collision and numerous other on-orbit fragmentations. Such events highlight the importance of measurements and modeling of the debris environment and the need for international collaborations such as the IADC 24-Hour Campaigns to provide accurate risk assessment to both manned spaceflight and satellite operators.

6.0 References

- [1] Anz-Meador, P., "IADC_24hrCamp_Bus_170217.xlsx." Message to Christopher Blackwell. 2017 February 17. Email.
- [2] Eshbaugh, J., Morrison Jr, R., Hoen, E., Hiett, T., Benitz, G., "HUSIR Signal Processing." Lincoln Laboratory Journal. Volume 21. Issue 1. (2014). Web.
- [3] Horstman, M., Papanyan, V., Juarez, Q., Hamilton, J., *Haystack and HAX Radar Measurements of the Orbital Debris Environment: 2006-2012*. NASA/TP-2014-217391. NASA/JSC.
- [4] Johnson, N., Stansbery, E., Whitlock, D., Abercromby, D., and Shoots, D. *History of On-orbit Satellite Fragmentations, 14th Edition*. NASA/TM-2008-214779. NASA/JSC
- [5] Slade, Martin. Stanchfield, Kevin. "Solar System Radar Group: Group 332F." NASA JPL. 15 January 2016. Web. 20 February 2017. <http://gssr.jpl.nasa.gov/>
- [6] Stansbery, E., Leushacke, L., "International 24-hr LEO Space Debris Measurement Campaign 2008." IADC. IADC-13-05. (2013). Print.
- [7] Usoff, Joseph. "Haystack Ultrawideband Satellite Imaging Radar." MIT Lincoln Laboratory Tech Notes. September 2014. Web. 21 February 2017.
<https://www.ll.mit.edu/publications/technotes/TechNote_HUSIR.pdf>

7.0 Definitions and Acronyms

Al ₂ O ₃	Aluminum oxide
ASAT	Anti-satellite Test
BPE	Beam Park Experiment
CPA	Closest Point of Approach
dB	Decibel
ecc	Eccentricity
EISCAT	European Incoherent Scatterer Scientific Association
EL	Elevation Difference
EMC	Electromagnetic Compatibility
ESA	European Space Agency
ESR	European (incoherent scatter) Svalbard Radar
FY-1C	Fengyun 1-C
FHR	Fraunhofer Research Institute for High Frequency Physics and Radar Techniques
HAX	Haystack Auxiliary Radar
HUSIR	Haystack Ultrawideband Satellite Imaging Radar
IADC	Inter-Agency Space Debris Coordination Committee
LEO	Low Earth Orbit
MIT/LL	Massachusetts Institute of Technology's Lincoln Laboratory
NaK	Sodium (Na) Potassium (K)
NERCS	Noise Equivalent RCS
ODPO	Orbital Debris Program Office
OP	Orthogonal Polarization
PP	Principal Polarization
PRF	Pulse Repetition Frequency
PROOF	Program for Radar and Optical Observation Forecasting
RCS	Radar cross section
RORSAT	Radar Ocean Reconnaissance Satellite

SEM	Size Estimation Model
SNR	Signal-to-noise ratio
SSN	Space Surveillance Network
TAGGED	Cataloged objects
TCA	Time of Closest Approach
TIRA	Tracking and Imaging
TR	Traverse Difference
T/R	Transmit/Receive
TWT	Traveling Wave Tube
UCTs	Uncorrelated targets
UNASSO	Unassociated targets
USSPACECOM	United States Space Command

8.0 Appendices

Appendix A

TIRA Radar

A.1 Experiment Setup

Tables A.1 and A.2 list the instrument and campaign parameters for the 2015 campaign. Concerning the new beampark antenna pointing, some particularities have to be considered. Due to the low elevation angle of 10° a significant reduction of transmit power (down to 34% of the power value used in former BPE with high antenna elevation) was necessary to be compliant with the national Electromagnetic Compatibility (EMC) regulations. As a consequence, the detection sensitivity degraded by approximately 3 dB.

Table A-1 – Instrument Parameters used by the TIRA Radar for the 2015 Campaign

Parameter	Unit	Value
Geocentric latitude of sensor	deg	50.62
Geocentric longitude of sensor	deg	7.13
Geodetic altitude of sensor	km	0.293
Wavelength	m	0.225
Beam width for incoherent integration	deg	0.49
Antenna constant (gain)	dB	49.7
Transmitted power (peak)	kW	450
Pulse period	ms	29
Pulse duration	ms	1
Desired false alarm time (Marcum)	s	36000
Number of independent threshold decisions per pulse	-	5667
Maximum number of pulses to integrate	-	89
Noise equivalent RCS (NERCS)	dBsm	-47.5
Transmitted power for NERCS	kW	1500
Pulse duration for NERCS	ms	1
Range for NERCS	km	1000

Table A-2 – Campaign Parameters for the TIRA Radar for the 2015 Campaign

Parameter	Unit	Value
Date of campaign start	YY MM DD	15 12 08
Time of campaign start (UTC)	HH:MM	12:00
Maximum range	km	3000
Minimum range	km	1500
Azimuth of line-of-sight	deg	165.0
Elevation of line-of-sight	deg	10.0
Duration of campaign	hrs	24
Total recorded data	hrs	24

A.2 Data Processing

In Figure A-1, an overview of the processing is given. It starts with detecting possible object echoes in raw radar data by incoherent integration over several pulse records. This is only limited by a false alarm time of 10 h. Consecutive pulse records containing possible object echoes are grouped.

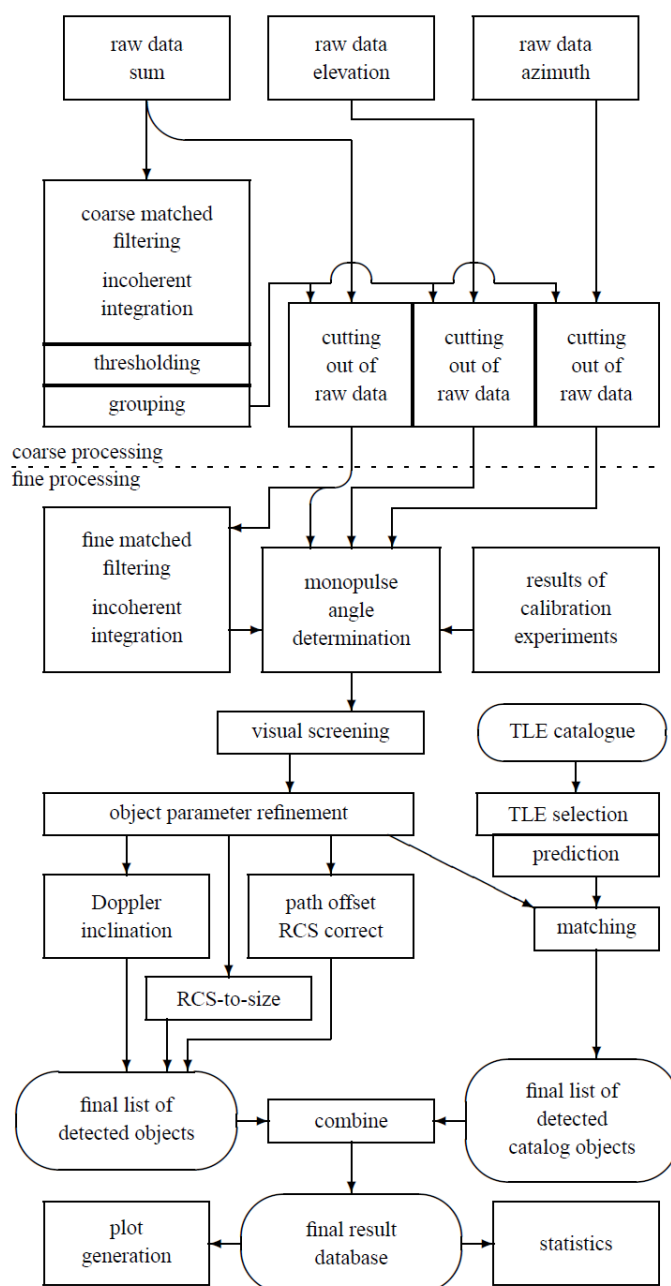


Figure A-1. Processing flow chart.

During reprocessing of these grouped data, range and Doppler-frequency shifts are determined more precisely, and tracks of the detections are kept. For each object, time, signal amplitude, range, and Doppler-frequency values, as well as the monopulse angle offsets of consecutive echoes, are determined. The squared amplitudes lead to the radar cross section (RCS) of the objects.

There is a problem of side lobe detections using radars for BPEs. The identification is difficult because, in many cases, the visual screening does not give any consistent clues that would not be plausible for main lobe detections also. Consider TIRA's L-band far field pattern in Figure A-2.

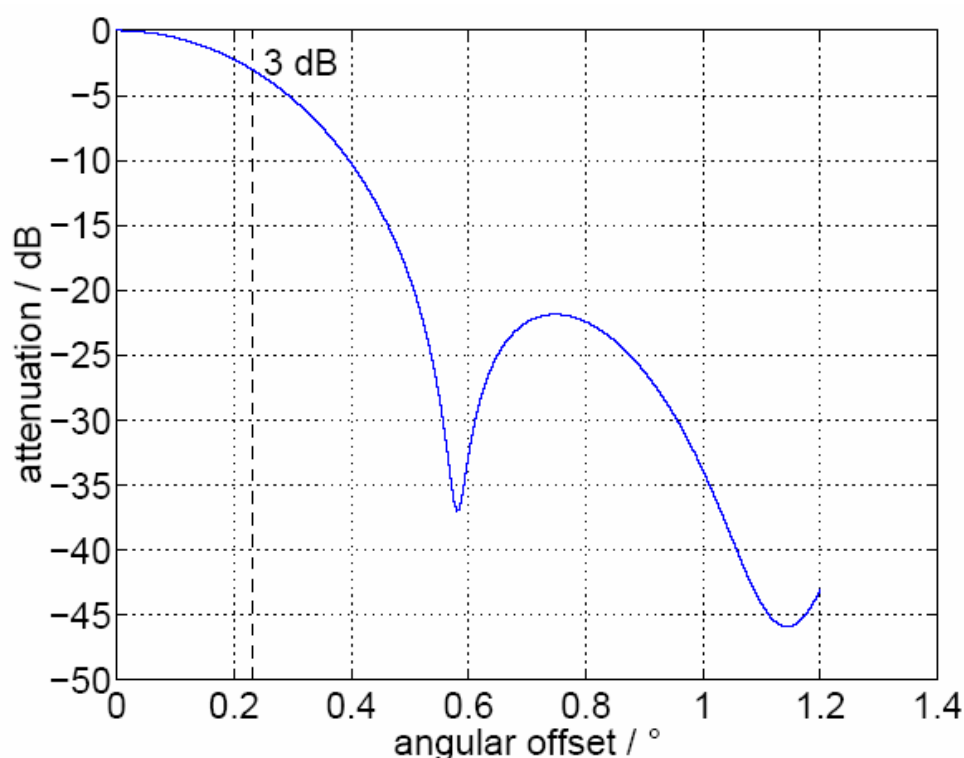


Figure A-2. TIRA's L-band far field radiation pattern (one-way).

The 3-decibel (dB) beam width of the 34-m parabolic antenna at L-band frequency is 0.5° ; the corresponding angular offset is half of this value, namely 0.25° . The first null of the antenna radiation pattern appears at an angular offset of 0.6° , and the maximum of the first side lobe at 0.74° . The maximum of the first side lobe is about 22 dB below the main beam (one-way pattern). For reliable monopulse angle measurements the angular offset must be $<0.35^\circ$. Side lobe detections might happen when a larger space object (which is most likely catalogued) passes outside the main beam but crossing, e.g., the first side lobe. It would appear as a small object passing the main beam. However, the maximum signal-to-noise ratio (SNR) is not generated at closest point of approach (CPA) but when the object crosses, e.g., the maximum of TIRA's sidelobe several seconds before or after the time of closest approach (TCA), which

is computed for the cross-check. Another hint for side lobe detections is look angle differences of more than 0.6° .

RCS is converted to a characteristic length using the NASA Size Estimation Model (SEM), which is described in Appendix E.

A.3 Detection List

The output format for the detection list was slightly modified, as a unique Doppler inclination cannot be provided for each detected object:

- col **DOPINC** was replaced by cols **DOPINC1** and **DOPINC2**, where **DOPINC1** is the selected solution from the beam crossing direction,
- If a non-valid, i.e. complex, solution is provided for the Doppler inclination due to high range rates **DOPINC1** and **DOPINC2** contain the dummy value **999.00**,
- col **DEL-I** was replaced by cols **DEL-I1** and **DEL-I2**.

Table A-3 – TIRA Detection Results of S-BPE-115 on DOY 15342

D-EPOCH [sec]	D-RANGE [km]	D-RRATE [km/s]	RCS [dBsm]	ALTITUDE [km]	DOPINC1 [deg]	DOPINC2 [deg]	DIA [m]	OFFSET [deg]	RMSERR [deg]	C-EPOCH [sec]	OBJ [number]	C-RANGE [km]	C-RRATE [km/s]	T-INC [deg]	T-ECC [deg]	DEL-T [sec]	DEL-R [km]	DEL-RR [m/s]	DEL-I1 [deg]	DEL-I2 [deg]
15342.50303	1896.89	4.2015	-20.04	584.923	121.26	43.56	0.077448	0.050237	0.1702											
15342.50424	1564.17	0.8649	-26.63	447.881	38.14	137.96	0.045304	0.014534	0.2521											
15342.50822	2309.796	5.99424	-18.19	772.907	99.27	62.28	0.114111	0.010255	0.1721											
15342.51209	1888.856	7.25392	-12.76	581.458	999	999	0.24496	0.069191	0.0834											
15342.51277	1521.539	6.54325	-24.59	431.299	65.13	96.47	0.049269	0.026485	0.1399											
15342.51672	2184.434	-6.76981	-21.57	713.817	999	999	0.06125	0.100011	0.2062	15342.51671	26306	2184.488	-6.76211	98.53	0.01	-0.39	0.05	7.71	900.47	900.47
15342.51708	2097.103	-0.35432	-23.95	673.679	144.94	36.4	0.050898	0.031983	0.2184											
15342.51926	2332.957	-6.6204	9.73	784.011	999	999	3.458063	0.309126	0.0325	15342.51926	25940	2331.879	-6.6185	98.43	0.0004	-0.13	-1.08	1.89	900.57	900.57
15342.52134	2302.745	0.90601	-20.99	769.538	32.68	142.43	0.065693	0.162744	0.3155											
15342.52702	2512.464	5.76196	-19.38	872.006	60.01	101.62	0.089995	0.001014	0.2195											
15342.53086	1997.267	-6.84339	-20.04	628.846	999	999	0.077463	0.06706	0.1694											
15342.53185	1676.97	5.26137	-24.37	492.841	112.06	51.15	0.049797	0.003087	0.1359											
15342.53192	2737.917	-2.06373	-18.04	987.238	40.77	149.47	0.117387	0.020608	0.2319											
15342.53193	2727.003	6.63565	-17.9	981.543	999	999	0.120469	0.015629	0.1894											
15342.53193	2816.97	-4.87108	-18.99	1028.845	132.29	65.18	0.09738	0.062919	0.2243											
15342.56144	2843.67	0	-18.83	1043.035	30.55	149.01	0.100554	0.09341	0.4148											
15342.5641	1773.72	0	-25.61	532.639	141.86	37.8	0.047099	0.048339	0.3062											
15342.5658	1911.57	7.36534	-25.76	591.274	999	999	0.04681	0.081558	0.1105											
15342.56614	2736.699	0.00112	-15.28	986.602	31.22	148.34	0.177995	0.011044	0.2463											
15342.56858	2846.37	0.00157	-15.34	1044.474	30.53	149.02	0.176614	0.042845	0.1673											
15342.56914	1646.282	-0.00616	-26.12	480.455	38.76	140.95	0.046168	0.032536	0.1686											
15342.57201	2757.591	-0.03074	-16.28	997.536	148.57	31.17	0.155657	0.077648	0.2559											
15342.57447	2787.409	1.11846	-3.92	1013.215	143.99	29.34	0.718333	0.251029	0.1515	15342.57447	2328	2787.561	1.11575	144.23	0.0009	-0.05	0.15	-2.71	0.24	114.89
15342.59531	2577.064	5.93113	-14.24	904.497	97.49	63.93	0.203099	0.006399	0.181											
15342.60044	2319.67	6.42358	-18.9	777.634	86.66	74.48	0.099279	0.025414	0.162											

D-EPOCH [sec]	D-RANGE [km]	D-RRATE [km/s]	RCS [dBsm]	ALTITUDE [km]	DOPINC1 [deg]	DOPINC2 [deg]	DIA [m]	OFFSET [deg]	RMSERR [deg]	C-EPOCH [sec]	OBJ [number]	C-RANGE [km]	C-RRATE [km/s]	T-INC [deg]	T-ECC [deg]	DEL-T [sec]	DEL-R [km]	DEL-RR [m/s]	DEL-I1 [deg]	DEL-I2 [deg]
15342.60072	2339.299	6.425	6.36	787.062	85.77	75.36	2.3467	0.183794	0.0193	15342.60072	25431	2336.96	6.42202	86.4	0.0002	-0.37	-2.34	-2.98	0.63	11.04
15342.60098	2277.308	-6.6687	-17.7	757.429	999	999	0.124812	0.018678	0.1407	15342.60098	31759	2275.234	-6.65967	98.59	0.0004	0.09	-2.07	9.03	900.41	900.41
15342.60585	2395.145	-5.70461	6.72	814.11	74.08	123.96	2.446729	0.206337	0.038	15342.60585	20433	2392.726	-5.70192	74.04	0.0042	0.21	-2.42	2.69	-0.04	-49.92
15342.60721	1858.594	7.43527	-23.16	568.475	999	999	0.053436	0.0377	0.1494											
15342.60848	2497.523	5.90396	-16.05	864.553	99.04	62.46	0.160702	0.063571	0.1413											
15342.60979	2242.23	6.17536	-23.57	740.846	65.15	96.28	0.052029	0.008265	0.1713											
15342.61193	2427.868	-6.50519	-12.18	830.113	105.45	93.41	0.263621	0.145889	0.1058	15342.61192	35275	2426.408	-6.50157	98.69	0.014	-0.17	-1.46	3.62	-6.76	5.28
15342.61479	2003.492	-6.41212	5.87	631.608	82.78	115.7	2.219228	0.057903	0.02	15342.61479	19574	2002.992	-6.40707	82.53	0.0023	0.04	-0.5	5.06	-0.25	-33.17
15342.61658	2701.499	-6.02249	20.67	968.278	82.82	115.8	12.189191	0.410133	0.0689	15342.61658	17291	2699.739	-6.01809	82.47	0.0012	0.02	-1.76	4.39	-0.35	-33.33
15342.61668	2220.252	-2.37547	-20.95	730.525	145.77	44.55	0.065998	0.016734	0.1728											
15342.61717	2127.288	0.06991	15.97	687.456	35.12	144.17	7.096771	0.071637	0.0134	15342.61717	3598	2126.371	0.07111	34.99	0.0049	0.19	-0.92	1.2	-0.13	109.18
15342.64213	2350.441	6.41059	-9.8	792.431	74.9	86.24	0.359752	0.112848	0.0768	15342.64213	34045	2350.041	6.4074	74.04	0.0026	-0.23	-0.4	-3.18	-0.86	-12.2
15342.64361	1647.838	6.46274	-24.62	481.08	96.84	64.75	0.049182	0.021592	0.1636											
15342.64763	2473.821	6.24427	7.28	852.777	70.84	90.37	2.608105	0.307369	0.0471	15342.64764	22566	2481.483	6.24561	71.01	0.0013	1.11	7.66	1.34	0.17	-19.36
15342.65213	1497.898	-3.46195	-21.82	422.201	53.58	138.68	0.059647	0.03008	0.1531											
15342.66027	1963.938	-5.88387	-20.91	614.132	74.11	123.72	0.066325	0.051376	0.165											
15342.66058	2255.037	6.47439	-5.47	746.885	86.1	75.03	0.600978	0.023497	0.0697	15342.66058	34079	2253.573	6.47438	86.39	0.001	0.02	-1.46	-0.02	0.29	11.36
15342.66116	1973.229	-6.87185	-11.76	618.221	999	999	0.27789	0.025471	0.0504	15342.66116	38318	1971.237	-6.86769	97.45	0.0142	0.02	-1.99	4.17	901.55	901.55
15342.66179	2721.859	-0.01649	-18.39	978.862	31.36	148.3	0.109755	0.058171	0.2297											
15342.66284	2421.078	5.98273	1.02	826.783	98.29	63.2	1.268349	0.229769	0.0438	15342.66284	3522	2420.303	5.9788	98.3	0.0029	-0.27	-0.77	-3.93	0.01	35.1
15342.66569	1674.333	-6.29781	10.46	491.772	119.82	78.24	3.763317	0.370073	0.2051											
15342.66652	2643.276	-6.55037	8.25	938.241	999	999	2.916233	0.154978	0.0188	15342.66652	28367	2642.583	-6.54455	98.17	0.0352	0.12	-0.69	5.82	900.83	900.83
15342.67153	2139.832	-5.81875	-17.3	693.211	74.16	123.77	0.13325	0.08585	0.1206	15342.67153	18501	2138.44	-5.82112	74.06	0.001	0.1	-1.39	-2.37	-0.1	-49.71
15342.6771	2073.049	5.53456	-10	662.774	54.38	107.93	0.350402	0.127259	0.1084											
15342.67791	2645.484	6.29016	-15.25	939.373	999	999	0.178505	0.054307	0.178	15342.67791	13018	2627.118	6.29327	82.68	0.0052	0.45	18.37	3.11	916.32	916.32
15342.67845	1881.664	5.2996	-23.85	578.363	51.59	111.28	0.05117	0.093241	0.1928											

D-EPOCH [sec]	D-RANGE [km]	D-RRATE [km/s]	RCS [dBsm]	ALTITUDE [km]	DOPINC1 [deg]	DOPINC2 [deg]	DIA [m]	OFFSET [deg]	RMSERR [deg]	C-EPOCH [sec]	OBJ [number]	C-RANGE [km]	C-RRATE [km/s]	T-INC [deg]	T-ECC [deg]	DEL-T [sec]	DEL-R [km]	DEL-RR [m/s]	DEL-I1 [deg]	DEL-I2 [deg]
15342.68011	2074.17	0.02045	-21.62	663.28	35.61	143.93	0.060905	0.065289	0.1688											
15342.68018	2366.437	0.00713	-20.63	800.164	145.95	33.63	0.069226	0.003606	0.1814											
15342.68208	2458.2	-6.54343	-6.03	845.048	999	999	0.563319	0.26902	0.2174											
15342.68264	2254.093	0.74833	-17.11	746.439	33.14	142.78	0.137384	0.00552	0.1274											
15342.68266	2463.651	-6.53286	-15.42	847.742	999	999	0.174758	0.139161	0.1833	15342.68265	40415	2466.277	-6.52888	98.76	0.0007	-1.36	2.63	3.99	900.24	900.24
15342.68276	1981.013	-5.8864	-16.77	621.654	74.23	123.62	0.144847	0.106626	0.1368	15342.68276	14866	1980.952	-5.8728	74.04	0.0003	0.31	-0.06	13.59	-0.19	-49.58
15342.68345	2277.794	6.44968	2.35	757.66	74.44	86.71	1.478327	0.312128	0.0876	15342.68345	10962	2277.529	6.44435	74.08	0.0026	0.01	-0.26	-5.32	-0.36	-12.63
15342.689	2517.651	6.35724	-16.61	874.599	999	999	0.148397	0.03368	0.162	15342.68899	36356	2513.291	6.34858	82.52	0.0016	-0.47	-4.36	-8.66	916.48	916.48
15342.68994	1799.875	-6.51521	25.69	543.592	115.69	82.74	21.731209	0.271354	0.2049	15342.68994	17295	1800.401	-6.51396	82.51	0.0002	0.06	0.53	1.25	-33.18	-0.23
15342.69016	2538.734	0.02685	-17.4	885.167	32.43	147.01	0.13104	0.026587	0.2048											
15342.69021	2432.853	-6.55845	-7.95	832.561	999	999	0.451957	0.114232	0.0853	15342.69021	28055	2429.358	-6.55643	98.56	0.0002	0.18	-3.5	2.02	900.44	900.44
15342.69173	2496.787	-6.52949	-11.54	864.186	999	999	0.285913	0.000355	0.0775	15342.69174	29776	2494.068	-6.52528	99.12	0.0025	0.26	-2.72	4.22	899.88	899.88
15342.69191	2036.97	-0.01952	-20.31	646.539	35.96	143.78	0.073253	0.000449	0.1758											
15342.69302	2290.465	-6.65323	-12.01	763.683	999	999	0.269153	0.118273	0.0832	15342.69302	21576	2288.013	-6.65042	98.75	0.0004	-0.01	-2.45	2.81	900.25	900.25
15342.69912	2459.108	-6.5144	-17.18	845.496	103.27	95.61	0.135946	0.063128	0.1531											
15342.70149	2419.991	-6.57187	-12.15	826.251	999	999	0.264511	0.093634	0.1139	15342.70149	27846	2419.207	-6.56621	98.68	0.001	0.11	-0.78	5.66	900.32	900.32
15342.70209	1706.895	2.09633	-26.08	505.03	37.33	133.83	0.046234	0.064932	0.1986											
15342.70208	2451.72	1.83847	-15.26	841.849	138.59	32.09	0.178311	0.079543	0.1549											
15342.70363	2725.966	1.43828	1.45	981.002	29.88	142	1.333592	0.075073	0.0317	15342.70364	5126	2725.092	1.44174	29.68	0.0012	0.32	-0.87	3.45	-0.2	112.32
15342.70564	2845.987	-4.91269	-12.33	1044.27	65.82	131.75	0.258479	0.099365	0.1357											
15342.70613	2412.151	5.94462	-13.43	822.413	99.17	62.36	0.224866	0.172087	0.1674	15342.70613	35378	2409.095	5.94509	97.74	0.0176	-0.32	-3.06	0.46	-1.43	35.38
15342.71212	1976.97	4.94648	-23.19	619.87	48.61	114.69	0.053311	0.050343	0.1243											
15342.71212	1906.19	-5.31883	-25.97	588.943	129.55	67.4	0.046436	0.001252	0.1969											
15342.71308	2306.167	6.43581	-15.32	771.172	86.45	74.69	0.176893	0.046809	0.1625	15342.71308	34522	2304.056	6.43531	86.37	0.0058	0.01	-2.11	-0.51	-0.08	11.68
15342.71463	2157.703	6.04459	-18.31	701.441	99.82	61.81	0.11156	0.000961	0.1729											
15342.71748	2288.447	-6.63735	-8.68	762.723	102.06	96.84	0.414552	0.201352	0.1309	15342.71748	12200	2286.016	-6.63085	98.34	0.0112	0.14	-2.43	6.5	-3.72	1.5

D-EPOCH [sec]	D-RANGE [km]	D-RRATE [km/s]	RCS [dBsm]	ALTITUDE [km]	DOPINC1 [deg]	DOPINC2 [deg]	DIA [m]	OFFSET [deg]	RMSERR [deg]	C-EPOCH [sec]	OBJ [number]	C-RANGE [km]	C-RRATE [km/s]	T-INC [deg]	T-ECC [deg]	DEL-T [sec]	DEL-R [km]	DEL-RR [m/s]	DEL-I1 [deg]	DEL-I2 [deg]
15342.7201	1841.75	2.60731	-22.94	561.295	37.38	131.78	0.05422	0.035916	0.1378											
15342.72069	2096.683	6.31182	-22.94	673.488	95.03	66.37	0.054251	0.0279	0.1679											
15342.72343	2068.932	-6.79432	-12.08	660.914	999	999	0.267055	0.096455	0.1285	15342.72342	38270	2065.897	-6.78973	97.22	0.0151	-0.02	-3.04	4.59	901.78	901.78
15342.72362	2675.134	5.91939	4.86	954.634	64.96	96.41	1.973442	0.000637	0.085	15342.72361	7005	2668.993	5.91906	65.44	0.0064	-0.85	-6.14	-0.33	0.48	-30.97
15342.72513	1692.214	0.00874	-23.42	499.037	38.39	141.25	0.052527	0.000291	0.2138											
15342.73131	2720.286	6.22217	-2.82	978.043	999	999	0.815539	0.002909	0.0912	15342.7313	11803	2715.121	6.21699	82.94	0.0023	-0.57	-5.17	-5.19	916.06	916.06
15342.73503	1856.714	1.21351	-10.37	567.672	35.76	138.56	0.334106	0.008688	0.2405	15342.73503	20303	1855.517	1.21934	35.63	0.0119	0.4	-1.2	5.83	-0.13	102.93
15342.73765	2063.02	3.30226	-19.36	658.246	38.49	128.14	0.090353	0.061792	0.0636											
15342.74445	2672.434	6.21668	-0.49	953.241	76.13	84.99	1.066947	0.007712	0.2394											
15342.75102	2228.868	2.60751	0.83	734.565	35.17	133.17	1.241078	0.005158	0.085	15342.75102	3597	2228.968	2.60445	34.99	0.0005	0.17	0.1	-3.06	-0.18	-98.18
15342.75249	2043.431	6.59433	-18.58	649.436	86.94	74.21	0.105698	0.039288	0.1709											
15342.7541	1559.803	1.35339	-27.21	446.172	37.96	136.2	0.044367	0.036266	0.1551											
15342.7552	2333.625	6.6138	-17.86	784.332	999	999	0.121219	0.009221	0.1538											
15342.7561	2357.206	-6.63458	-16.78	795.698	999	999	0.144594	0.029337	0.1492											
15342.75863	2700.661	5.92112	-16.46	967.843	95.98	65.37	0.151648	0.017026	0.1571											
15342.75911	2372.175	-4.99209	-15.45	802.944	65.07	132.01	0.173969	0.002481	0.1148	15342.75911	39647	2369.979	-4.98549	65.01	0.0021	0.52	-2.2	6.59	-0.06	-67
15342.7611	1670.733	-7.04554	-4.07	490.315	999	999	0.706166	0.17183	0.1607	15342.7611	39026	1668.609	-7.03837	97.27	0.0044	0.26	-2.12	7.16	901.73	901.73
15342.76143	2222.418	6.53578	-14.26	731.539	82.24	78.86	0.202348	0.019076	0.0989	15342.76142	38030	2218.353	6.53465	86.37	0.009	-0.97	-4.06	-1.13	4.13	7.51
15342.76416	2096.67	2.16903	-19.95	673.482	34.87	135.26	0.079008	0.061561	0.1273											
15342.7642	2397.662	-0.00113	-18.63	815.337	33.44	146.17	0.104718	0.010026	0.2174											
15342.76441	2711.806	-6.02558	8.24	973.631	83.04	115.59	2.914458	0.003118	0.0728	15342.76442	11379	2708.755	-6.02087	82.94	0.002	0.22	-3.05	4.71	-0.1	-32.65
15342.76712	2663.393	-6.04184	-14.41	948.58	115.85	82.75	0.198587	0.015342	0.1603	15342.76713	13797	2658.795	-6.03702	82.84	0.0051	0.43	-4.6	4.82	-33.01	0.09
15342.77177	2433.877	6.11439	-9.91	833.064	66.27	95.08	0.35465	0.018783	0.1424	15342.77177	147	2433.917	6.11079	66.62	0.0061	-0.05	0.04	-3.6	0.35	-28.46
15342.77606	2402.528	-6.58787	-18.3	817.711	999	999	0.111753	0.0104	0.1472	15342.77606	37470	2402.103	-6.58459	98.87	0.003	0.27	-0.42	3.28	900.13	900.13
15342.77726	1744.783	-7.00208	-21.28	520.618	999	999	0.063285	0.027806	0.1638	15342.77725	35273	1746.719	-6.99166	97.63	0.0014	-0.03	1.94	10.42	901.37	901.37
15342.77938	2475.932	5.98167	-17.59	853.823	97.65	63.8	0.127012	0.019165	0.1907											

D-EPOCH [sec]	D-RANGE [km]	D-RRATE [km/s]	RCS [dBsm]	ALTITUDE [km]	DOPINC1 [deg]	DOPINC2 [deg]	DIA [m]	OFFSET [deg]	RMSERR [deg]	C-EPOCH [sec]	OBJ [number]	C-RANGE [km]	C-RRATE [km/s]	T-INC [deg]	T-ECC [deg]	DEL-T [sec]	DEL-R [km]	DEL-RR [m/s]	DEL-I1 [deg]	DEL-I2 [deg]
15342.78097	2480.275	6.23008	-9.81	855.977	90.74	70.47	0.359406	0.050653	0.1267	15342.78097	4154	2479.626	6.22748	70.07	0.0048	0.09	-0.65	-2.6	-20.67	-0.4
15342.78434	1844.85	4.12372	-9.33	562.614	121.81	43.26	0.382098	0.029321	0.1274											
15342.78879	2649.009	5.91745	-17.14	941.183	64.55	96.83	0.136815	0.021622	0.1745	15342.78877	27910	2642.976	5.92363	65.05	0.0062	-1.75	-6.03	6.17	0.5	-31.78
15342.789	2429.277	5.19203	-3.89	830.805	51.72	110.64	0.72119	0.002054	0.062	15342.789	506	2428.984	5.18744	52	0.0278	-0.03	-0.29	-4.59	0.28	-58.64
15342.79036	2297.626	6.01667	-15.66	767.096	98.96	62.58	0.169439	0.005648	0.1635											
15342.79154	1940.647	0.86197	-17.8	603.926	140.42	35.31	0.122605	0.076045	0.1909											
15342.79216	1983.1	6.62843	-18.52	622.576	74.03	87.13	0.107004	0.116761	0.1709	15342.79216	6063	1986.297	6.62821	74.04	0.0006	0.05	3.2	-0.22	0.01	-13.09
15342.80003	1595.551	6.82571	-18.95	460.232	72.59	88.63	0.098266	0.012664	0.1015											
15342.80034	1781.584	6.89507	-21.37	535.924	999	999	0.062602	0.005955	0.1572											
15342.80176	2248.671	-5.77383	-16.79	743.881	74.16	123.82	0.144343	0.006236	0.1268	15342.80177	14812	2246.624	-5.7721	74.06	0.0017	0.19	-2.05	1.73	-0.1	-49.76
15342.80307	1889.102	-0.01971	-24.31	581.564	37.01	142.74	0.049933	0.042547	0.2557											
15342.80391	1904.756	0.04775	-22.4	588.323	36.75	142.68	0.056553	0.103538	0.2575											
15342.80911	1621.358	3.5948	-23.09	470.48	41.67	125.08	0.05366	0.055749	0.3248											
15342.81127	1894.488	0.01473	-21.66	583.886	142.69	36.9	0.060681	0.050386	0.219											
15342.81292	2055.99	0.8844	-19.9	655.079	34.45	141.05	0.080035	0.019316	0.0902											
15342.81417	1826.55	6.25909	-23.5	554.845	98.93	62.73	0.052254	0.019176	0.1576											
15342.81451	1888.161	0.85686	-20.33	581.159	140.11	35.7	0.073025	0.028119	0.1894											
15342.81681	2365.334	6.00066	-15.91	799.63	98.55	62.96	0.163701	0.014061	0.1614	15342.81681	31562	2365.213	5.99578	99.28	0.0069	0.09	-0.12	-4.88	0.73	36.32
15342.81928	2845.795	2.6812	-7.03	1044.168	32.56	134.18	0.502186	0.005863	0.2036	15342.81929	204	2868.413	2.69026	32.44	0.0099	0.91	22.62	9.07	-0.12	101.74
15342.81932	2300.272	-6.6005	-13.92	768.358	104.65	94.22	0.211437	0.008152	0.1631	15342.81929	40265	2311.533	-6.59471	97.9	0.0197	-1.99	11.26	5.79	-6.75	3.68
15342.82013	1543.447	-6.06312	-24.41	439.792	74.58	123.03	0.049686	0.007439	0.1401											
15342.8246	2413.141	-6.52864	9.91	822.897	104.55	94.32	3.532673	0.202408	0.2174											
15342.82496	1968.863	-5.71429	-20.55	616.299	71.99	125.62	0.070152	0.000817	0.1681											
15342.83007	2337.578	-0.02282	-20.19	786.233	145.84	33.9	0.075122	0.001658	0.1932											
15342.835	2280.038	-5.1672	-13.87	758.725	66.73	130.49	0.212807	0.072344	0.2004	15342.835	18765	2282.42	-5.16207	66.58	0.0011	-0.09	2.38	5.13	-0.15	-63.91
15342.83631	1879.43	6.74824	8.85	577.403	77.72	83.39	3.124744	0.007235	0.1053	15342.83632	10095	1880.381	6.74804	75.83	0.0038	0.05	0.95	-0.2	-1.89	-7.56

D-EPOCH [sec]	D-RANGE [km]	D-RRATE [km/s]	RCS [dBsm]	ALTITUDE [km]	DOPINC1 [deg]	DOPINC2 [deg]	DIA [m]	OFFSET [deg]	RMSERR [deg]	C-EPOCH [sec]	OBJ [number]	C-RANGE [km]	C-RRATE [km/s]	T-INC [deg]	T-ECC [deg]	DEL-T [sec]	DEL-R [km]	DEL-RR [m/s]	DEL-I1 [deg]	DEL-I2 [deg]
15342.83865	2246.015	0.02282	-18.75	742.629	145.1	34.41	0.10217	0.058308	0.1514											
15342.83939	1707.59	6.81606	-26.82	505.315	74.98	86.18	0.044987	0.012843	0.2239											
15342.83954	1797.831	6.81368	-24.39	542.733	999	999	0.049726	0.036286	0.4953	15342.83954	17191	1795.801	6.81582	82.47	0.0005	0.19	-2.03	2.14	916.53	916.53
15342.83965	2290.93	-3.88991	-18.76	763.905	54.77	140.14	0.10195	0.006082	0.0978											
15342.84083	1737.041	0.87288	-25.99	517.419	139.08	36.82	0.046401	0.02795	0.1754											
15342.85117	1992.339	-6.78594	-21.76	626.662	105.31	93.55	0.060018	0.00002	0.146											
15342.85272	2751.163	-5.27569	-3.29	994.167	70.13	127.77	0.773	0.002927	0.0839											
15342.8547	2013.919	0.02012	-23.87	636.245	143.52	36.03	0.051122	0.052423	0.2319											
15342.85682	2000.736	-6.84542	2.32	630.384	999	999	1.474289	0.060481	0.0957	15342.85682	33320	1997.934	-6.84262	98.01	0.0027	-0.04	-2.8	2.8	900.99	900.99
15342.85882	2020.34	-5.71424	-5.13	639.106	72.2	125.46	0.624939	0.008204	0.0579											
15342.86432	2324.514	-5.81781	-14.5	779.956	75.3	122.81	0.196475	0.011148	0.1589	15342.86432	33823	2322.61	-5.81027	73.81	0.022	0.43	-1.9	7.54	-1.49	-49
15342.8669	2537.006	-0.00848	-18.14	884.299	32.53	147.1	0.115196	0.016589	0.178											
15342.86695	2435.628	-6.55765	5.15	833.925	999	999	2.04057	0.374957	0.1432	15342.86694	33396	2434.853	-6.5548	98.75	0.0001	-0.23	-0.78	2.85	900.25	900.25
15342.86747	2745.485	-6.34486	-15.17	991.195	999	999	0.180297	0.091662	0.1721	15342.86748	41052	2737.335	-6.34633	99.01	0.0172	0.79	-8.15	-1.46	899.99	899.99
15342.86835	2185.778	-6.75601	-19.9	714.441	999	999	0.079945	0.050262	0.1781	15342.86835	29878	2184.897	-6.75522	97.01	0.0128	0.25	-0.88	0.78	901.99	901.99
15342.86877	2386.2	-6.60411	-17.68	809.755	999	999	0.125088	0.017759	0.1529											
15342.86892	1772.899	6.05471	-23.54	532.297	59.45	102.52	0.052118	0.075312	0.1226											
15342.86907	2392.193	-6.59413	-18.4	812.672	999	999	0.109559	0.017526	0.162											
15342.86917	2442.492	-6.56723	-10.47	837.302	999	999	0.32977	0.002752	0.0882											
15342.86933	2406.683	-6.59252	-17.58	819.74	999	999	0.127213	0.012817	0.1463											
15342.87007	2095.822	-6.77793	4.34	673.096	999	999	1.860274	0.001853	0.0852	15342.87007	26384	2094.747	-6.77515	98.09	0.0015	-0.14	-1.08	2.78	900.91	900.91
15342.87045	2216.676	-6.75492	-19.2	728.85	999	999	0.09336	0.051214	0.1446											
15342.87271	2457.978	6.25519	14.79	844.938	70.88	90.33	6.19049	0.346547	0.17	15342.87272	20625	2461.038	6.25228	71	0.0016	0.41	3.06	-2.91	0.12	-19.33
15342.87489	1713.572	-7.07617	-22.26	507.765	999	999	0.057259	0.020665	0.1583											
15342.87852	2468.135	6.32365	-16.72	849.961	86.88	74.26	0.145804	0.012795	0.1666											
15342.88042	2758.937	-0.00436	-18.89	998.241	31.09	148.5	0.099385	0.071196	0.2238											

D-EPOCH [sec]	D-RANGE [km]	D-RRATE [km/s]	RCS [dBsm]	ALTITUDE [km]	DOPINC1 [deg]	DOPINC2 [deg]	DIA [m]	OFFSET [deg]	RMSERR [deg]	C-EPOCH [sec]	OBJ [number]	C-RANGE [km]	C-RRATE [km/s]	T-INC [deg]	T-ECC [deg]	DEL-T [sec]	DEL-R [km]	DEL-RR [m/s]	DEL-I1 [deg]	DEL-I2 [deg]
15342.88378	1989.799	-6.84674	7.23	625.538	999	999	2.593802	0.083636	0.0974	15342.88379	28649	1987.052	-6.84492	97.92	0.0003	0.12	-2.75	1.82	901.08	901.08
15342.88411	2505.209	-0.02474	-16.89	868.384	146.94	32.78	0.142157	0.009365	0.2466											
15342.88411	2491.957	-7.15522	-22.75	861.782	999	999	0.054977	0.016451	0.3012											
15342.8852	2420.337	-6.58005	-16.16	826.42	999	999	0.158236	0.065709	0.1684	15342.88519	38818	2423.808	-6.57387	98.64	0.0098	-0.48	3.47	6.18	900.36	900.36
15342.88734	2085.12	0.88522	-21.22	668.238	141.23	34.24	0.063766	0.069222	0.124											
15342.88862	1918.123	-0.01508	-22.73	594.117	36.79	142.93	0.055079	0.012267	0.2202											
15342.88922	2477.835	6.26279	-19.14	854.767	71.66	89.53	0.094503	0.02684	0.1768											
15342.88978	2284.545	1.87228	-9.11	760.867	137.7	33.19	0.392716	0.02191	0.0474											
15342.89374	2274.37	6.24865	-12.52	756.035	67.29	94.04	0.25253	0.043219	0.1399	15342.89374	260	2275.826	6.25173	66.77	0.0046	-0.03	1.46	3.09	-0.52	-27.27
15342.89574	2088.607	-6.29882	-17.82	669.819	81.44	116.98	0.122092	0.03956	0.1515	15342.89574	36902	2087.61	-6.28969	81.17	0.0007	-0.14	-1	9.13	-0.27	-35.81
15342.89907	2345.038	6.44519	-17.69	789.826	77.38	83.73	0.125044	0.005884	0.155											
15342.89975	1497.011	-6.20712	4.53	421.861	76.16	121.6	1.901362	0.003078	0.0629											
15342.90544	2845.695	-5.03952	-16.02	1044.115	67.44	130.28	0.161237	0.010026	0.1514											
15342.90591	2150.797	-6.92538	-20.62	698.256	999	999	0.069361	0.002111	0.1514											
15342.90689	2040.42	0.00516	-20.48	648.085	35.88	143.74	0.070978	0.007385	0.2234											
15342.90742	2392.847	-6.58711	-19.18	812.991	999	999	0.093833	0.041409	0.1431											
15342.91235	2471.384	6.19656	-17.03	851.569	92.09	69.16	0.139215	0.006417	0.1714											
15342.91459	2539.208	-6.15296	-18.47	885.404	83.68	114.95	0.107973	0.06467	0.1853	15342.91459	17633	2541.891	-6.14681	83.07	0.0184	-0.13	2.68	6.15	-0.61	-31.88
15342.91487	1907.904	3.96622	-24.67	589.686	123.08	42.22	0.049068	0.033967	0.1715											
15342.91984	2785.415	5.53506	-15.82	1012.164	58.48	103.16	0.165786	0.038291	0.1695											
15342.91984	2677.556	7.52516	-20.39	955.884	999	999	0.072109	0.053059	0.1813											
15342.92269	1867.592	-0.8624	-22.75	572.324	39.52	144.02	0.05498	0.06446	0.1654											
15342.92479	1497.303	6.15784	-26.29	421.973	59.56	102.54	0.045866	0.011172	0.1408											
15342.92622	2583.259	-6.45813	-12.7	907.635	999	999	0.246881	0.212053	0.1781	15342.92623	30023	2580.153	-6.45254	99.06	0.0045	0.26	-3.11	5.6	899.94	899.94
15342.92624	1766.98	-0.00713	-24.79	529.83	141.83	37.87	0.048796	0.046323	0.2245											
15342.92817	1716.052	-7.05875	-21.2	508.782	999	999	0.063933	0.118875	0.173											

D-EPOCH [sec]	D-RANGE [km]	D-RRATE [km/s]	RCS [dBsm]	ALTITUDE [km]	DOPINC1 [deg]	DOPINC2 [deg]	DIA [m]	OFFSET [deg]	RMSERR [deg]	C-EPOCH [sec]	OBJ [number]	C-RANGE [km]	C-RRATE [km/s]	T-INC [deg]	T-ECC [deg]	DEL-T [sec]	DEL-R [km]	DEL-RR [m/s]	DEL-I1 [deg]	DEL-I2 [deg]
15342.92855	2153.427	6.15703	-18.84	699.469	97.71	63.8	0.100468	0.075651	0.1736											
15342.92973	2818.101	-0.02355	-16.26	1029.445	30.77	148.92	0.155972	0.028061	0.2302											
15342.92979	2580.68	0.0014	-19.95	906.328	147.36	32.22	0.079135	0.014913	0.2274											
15342.93477	2804.17	6.12415	-12.97	1022.067	75.67	85.45	0.238434	0.083842	0.2391	15342.93476	13507	2785.423	6.0988	65.76	0.0878	-1	18.75	25.35	-9.91	-19.69
15342.93864	1496.97	5.3299	-28.12	421.845	51.73	111.62	0.042997	0.015042	0.1791											
15342.94811	2219.481	6.41451	-12.71	730.163	89.96	71.26	0.246306	0.019393	0.1767											
15342.94818	1920.633	-0.00974	-25.72	595.207	142.94	36.76	0.04688	0.012439	0.2414											
15342.94825	2301.861	6.46191	-15.95	769.116	84.83	76.29	0.162934	0.054102	0.1348											
15342.94877	2388.457	6.01703	-7.96	810.853	97.94	63.53	0.451049	0.008668	0.0792	15342.94877	30358	2385.136	6.01628	98.79	0.0097	-0.34	-3.32	-0.75	0.85	35.26
15342.95008	2839.513	6.13206	-15.68	1040.822	999	999	0.168826	0.021759	0.1382											
15342.95053	2326.738	6.43003	-1.61	781.024	75.16	85.98	0.93711	0.282399	0.1864	15342.95053	25039	2321.194	6.42605	86.4	0.0002	-0.44	-5.54	-3.98	11.24	0.42
15342.95597	2808.57	5.05453	-19.04	1024.395	51.59	110.53	0.09652	0.006319	0.2911											
15342.95598	2813.027	0.00322	-19.05	1026.755	148.81	30.73	0.096237	0.022569	0.2365											
15342.95823	2070.57	3.92141	-14.5	661.653	41.49	123.61	0.196365	0.107928	0.0435											
15342.95835	1587.21	5.27986	-23.86	456.937	112	51.31	0.05115	0.008247	0.1439											
15342.95844	2275.695	-0.0023	-18.61	756.664	145.37	34.26	0.10507	0.025089	0.1792											
15342.96103	2722.476	0.55592	-18.01	979.183	30.16	146.27	0.117914	0.038255	0.4625											
15342.96103	2666.97	7.34279	-18.47	950.423	999	999	0.108092	0.049385	0.2154											
15342.96326	1614.47	1.54491	-28.32	467.737	135.77	37.57	0.042718	0.018699	0.2159											
15342.96356	2842.47	-0.02412	-14.59	1042.396	149.07	30.62	0.194141	0.094767	0.186											
15342.9646	2395.65	-6.65354	-22.05	814.356	999	999	0.058329	0.01299	0.1498	15342.9646	30436	2393.173	-6.64373	98.44	0.0139	0.62	-2.48	9.81	900.56	900.56
15342.96693	2733.532	0.88761	-13.09	984.949	144.86	29.75	0.234863	0.028862	0.153											
15342.96827	1915.17	-1.68613	-24.86	592.835	144.62	42.47	0.048637	0.054327	0.1456											
15342.96837	2168.681	2.49656	11.39	706.514	35.18	133.65	4.186397	0.002753	0.0334	15342.96838	6153	2167.648	2.49664	35.01	0.0007	0.33	-1.03	0.08	-0.17	-98.64
15342.9695	1571.67	-0.02511	-28.13	450.822	140.44	39.35	0.042988	0.033017	0.1966											
15342.97331	2416.41	-6.53621	-14.79	824.497	103.82	95.06	0.189162	0.024109	0.1228	15342.97332	31206	2409.841	-6.52907	98.83	0.0087	0.33	-6.57	7.14	-4.99	3.77

D-EPOCH [sec]	D-RANGE [km]	D-RRATE [km/s]	RCS [dBsm]	ALTITUDE [km]	DOPINC1 [deg]	DOPINC2 [deg]	DIA [m]	OFFSET [deg]	RMSERR [deg]	C-EPOCH [sec]	OBJ [number]	C-RANGE [km]	C-RRATE [km/s]	T-INC [deg]	T-ECC [deg]	DEL-T [sec]	DEL-R [km]	DEL-RR [m/s]	DEL-I1 [deg]	DEL-I2 [deg]
15342.97398	2481.33	3.70249	-18.79	856.501	125.64	39.18	0.101393	0.038897	0.619											
15342.97399	1596.57	6.70262	-25.55	460.635	69.07	92.28	0.047201	0.153536	0.0308											
15342.97401	2606.351	0.02268	-20.85	919.367	147.46	32	0.066948	0.050031	0.2451											
15342.98266	1847.841	-3.91539	-20.4	563.888	55.54	138.57	0.071957	0.007343	0.1379											
15342.98285	1996.164	-0.016	-21.94	628.357	143.48	36.24	0.058984	0.040969	0.2499											
15342.98614	1892.028	6.68102	-12.34	582.826	73.86	87.31	0.258279	0.102756	0.1384	15342.98613	35468	1890.89	6.67833	74.03	0.0037	-1.05	-1.14	-2.69	0.17	-13.28
15342.99201	2725.884	-6.14733	5.65	980.959	112.16	86.58	2.162793	0.001917	0.1212											
15342.99398	2455.97	-0.0159	-19.05	843.947	146.6	33.09	0.096288	0.027209	0.1443											
15342.99415	2795.366	2.39641	-8.27	1017.414	31.62	136.16	0.435688	0.015226	0.1056	15342.99416	700	2798.197	2.40199	30.48	0.0724	0.85	2.83	5.58	-1.14	105.68
15342.99453	1863.115	4.63742	-7.94	570.408	46.38	117.64	0.45222	0.004237	0.1064											
15342.99679	2845.494	3.95085	-12.11	1044.007	123.17	40.51	0.265922	0.077844	0.2887											
15343.00359	2278.918	6.02349	-18.22	758.193	99.03	62.52	0.113467	0.00837	0.1479											
15343.00531	1706.22	6.15076	-26.15	504.754	60.39	101.52	0.046111	0.024142	0.1859											
15343.00607	2569.709	6.0946	5.4	900.775	67.9	93.37	2.101221	0.003146	0.0975	15343.00607	116	2568.216	6.09236	66.81	0.0069	-0.08	-1.49	-2.24	-1.09	-26.56
15343.01186	2059.742	6.26582	-18.91	656.768	96.51	64.96	0.09901	0.005675	0.1435	15343.01186	33679	2060.961	6.26797	99.35	0.0342	-0.15	1.22	2.16	2.84	34.39
15343.01652	2692.416	5.83218	-16.36	963.57	98.23	63.2	0.153852	0.002546	0.1394	15343.01651	30933	2687.452	5.83014	99.08	0.0122	-0.32	-4.96	-2.04	0.85	35.88
15343.01806	1643.583	0.01761	-26.17	479.371	140.87	38.73	0.046069	0.023606	0.1672											
15343.02168	2393.189	3.21467	-8.32	813.157	129.41	36.77	0.432748	0.09501	0.2587											
15343.0228	2083.587	-6.78583	-12.76	667.543	999	999	0.245008	0.185045	0.151	15343.0228	33497	2084.977	-6.78062	98.2	0.0002	-0.15	1.39	5.21	-900.8	-900.8
15343.02288	1651.32	-0.00526	-26.44	482.481	38.72	140.98	0.045621	0.068351	0.1997											
15343.02603	2034.475	6.37606	-12.04	645.422	67.04	94.34	0.268249	0.022268	0.0749	15343.02603	18819	2030.986	6.3647	66.56	0.002	-0.34	-3.49	11.36	-0.48	-27.78
15343.02986	2028.603	6.14505	-20.37	642.795	99.19	62.44	0.072459	0.01444	0.1912											
15343.0302	2364.059	6.00598	-5.36	799.013	98.46	63.05	0.609005	0.003322	0.0801	15343.0302	20442	2363.92	6.00636	98.53	0.0012	-0.16	-0.14	0.38	0.07	35.48
15343.0326	2174.017	6.62197	0.78	708.985	999	999	1.234086	0.005384	0.083	15343.0326	22562	2171.175	6.62147	75.76	0.0165	-0.37	-2.84	-0.5	923.24	923.24
15343.03444	1735.564	5.90502	-20.27	516.809	104.74	57.45	0.07393	0.036521	0.1879											
15343.03899	2794.926	-5.96602	0.23	1017.181	82.78	115.85	1.158973	0.00043	0.0681	15343.03899	22207	2793.086	-5.96096	82.92	0.0032	0.08	-1.84	5.06	0.14	-32.93

D-EPOCH [sec]	D-RANGE [km]	D-RRATE [km/s]	RCS [dBsm]	ALTITUDE [km]	DOPINC1 [deg]	DOPINC2 [deg]	DIA [m]	OFFSET [deg]	RMSERR [deg]	C-EPOCH [sec]	OBJ [number]	C-RANGE [km]	C-RRATE [km/s]	T-INC [deg]	T-ECC [deg]	DEL-T [sec]	DEL-R [km]	DEL-RR [m/s]	DEL-I1 [deg]	DEL-I2 [deg]
15343.03992	2331.073	6.03914	-16.64	783.106	98.15	63.35	0.147668	0.002172	0.1675											
15343.04023	1910.023	6.06818	-23.11	590.603	101.43	60.39	0.053591	0.038783	0.171											
15343.04577	2297.405	6.4384	8.33	766.99	74.51	86.63	2.943305	0.000642	0.1021	15343.04576	20433	2291.072	6.43393	74.04	0.0042	-1.07	-6.33	-4.47	-0.47	-12.59
15343.04669	2262.288	-0.33068	4.51	750.312	35.23	146.05	1.895545	0.002409	0.0474	15343.04669	2144	2262.221	-0.32501	35.04	0.0008	0.13	-0.07	5.67	-0.19	111.01
15343.05944	2071.682	6.20049	-18.19	662.156	97.72	63.81	0.11399	0.000861	0.1616	15343.05944	31903	2068.798	6.19946	99.24	0.0163	-0.07	-2.88	-1.03	1.52	35.43
15343.05959	2399.322	5.46244	-3.61	816.147	54.85	107.21	0.744928	0.006028	0.0815											
15343.06443	2396.95	5.97689	-13.06	814.99	98.68	62.82	0.235825	0.002193	0.1069	15343.06445	25397	2401.225	5.98337	98.54	0.0002	1.39	4.27	6.48	-0.14	35.72
15343.0671	1997.939	-5.98781	-19.52	629.144	75.71	122.28	0.087106	0.005639	0.1519											
15343.06727	2793.72	6.07407	-17.49	1016.545	88.9	72.27	0.12912	0.058663	0.1725											
15343.06977	1658.67	6.12282	-15.49	485.441	59.79	102.2	0.173239	0.025165	0.3122											
15343.07179	2604.175	6.32178	-15.19	918.259	999	999	0.179999	0.00426	0.1531											
15343.07258	2358.114	-2.56291	-3.51	796.137	45.18	146.1	0.752933	0.000958	0.0636	15343.07258	25479	2354.761	-2.55554	45.01	0.0006	0.15	-3.35	7.37	-0.17	101.09
15343.07459	2323.061	-2.52795	-15.01	779.26	45.08	146	0.18413	0.002247	0.1696	15343.07459	25481	2318.365	-2.52299	45.01	0.0002	0.23	-4.7	4.96	-0.07	100.99
15343.08128	2533.754	6.09764	-15.19	882.666	93.92	67.37	0.180039	0.091423	0.2099											
15343.08152	1922.97	-0.00896	-27.52	596.223	36.74	142.95	0.043885	0.018975	0.1939											
15343.0816	2398.445	-0.003	-18.96	815.719	146.19	33.44	0.0981	0.013424	0.161											
15343.09128	2813.52	-0.0173	-14.33	1027.017	30.78	148.88	0.200754	0.01069	0.2374											
15343.09246	2845.519	6.08002	-13.1	1044.021	74.45	86.68	0.234431	0.019996	0.1828	15343.09247	12720	2854.382	6.06817	83.25	0.0116	0.74	8.86	11.86	8.8	-3.43
15343.09475	1908.074	-5.90382	-22.23	589.759	74.1	123.69	0.057387	0.002089	0.1934	15343.09475	35598	1909.096	-5.90182	73.9	0.0091	0.27	1.02	2.01	-0.2	-49.79
15343.0955	2183.157	0.04251	-20.79	713.224	34.8	144.62	0.067493	0.075952	0.179											
15343.09594	2207.57	6.42753	-22.71	724.593	71.46	89.74	0.055179	0.024957	0.1514	15343.09594	35661	2221.62	6.41959	74.02	0.0134	-0.52	14.05	-7.94	2.56	-15.72
15343.09765	2592.666	0.00621	-16.13	912.408	147.42	32.13	0.158942	0.005684	0.2083											
15343.09766	2670.384	6.76771	-18.44	952.183	999	999	0.108603	0.045448	0.2003											
15343.10273	1881.383	7.36678	-24.18	578.242	999	999	0.05027	0.04886	0.1515											
15343.10784	2489.295	2.66109	-5.53	860.458	34.03	133.57	0.596902	0.172188	0.0639											
15343.1103	2127.695	-6.50469	-16.23	687.642	86.47	112.2	0.15671	0.005253	0.1436	15343.11031	34104	2125.579	-6.49918	86.35	0.0012	0.63	-2.12	5.51	-0.12	-25.85

D-EPOCH [sec]	D-RANGE [km]	D-RRATE [km/s]	RCS [dBsm]	ALTITUDE [km]	DOPINC1 [deg]	DOPINC2 [deg]	DIA [m]	OFFSET [deg]	RMSERR [deg]	C-EPOCH [sec]	OBJ [number]	C-RANGE [km]	C-RRATE [km/s]	T-INC [deg]	T-ECC [deg]	DEL-T [sec]	DEL-R [km]	DEL-RR [m/s]	DEL-I1 [deg]	DEL-I2 [deg]
15343.11034	2662.081	5.8553	-15	947.905	63.33	98.1	0.184271	0.031134	0.1577											
15343.1126	2375.205	6.33383	-3.49	804.414	89.29	71.9	0.75536	0.004411	0.1009	15343.1126	23814	2374.818	6.32823	90.12	0.0024	-0.19	-0.39	-5.61	0.83	18.22
15343.11372	2077.086	6.17418	-21.39	664.599	98.18	63.38	0.062474	0.046344	0.1907	15343.11372	37885	2084.622	6.1788	98.34	0.0044	-0.1	7.54	4.62	0.16	34.96
15343.11394	2352.682	-0.02005	-16.78	793.513	33.79	145.93	0.144569	0.011328	0.1971											
15343.11669	2320.053	6.38857	-14.56	777.817	72.74	88.43	0.194808	0.114951	0.1767	15343.11669	35716	2317.323	6.38897	74	0.0095	-0.18	-2.73	0.41	1.26	-14.43
15343.12151	2846.368	0.54037	1.71	1044.473	29.37	147.02	1.373513	0.006911	0.0496											
15343.12786	2787.061	-5.9839	-9.79	1013.031	83.1	115.53	0.360324	0.034208	0.132	15343.12786	20804	2782.988	-5.97475	82.94	0.0037	0.61	-4.07	9.15	-0.16	-32.59
15343.12819	2846.215	0.00041	-15.09	1044.392	30.53	149.02	0.182176	0.005897	0.2398											
15343.12822	1853.624	6.62332	-21.15	566.353	70.85	90.4	0.064317	0.010092	0.1592											
15343.13072	2725.516	6.05227	-18.09	980.767	91.59	69.63	0.116303	0.04165	0.1609											
15343.13945	2314.825	6.04076	-12.02	775.313	98.3	63.21	0.269004	0.00218	0.1363	15343.13945	35274	2311.059	6.0402	98.94	0.017	-0.08	-3.77	-0.56	0.64	35.73
15343.14283	1497.204	-0.47487	5.19	421.935	40.94	140.71	2.050743	0.002453	0.041											
15343.14392	1971.353	-6.61142	-21.37	617.395	86.89	111.77	0.06263	0.010872	0.1573											
15343.14853	1840.132	5.63576	-25.84	560.607	54.8	107.64	0.04666	0.013165	0.4016											
15343.15064	2638.11	6.0588	-16.17	935.592	93.18	68.08	0.157951	0.059487	0.3661											
15343.15065	2331.39	-0.01211	-18.69	783.258	145.77	33.91	0.103506	0.036254	0.2063											
15343.15843	2504.458	-0.01842	-17.59	868.009	146.92	32.77	0.127005	0.013133	0.1893											
15343.16063	2000.737	6.1546	-24.31	630.385	99.27	62.37	0.049936	0.015621	0.1664											
15343.16779	2545.33	6.30493	4.06	888.482	84.6	76.52	1.801445	0.025152	0.081	15343.16779	6257	2544.922	6.3034	81.26	0.0056	0.02	-0.41	-1.53	-3.34	4.74
15343.17433	2516.624	5.90099	-15.37	874.085	98.88	62.61	0.175919	0.018337	0.1393	15343.17433	35231	2515.941	5.90038	99.02	0.0037	0.12	-0.68	-0.61	0.14	36.41
15343.17712	1872.032	6.7285	-20.06	574.227	75.75	85.39	0.077111	0.000375	0.1386											
15343.18076	1614.338	0.01099	-28.42	467.684	140.67	38.96	0.042573	0.015269	0.2099											
15343.1808	2183.58	6.17808	-21.41	713.42	96.94	64.53	0.062326	0.126781	0.1751											
15343.18185	2210.37	6.13316	-20.53	725.901	97.57	63.92	0.070324	0.013474	0.082											
15343.18186	2641.941	-6.04028	-19.92	937.556	116.16	82.42	0.079518	0.053246	0.1792											
15343.18291	2516.97	6.17287	-21.69	874.258	69.31	91.94	0.060452	0.026098	0.0761											

D-EPOCH [sec]	D-RANGE [km]	D-RRATE [km/s]	RCS [dBsm]	ALTITUDE [km]	DOPINC1 [deg]	DOPINC2 [deg]	DIA [m]	OFFSET [deg]	RMSERR [deg]	C-EPOCH [sec]	OBJ [number]	C-RANGE [km]	C-RRATE [km/s]	T-INC [deg]	T-ECC [deg]	DEL-T [sec]	DEL-R [km]	DEL-RR [m/s]	DEL-I1 [deg]	DEL-I2 [deg]
15343.18551	1590.158	4.98594	-27.96	458.1	114.67	49.14	0.04323	0.018567	0.1687											
15343.18604	2223.114	-5.77989	-16.71	731.866	74.1	123.87	0.146204	0.009592	0.1172											
15343.18619	1758.574	6.46148	-22.3	526.335	95.78	65.72	0.057028	0.017265	0.2081											
15343.18628	1820.893	6.50954	-22.63	552.452	94	67.4	0.055516	0.008187	0.1755											
15343.19086	2334.689	-5.73104	5.28	784.844	74.08	123.94	2.073318	0.002068	0.0719	15343.19086	11870	2331.394	-5.72536	74.05	0.0017	0.43	-3.29	5.67	-0.03	-49.89
15343.19709	1557.37	6.12427	-22.59	445.221	102.7	59.39	0.055683	0.078822	0.2226											
15343.19717	1645.746	-0.02439	-27.37	480.24	38.8	140.98	0.044118	0.004269	0.2252											
15343.19823	2693.161	-6.32082	-15.7	963.956	106.13	92.73	0.168548	0.003683	0.1633	15343.19824	31257	2693.243	-6.31529	98.67	0.0132	0.57	0.08	5.54	-7.46	5.94
15343.19993	2304.272	-5.75212	-15.23	770.267	74.19	123.82	0.179065	0.005323	0.1367	15343.19994	33948	2301.898	-5.75269	74.03	0.0024	0.09	-2.37	-0.58	-0.16	-49.79
15343.20497	2194.119	6.45926	-18.46	718.321	72.37	88.82	0.108321	0.041584	0.1719											
15343.20543	2550.817	5.90172	-13.53	891.244	98.47	63	0.221991	0.022149	0.1809	15343.20544	12222	2552.177	5.90069	98.75	0.0072	0.16	1.36	-1.03	0.28	35.75
15343.21091	2503.735	0.01056	-20.57	867.649	32.7	146.83	0.069827	0.048622	0.2622											
15343.21091	2016.17	5.56815	-19.19	637.247	107.76	54.57	0.093658	0.031016	0.0641											
15343.21424	1880.302	6.13615	-22.08	577.778	100.57	61.2	0.058207	0.033284	0.1979											
15343.21504	2282.27	-0.01633	-19.36	759.786	145.45	34.25	0.090358	0.011318	0.2552											
15343.22555	2542.479	-6.36172	-16.69	887.048	90.04	108.76	0.146519	0.0001	0.1418											
15343.22876	2217.706	-5.50366	-15.77	729.332	70.44	127.17	0.16697	0.007658	0.1278	15343.22877	4218	2210.366	-5.50306	70.1	0.0037	0.34	-7.34	0.6	-0.34	-57.07
15343.22997	2451.447	0.76311	-10.06	841.714	31.75	143.88	0.347985	0.009011	0.1857	15343.22997	25510	2448.862	0.77087	31.44	0.0329	0.46	-2.58	7.75	-0.31	112.44
15343.23432	2337.56	-0.0126	-18.07	786.225	145.81	33.87	0.116733	0.010397	0.2319											
15343.23433	2729.991	6.1686	-16.27	983.101	75.32	85.8	0.155761	0.042076	0.2205											
15343.23549	2069.866	5.79616	-9.18	661.335	104.45	57.54	0.389456	0.124131	0.3098											
15343.23727	2443.32	0.02156	-25.67	837.709	33.08	146.41	0.046983	0.027327	0.2619											
15343.23733	1809.017	6.35953	-3.04	547.439	97.27	64.3	0.795238	0.003713	0.1491	15343.23733	40902	1806.638	6.359	97.45	0.0015	0.07	-2.38	-0.52	0.18	33.15
15343.24004	1497.467	4.89068	-11.56	422.036	48.65	115.47	0.285272	0.001991	0.1762	15343.24003	25721	1473.109	4.8863	48.45	0.001	-0.36	24.36	-4.37	-0.2	-67.02
15343.24138	2144.073	7.5194	-16.23	695.161	999	999	0.156699	0.023055	0.1316											
15343.24601	2008.11	0.87902	-23.97	633.66	140.78	34.8	0.050835	0.041763	0.2348											

D-EPOCH [sec]	D-RANGE [km]	D-RRATE [km/s]	RCS [dBsm]	ALTITUDE [km]	DOPINC1 [deg]	DOPINC2 [deg]	DIA [m]	OFFSET [deg]	RMSERR [deg]	C-EPOCH [sec]	OBJ [number]	C-RANGE [km]	C-RRATE [km/s]	T-INC [deg]	T-ECC [deg]	DEL-T [sec]	DEL-R [km]	DEL-RR [m/s]	DEL-I1 [deg]	DEL-I2 [deg]
15343.24824	2572.727	5.87391	-18.53	902.302	98.8	62.68	0.106783	0.079533	0.1607	15343.24825	20322	2584.299	5.8777	98.98	0.0009	1	11.57	3.8	0.18	36.3
15343.24931	1567.727	7.07029	-25.32	449.275	999	999	0.047662	0.095962	0.1493											
15343.25085	2596.059	-6.12554	-8.25	914.132	83.82	114.81	0.436566	0.056077	0.1698	15343.25085	13478	2596.226	-6.11758	82.87	0.0097	0.04	0.17	7.96	-0.95	-31.94
15343.25829	2591.334	5.83995	-4.41	911.731	99.29	62.2	0.679349	0.002262	0.1582	15343.25829	4614	2587.398	5.83746	100.12	0.0082	-0.49	-3.94	-2.49	0.83	37.92
15343.26066	2096.395	-0.00886	-21.45	673.357	144.16	35.52	0.062079	0.06853	0.1522											
15343.26078	2117.516	6.11817	-21.63	682.984	98.84	62.74	0.060848	0.014991	0.186	15343.26077	40604	2110.707	6.11045	98.73	0.014	-0.49	-6.81	-7.71	-0.11	35.99
15343.26181	2694.045	0.91173	-19.01	964.414	144.55	30	0.096977	0.05806	0.0672											
15343.26231	2113.882	6.11773	-17.57	681.324	98.89	62.7	0.127564	0.010708	0.1625											
15343.26964	2097.237	-0.02361	-22.37	673.739	35.55	144.21	0.056702	0.009002	0.2051											
15343.26974	1980.49	5.25773	-22.45	621.423	51.33	111.48	0.056308	0.074965	0.1616											
15343.26982	2533.724	-4.97511	3.24	882.651	131.9	65.37	1.638816	0.000846	0.1276	15343.26982	3158	2532.014	-4.97073	65.33	0.0038	0.21	-1.71	4.37	-66.57	-0.04
15343.27117	2780.499	1.56133	-12.63	1009.574	141.52	29.67	0.248795	0.097889	0.1774											
15343.27175	1916.07	-0.05247	-21.07	593.226	143	36.89	0.064941	0.056451	0.2004											
15343.27183	1991.624	0.62011	0.49	626.346	141.6	35.17	1.194087	0.001099	0.1481	15343.27184	6155	1993.539	0.62597	35	0.0037	0.39	1.91	5.86	-106.6	-0.17
15343.27343	2324.338	6.03729	-19.49	779.872	98.26	63.24	0.087713	0.022098	0.1838											
15343.27408	2541.213	-6.12018	-13.66	886.412	82.93	115.67	0.218515	0.01619	0.1401											
15343.27527	1739.017	-1.09707	-6.04	518.234	143.25	41.17	0.562732	0.002764	0.1198											
15343.28064	2482.47	-6.59423	-18.14	857.067	999	999	0.115122	0.004466	0.1919	15343.28064	30920	2485.197	-6.59448	98.91	0.0152	-0.3	2.73	-0.25	900.09	900.09
15343.28476	2282.57	-6.69218	-21.5	759.928	999	999	0.061687	0.053774	0.1888	15343.28477	31562	2276.835	-6.6907	99.28	0.0069	0.16	-5.73	1.49	899.72	899.72
15343.28666	2071.083	-2.96002	-5.98	661.885	143.37	48.6	0.566667	0.002532	0.1168	15343.28666	33061	2066.841	-2.95455	48.45	0.0005	0.19	-4.24	5.47	-94.92	-0.15
15343.29028	1872.87	6.13449	-28.46	574.587	61.12	100.65	0.042509	0.017804	0.151											
15343.29037	2253.457	0.00453	-21.42	746.139	34.4	145.2	0.062254	0.063463	0.1865											
15343.29473	2693.47	2.20216	-9.5	964.116	31.5	137.22	0.373753	0.021027	0.0627											
15343.2956	1951.77	6.15408	-22.49	608.793	61.98	99.7	0.056131	0.053824	0.1077											
15343.29609	2006.37	6.25053	12.19	632.887	64.12	97.41	4.590216	0.00109	0.1608	15343.29609	32786	2002.275	6.24669	97.64	0.0011	-0.16	-4.09	-3.85	33.52	0.23
15343.29722	2297.244	-6.68131	-17.75	766.913	999	999	0.123598	0.006715	0.1564	15343.29722	37904	2297.509	-6.67885	98.3	0.0082	0.07	0.26	2.46	-900.7	-900.7

D-EPOCH [sec]	D-RANGE [km]	D-RRATE [km/s]	RCS [dBsm]	ALTITUDE [km]	DOPINC1 [deg]	DOPINC2 [deg]	DIA [m]	OFFSET [deg]	RMSERR [deg]	C-EPOCH [sec]	OBJ [number]	C-RANGE [km]	C-RRATE [km/s]	T-INC [deg]	T-ECC [deg]	DEL-T [sec]	DEL-R [km]	DEL-RR [m/s]	DEL-I1 [deg]	DEL-I2 [deg]
15343.29832	2436.613	5.98276	-16.7	834.409	98.1	63.37	0.146263	0.000597	0.1511	15343.29831	31691	2432.663	5.97609	99.1	0.0077	-0.84	-3.95	-6.67	1	35.73
15343.30243	2481.361	5.9314	-16.49	856.517	98.66	62.83	0.150935	0.017803	0.1579	15343.30243	30829	2483.398	5.92966	99	0.0038	-0.28	2.04	-1.74	0.34	36.17
15343.30391	1824.297	6.1285	-23.21	553.891	101.09	60.73	0.053245	0.03418	0.1628											
15343.30467	1827.87	4.30643	-17.29	555.404	44.35	120.37	0.133498	0.007187	0.0946											
15343.30864	2056.179	-0.0232	-20.56	655.164	143.92	35.83	0.069981	0.006054	0.1967											
15343.30954	2341.181	6.40694	2.1	787.968	86.82	74.33	1.437679	0.005398	0.1141	15343.30954	17304	2341.72	6.40503	74.06	0.003	-0.07	0.54	-1.91	-12.76	-0.27
15343.3117	2846.227	6.49192	-18.75	1044.398	999	999	0.102128	0.009979	0.2479											
15343.31679	1811.458	0.01087	-22.46	548.468	142.11	37.51	0.056261	0.066428	0.1498											
15343.31813	2465.659	5.93792	-15.11	848.735	98.7	62.79	0.181718	0.000651	0.1629	15343.31813	31423	2463.237	5.93869	98.71	0.0037	-0.18	-2.42	0.77	0.01	35.92
15343.32434	1970.287	0.52554	-24.25	616.925	141.77	35.45	0.050098	0.032403	0.2014											
15343.32456	1896.244	-6.90975	-21.59	584.644	999	999	0.061107	0.017666	0.1855											
15343.3253	2257.326	-5.87137	-17.72	747.966	122.46	75.65	0.124347	0.001483	0.1574	15343.32531	35445	2256.91	-5.85737	74.04	0.021	0.52	-0.42	14	-48.42	-1.61
15343.32646	2719.715	-6.04974	-15.84	977.746	83.75	114.9	0.165267	0.025825	0.2772	15343.32646	17067	2715.78	-6.04509	82.94	0.0036	-0.03	-3.94	4.65	-0.81	-31.96
15343.3279	2300.765	6.03925	3.19	768.593	63.03	98.48	1.629048	0.00008	0.1882	15343.3279	21610	2298.591	6.04021	98.68	0.0004	-0.09	-2.17	0.96	35.65	0.2
15343.33594	2306.37	-6.23084	-20.36	771.269	82.43	116.1	0.072506	0.02833	0.1822											
15343.33771	1647.176	-0.30535	-23.92	480.814	39.42	141.56	0.050985	0.013187	0.1693											
15343.33771	1703.779	-1.85252	-27.42	503.756	44.38	143.02	0.044035	0.039976	0.2484											
15343.339	2321.05	0.00383	-22.18	778.295	145.65	33.94	0.057665	0.026507	0.2698											
15343.3391	2317.28	-5.77442	-8.65	776.489	123.45	74.6	0.415974	0.007333	0.1416	15343.3391	33844	2315.625	-5.76819	74.07	0.0052	0.23	-1.66	6.23	-49.38	-0.53
15343.34188	2360.799	4.44605	-22.92	797.435	119	44.57	0.054308	0.040805	0.206											
15343.34194	2498.27	6.68646	-21.15	864.925	999	999	0.064338	0.082368	0.217											
15343.34194	1546.613	-3.76927	-26.99	441.025	55.29	137.88	0.044707	0.000193	0.2192											
15343.34194	2775.345	-4.70387	-16.71	1006.861	134.13	63.06	0.146003	0.025633	0.0875											
15343.34195	2516.67	2.47769	-18.48	874.108	33.26	134.88	0.107815	0.069446	0.1081											
15343.34195	1840.59	7.25707	-16.98	560.802	999	999	0.140207	0.081021	0.0395											
15343.34196	2242.279	-0.4	-25.23	740.869	146.05	35.57	0.047853	0.036874	0.3014											

D-EPOCH [sec]	D-RANGE [km]	D-RRATE [km/s]	RCS [dBsm]	ALTITUDE [km]	DOPINC1 [deg]	DOPINC2 [deg]	DIA [m]	OFFSET [deg]	RMSERR [deg]	C-EPOCH [sec]	OBJ [number]	C-RANGE [km]	C-RRATE [km/s]	T-INC [deg]	T-ECC [deg]	DEL-T [sec]	DEL-R [km]	DEL-RR [m/s]	DEL-I1 [deg]	DEL-I2 [deg]
15343.34196	2665.641	4.0144	-8.91	949.739	122.77	41.08	0.40277	0.018931	0.0972											
15343.34197	1852.05	-5.96321	-15.25	565.682	123.21	74.6	0.178556	0.049929	0.0717											
15343.34197	2843.829	-3.75227	-18.68	1043.12	53.51	142.13	0.103683	0.041704	0.2167											
15343.34198	2318.145	-1.70625	-21.15	776.903	147.39	40.49	0.064287	0.010107	0.1867											
15343.34198	2378.77	6.3616	-24.23	806.145	73.23	87.94	0.050128	0.009664	0.192											
15343.34198	2338.17	-4.42484	-20.21	786.518	59.36	136.73	0.074744	0.012168	0.1738											
15343.342	2038.53	-1.53182	-23.71	647.238	145.55	41.1	0.051594	0.070142	0.1538											
15343.342	2675.295	6.25658	-19.78	954.717	999	999	0.082208	0.06857	0.1848											
15343.34201	2267.785	2.40658	-22.06	752.914	134.55	34.38	0.058274	0.027469	0.1766											
15343.34201	2217.247	-6.69915	-24.05	729.117	999	999	0.05061	0.006009	0.2348											
15343.34201	2301.87	-2.59689	-24.51	769.12	145.7	45.58	0.049446	0.090145	0.1058											
15343.34368	1617.933	6.49866	-13.36	469.115	65.13	96.44	0.22708	0.003983	0.0906	15343.34368	38269	1613.521	6.49706	97.34	0.012	-0.26	-4.41	-1.6	32.21	0.9
15343.34388	2091.622	2.47113	-20.61	671.188	35.56	133.53	0.069393	0.052971	0.1542											
15343.34407	2726.338	6.34641	-16.53	981.196	999	999	0.150131	0.007621	0.2872	15343.34407	12848	2730.19	6.33777	82.48	0.0613	-0.29	3.85	-8.63	916.52	916.52
15343.34559	1942.299	5.50996	-23.98	604.648	53.74	108.76	0.050806	0.005209	0.1132											
15343.34758	2346.407	-4.99491	-19.4	790.486	65.03	132.02	0.089597	0.003105	0.201											
15343.3477	2639.335	-0.00034	-16.18	936.219	31.85	147.73	0.157692	0.05803	0.1759											
15343.34775	1865.828	3.928	-26.02	571.569	123.31	42.16	0.046346	0.012569	0.5724											
15343.34775	1881.96	-0.27136	-23.78	578.49	143.23	37.66	0.051378	0.139857	0.2366											
15343.34862	2333.587	-4.99603	-19.92	784.314	132.03	65.01	0.079584	0.001298	0.1656											
15343.35186	2021.708	-5.98778	-19.35	639.716	75.85	122.17	0.09058	0.004445	0.1582	15343.35186	35359	2018.092	-5.9846	75.75	0.0073	0.05	-3.62	3.18	-0.1	-46.42
15343.35333	1670.714	-6.05132	2.23	490.307	74.92	122.81	1.458081	0.000356	0.1153	15343.35333	39195	1671.691	-6.04449	74.73	0.0003	0.24	0.98	6.83	-0.19	-48.08
15343.35381	1741.197	3.3251	-15.14	519.135	40.08	127.15	0.181126	0.001808	0.1078	15343.35381	27664	1741.098	3.32549	39.75	0.0179	0.14	-0.1	0.39	-0.33	-87.4
15343.35521	2161.47	6.12381	-18.02	703.18	98.29	63.25	0.117733	0.009169	0.1695	15343.3552	39440	2156.701	6.12253	97.7	0.008	-0.37	-4.77	-1.28	-0.59	34.45
15343.35726	1595.37	4.40293	-28.07	460.16	119.4	45.53	0.043067	0.042265	0.26											
15343.35726	2161.83	5.98758	-20.03	703.346	100.79	60.89	0.077669	0.114003	0.1662											

D-EPOCH [sec]	D-RANGE [km]	D-RRATE [km/s]	RCS [dBsm]	ALTITUDE [km]	DOPINC1 [deg]	DOPINC2 [deg]	DIA [m]	OFFSET [deg]	RMSERR [deg]	C-EPOCH [sec]	OBJ [number]	C-RANGE [km]	C-RRATE [km/s]	T-INC [deg]	T-ECC [deg]	DEL-T [sec]	DEL-R [km]	DEL-RR [m/s]	DEL-I1 [deg]	DEL-I2 [deg]
15343.35727	2458.395	4.87903	-20.11	845.144	114.26	48.49	0.076349	0.053979	0.2088											
15343.35728	2328.656	-0.77163	-23.34	781.944	36.29	147.24	0.052803	0.04886	0.2624											
15343.35729	2613.27	-1.9921	-20.71	922.893	148.89	40.79	0.068288	0.000661	0.2102											
15343.3573	1605.806	-4.16947	-25.4	464.294	57.8	136.45	0.047494	0.070978	0.2038											
15343.3573	1873.47	0.16933	-28.37	574.844	142.15	36.74	0.042646	0.08638	0.2019											
15343.3573	2276.97	3.94495	-22.82	757.269	123.54	41.13	0.054723	0.025413	0.2785											
15343.36098	2000.775	6.23292	2.3	630.402	97.81	63.74	1.470952	0.003406	0.0875	15343.36098	33323	2001.04	6.23451	97.72	0.0024	-0.28	0.27	1.59	-0.09	33.98
15343.36117	2138.903	-6.72022	-14.24	692.784	95.37	103.51	0.20308	0.001288	0.1036	15343.36117	40020	2135.473	-6.71258	97.91	0.0087	0.08	-3.43	7.64	2.54	-5.6
15343.36125	2395.645	-0.02438	-19.41	814.354	33.51	146.23	0.089414	0.110451	0.2743											
15343.36138	2536.721	5.87874	3.99	884.155	99.11	62.38	1.785553	0.002838	0.1699	15343.36138	21689	2535.95	5.87822	99.38	0.0026	-0.11	-0.77	-0.52	0.27	37
15343.3669	2463.656	-6.50566	-18.97	847.744	95.1	103.78	0.097885	0.00589	0.1753	15343.36691	36719	2455.229	-6.49952	98.54	0.0107	0.69	-8.43	6.15	3.44	-5.24
15343.37331	2255.695	1.09879	-22.37	747.196	141.35	32.92	0.05668	0.066317	0.1462											
15343.37447	2005.048	6.22189	-15.55	632.299	97.98	63.58	0.171909	0.003751	0.1669	15343.37447	29710	2004.862	6.22137	97.99	0.0003	-0.22	-0.19	-0.51	0.01	34.41
15343.37768	2161.139	6.58449	-19.15	703.027	999	999	0.094443	0.004899	0.1883											
15343.37796	2398.84	6.27346	3.04	815.912	91.02	70.21	1.60041	0.001926	0.127											
15343.38041	2662.044	6.247	-14.71	947.886	79.29	81.81	0.191234	0.024763	0.1943											
15343.38047	2690.405	6.25604	-10.28	962.528	999	999	0.337808	0.001931	0.1603	15343.38045	23774	2680.978	6.25167	82.98	0.0045	-1.5	-9.43	-4.36	916.02	916.02
15343.38171	2495.559	5.91831	-16.33	863.575	62.72	98.77	0.154372	0.013441	0.1499	15343.38171	30940	2492.804	5.91315	99	0.0043	-0.5	-2.75	-5.17	36.28	0.23
15343.38256	2603.924	-5.58878	-14.88	918.131	124.36	73.75	0.18715	0.0137	0.1247											
15343.38368	2388.073	-0.01409	-19.75	810.667	146.15	33.53	0.082664	0.028725	0.1696											
15343.39328	2729.912	6.07382	-19.18	983.059	70.52	90.68	0.09391	0.02685	0.2154	15343.39328	33822	2718.136	6.06928	74.08	0.0186	-0.06	11.78	-4.54	3.56	-16.6
15343.39485	1947.42	-4.9489	-22.94	606.888	63.86	132.55	0.054221	0.012186	0.1904											
15343.39487	1621.774	-0.00752	-26.18	470.646	38.94	140.77	0.046052	0.033439	0.2303											
15343.39582	1976.257	-0.02075	-23.67	619.556	36.39	143.35	0.051726	0.105267	0.2275											
15343.39759	2397.57	-0.00279	-20.41	815.292	33.44	146.18	0.071937	0.012102	0.2389											
15343.39767	2579.853	5.84532	-11.98	905.909	99.31	62.19	0.270328	0.001294	0.1036											

D-EPOCH [sec]	D-RANGE [km]	D-RRATE [km/s]	RCS [dBsm]	ALTITUDE [km]	DOPINC1 [deg]	DOPINC2 [deg]	DIA [m]	OFFSET [deg]	RMSERR [deg]	C-EPOCH [sec]	OBJ [number]	C-RANGE [km]	C-RRATE [km/s]	T-INC [deg]	T-ECC [deg]	DEL-T [sec]	DEL-R [km]	DEL-RR [m/s]	DEL-I1 [deg]	DEL-I2 [deg]
15343.39785	1724.363	6.8058	-24.42	512.195	74.97	86.18	0.049671	0.0056	0.1761											
15343.39813	1906.922	6.84338	-17.15	589.26	999	999	0.136555	0.007087	0.1154											
15343.39875	2010.884	5.12568	-24.2	634.894	112.81	50.16	0.050208	0.009601	0.1691											
15343.39934	2424.428	5.98973	-18.24	828.426	98.1	63.37	0.113035	0.01618	0.1741											
15343.39965	2448.32	5.95907	-12.49	840.172	98.46	63.02	0.253428	0.010403	0.1377											
15343.40255	1499.547	3.02624	-17.69	422.833	40.49	128.06	0.124881	0.014984	0.0802	15343.40255	39381	1470.718	3.0319	40.5	0.0006	-0.11	28.83	5.66	0.01	-87.56
15343.40304	2745.973	-4.96903	-13.23	991.45	131.43	66.09	0.230648	0.012386	0.1902	15343.40304	11750	2745.315	-4.96129	65.84	0.002	0.25	-0.66	7.74	-65.59	-0.25
15343.40369	2099.15	6.91283	-4.35	674.61	999	999	0.683976	0.000569	0.1898	15343.40369	12388	2096.909	6.90985	82.95	0.0681	-0.27	-2.24	-2.98	916.05	916.05
15343.4068	2127.452	-6.83429	-18.6	687.531	999	999	0.105292	0.005659	0.1335											
15343.4093	2693.628	5.86954	-14.76	964.198	97.35	64.04	0.189945	0.014761	0.1596											
15343.4099	2038.844	6.13852	-20.13	647.379	62.41	99.21	0.076047	0.012466	0.1893											
15343.41185	1958.621	-6.86612	10.08	611.797	999	999	3.602192	0.002812	0.0823	15343.41185	40049	1957.17	-6.86022	97.95	0.0012	-0.06	-1.45	5.9	901.05	901.05
15343.41616	2429.588	5.93051	-14.48	830.958	99.26	62.27	0.196927	0.019333	0.1627	15343.41616	4912	2428.546	5.92599	99.72	0.0046	-0.16	-1.04	-4.52	0.46	37.45
15343.41822	2158.195	6.15355	-16.66	701.668	97.73	63.78	0.147168	0.008088	0.2097	15343.41822	33331	2159.448	6.15248	98.09	0.0008	0.03	1.25	-1.06	0.36	34.31
15343.42366	1917.601	6.15326	-20.01	593.89	99.99	61.72	0.07808	0.008867	0.1652											
15343.42378	1982.677	6.22277	8.89	622.389	63.39	98.19	3.139521	0.002579	0.1205	15343.42379	38861	1988.914	6.2318	97.89	0.0018	1.06	6.24	9.04	34.5	-0.3
15343.42451	2315.097	6.42036	-13.71	775.443	74.14	87.01	0.217147	0.000852	0.1063	15343.42451	34401	2312.831	6.41154	74.05	0.0071	-0.2	-2.27	-8.82	-0.09	-12.96
15343.42606	1666.374	6.22218	-23.6	488.552	100.7	61.15	0.051951	0.026602	0.168											
15343.42886	1648.885	6.42553	-20.04	481.501	64.12	97.5	0.077534	0.000423	0.3556	15343.42886	40362	1648.791	6.4267	97.41	0.0004	0.31	-0.09	1.17	33.29	-0.09
15343.42981	2423.67	7.44712	-17.22	828.054	999	999	0.134914	0.064416	0.1684											
15343.43023	2298.512	6.44914	2.24	767.518	75.21	85.92	1.461077	0.007004	0.124	15343.43023	21015	2293.348	6.44563	74.05	0.0021	-0.77	-5.16	-3.52	-1.16	-11.87
15343.43426	2198.013	-5.79408	-18.02	720.134	123.81	74.15	0.117775	0.018913	0.1317											
15343.435	2258.402	2.80683	-21.1	748.474	131.98	35.67	0.064703	0.08137	0.3192	15343.43501	14670	2260.129	2.83822	36.12	0.3007	0.48	1.73	31.38	-95.86	0.45
15343.43694	2425.967	-6.56696	-19.34	829.18	999	999	0.09069	0.001215	0.1727											
15343.44033	2107.23	6.16322	-20.96	678.289	98.08	63.46	0.065914	0.010199	0.1998											
15343.44167	1744.652	-1.10436	-21.2	520.564	41.16	143.3	0.063872	0.006119	0.1277											

D-EPOCH [sec]	D-RANGE [km]	D-RRATE [km/s]	RCS [dBsm]	ALTITUDE [km]	DOPINC1 [deg]	DOPINC2 [deg]	DIA [m]	OFFSET [deg]	RMSERR [deg]	C-EPOCH [sec]	OBJ [number]	C-RANGE [km]	C-RRATE [km/s]	T-INC [deg]	T-ECC [deg]	DEL-T [sec]	DEL-R [km]	DEL-RR [m/s]	DEL-I1 [deg]	DEL-I2 [deg]
15343.44386	2338.344	-5.74209	4.24	786.602	74.26	123.77	1.838045	0.004078	0.0805	15343.44386	18095	2336.594	-5.73776	74.04	0.0014	0.25	-1.75	4.33	-0.22	-49.73
15343.44411	1772.709	5.26158	-24.58	532.218	51.17	111.91	0.049288	0.014143	0.2212											
15343.44959	2258.328	6.05773	-15.35	748.439	62.96	98.57	0.176305	0.002085	0.1554	15343.44959	30092	2257.697	6.05476	98.71	0.0094	-0.36	-0.63	-2.97	35.75	0.14
15343.45064	1796.07	-7.03613	-26.25	541.993	999	999	0.045937	0.006193	0.196											
15343.45107	2131.045	-5.18087	-20.55	689.178	130.57	66.47	0.070075	0.0189	0.1616											
15343.45697	2215.035	6.03336	-22.74	728.082	62.11	99.48	0.055017	0.002529	0.2327											
15343.46424	2832.188	4.27304	-11.95	1036.925	43.28	119.88	0.271382	0.016011	0.5319											
15343.46431	1857.357	-5.07871	-13.33	567.947	131.51	64.98	0.227846	0.004077	0.0899	15343.46431	39132	1858.129	-5.07317	64.88	0.0017	0.22	0.77	5.54	-66.63	-0.1
15343.46574	2337.319	-6.54728	-16.82	786.109	106.34	92.5	0.143716	0.005428	0.1758	15343.46574	37567	2338.815	-6.54301	97.98	0.015	-0.29	1.5	4.27	-8.36	5.48
15343.46885	2306.284	-0.01844	-24.03	771.228	145.61	34.1	0.05066	0.024233	0.2968											
15343.46921	2743.958	4.08015	-3.93	990.396	41.58	122.03	0.71768	0.027631	0.3558											
15343.47497	2788.185	7.05406	-17.64	1013.624	999	999	0.126105	0.010927	0.1557											
15343.48029	2834.61	5.84019	-14.73	1038.213	96	65.33	0.190636	0.052474	0.2291											
15343.49104	1586.867	6.48462	-22.8	456.802	96.97	64.64	0.054795	0.000715	0.1465											
15343.49202	2487.843	-0.01685	-20.4	859.736	32.88	146.81	0.072035	0.045389	0.2396											
15343.49299	2512.888	5.88357	-12.8	872.218	62.22	99.29	0.243649	0.026134	0.1459	15343.49299	29780	2507.167	5.87528	99.26	0.0046	-0.43	-5.72	-8.28	37.04	-0.03
15343.49503	2630.83	-6.67877	-14.71	931.863	999	999	0.191305	0.001749	0.1517	15343.49502	37441	2632.551	-6.67627	99.19	0.0526	-0.12	1.72	2.5	899.81	899.81
15343.49964	2238.57	0.00176	-20.69	739.123	145.11	34.51	0.06851	0.021159	0.1595											
15343.49971	1949.927	6.89323	-25.04	607.986	999	999	0.048254	0.004247	0.2262											
15343.50363	2402.748	6.06579	-19.04	817.818	96.69	64.72	0.096394	0.02964	0.1645	15343.50362	37022	2396.515	6.05903	98.48	0.0149	-0.55	-6.23	-6.76	1.79	33.76
15343.50484	1677.544	6.15423	-26.01	493.074	101.64	60.29	0.046354	0.02675	0.2263											
15343.50509	2262.738	6.43831	-20.06	750.525	87.81	73.35	0.077129	0.054107	0.158											
15343.51119	2485.295	1.7584	-19.74	858.47	139.18	31.76	0.08294	0.035509	0.2327											
15343.51427	1561.556	-2.58902	1.25	446.858	141.17	48.57	1.303385	0.003951	0.0678	15343.51427	25723	1563.521	-2.58603	48.42	0.0014	0.03	1.96	2.99	-92.75	-0.15
15343.51469	2264.423	6.45815	-17.88	751.322	86.71	74.43	0.120915	0.009706	0.1611	15343.51468	35658	2262.795	6.45287	74.02	0.0024	-0.45	-1.63	-5.28	-12.69	-0.41
15343.51617	1529.441	-5.66516	-28.84	434.355	70.21	126.78	0.041971	0.029793	0.1849											

D-EPOCH [sec]	D-RANGE [km]	D-RRATE [km/s]	RCS [dBsm]	ALTITUDE [km]	DOPINC1 [deg]	DOPINC2 [deg]	DIA [m]	OFFSET [deg]	RMSERR [deg]	C-EPOCH [sec]	OBJ [number]	C-RANGE [km]	C-RRATE [km/s]	T-INC [deg]	T-ECC [deg]	DEL-T [sec]	DEL-R [km]	DEL-RR [m/s]	DEL-I1 [deg]	DEL-I2 [deg]
15343.51617	1550.27	6.06894	-30.41	442.45	103.46	58.71	0.039848	0.053503	0.2545											
15343.51997	1849.77	-0.00553	-21.02	564.71	142.42	37.26	0.065406	0.034318	0.2475											
15343.51998	1499.47	-0.00177	-27.71	422.804	139.85	39.85	0.043604	0.021933	0.1857											
15343.52001	2029.625	7.38389	-23.32	643.252	999	999	0.052856	0.018925	0.1635											
15343.52006	2819.37	6.13153	-16.99	1030.118	83.72	77.39	0.139894	0.053227	0.2222											

A.4 References

- [1] Rosebrock, J., Leushacke, L. and Mehrholz, D. *Cooperative Debris Tracking and Development of Algorithms for Mid-Size Debris Detection with Radar*, Final Report of Study Contracts, ESA/ESOC, Darmstadt, Germany, 1999.
- [2] Banka, D., Leushacke, L. Mehrholz, D. Rosebrock, J. Kübbeler, K.-H. *Advanced Methods for Detection and Tracking of Small-Size Space Debris and Meteoroids and Radar Measurements of the Space Environment*, Final Report of Study Contract, ESA/ESOC, Darmstadt, Germany, 2002.

Appendix B

HUSIR Radar

B.1 Experimental Setup

During the 2015 IADC 24-Hour Campaign, 19.2 hours of HUSIR data were collected with the radar pointing at 20° elevation and at an azimuth of 180°. This pointing angle was chosen as an experiment in sampling the lower inclination debris population. The data was collected from approximately 12:16 GMT on 8 December 2015 until 11:42 on 9 December 2015.

The HUSIR radar is a high power, X-band, monopulse-tracking radar with very high sensitivity. To detect debris, a pulsed, single frequency waveform is used. The operating parameters for the HUSIR radar during the 2015 campaign are shown in Table B-1. For HUSIR, the single pulse SNR on a 1-m² target at 1000 km range is 59.7 dB. With HUSIR, objects as small as 1-cm diameter can be observed at ranges greater than 1000 km under normal operations.

**Table B-1 – Instrument Parameters used by the Haystack Radar
for the 2015 Campaign**

Instrument Parameters		
Geocentric latitude of sensor	42.62	deg
Geocentric longitude of sensor	-71.49	deg
Geodetic altitude	0.1157	km
Wavelength	0.03	m
Beam width for incoherent integration	0.116	deg
Antenna constant (Gain)	67.2	dB
Transmitted power (peak)	400.0	kW
Pulse period	16.67	msec
Pulse duration	1.638	msec
Desired false alarm time (Marcum)	36000	sec
Number of independent threshold decisions per pulse	12126	
Maximum number of pulses to integrate	16	
Noise equivalent RCS (NRCS)	-65.2	dB m ²
Transmitted power for NRCS	400	kW
Pulse duration for NRCS	1.638	msec
Range for NRCS	1000	km

For debris observations, the radar is operated in a staring, or "beam park," mode in which the antenna is pointed at a specified elevation and azimuth and remains there while debris objects randomly pass through the field-of-view. This operational mode provides a fixed detection volume important to the measurement of the debris flux, or number of objects detected per unit area per unit time. By operating the radar in a stare mode and not tracking detected debris objects, a precise measurement of the object's orbit is sacrificed. However, by examining the

signals from the monopulse angle channels operating in an open-loop mode, position in the radar beam for each pulse can be determined. From this path through the beam, rough orbital elements are deduced.

B.2 Data Processing

In the debris mode, the signal strength for each received pulse is recorded from four separate channels: the Principal Polarization (PP) sum channel, Orthogonal Polarization (OP) sum channel, Traverse Difference (TR) channel, and Elevation Difference (EL) channel (see Figure B-1). The ODAS software determines the signal strength, SNR ratio, TR and EL voltage ratios, range, and range rate. Other parameters are derived from these measurements. For an orbiting object passing through the radar field-of-view, the key step in the data processing is determining the location of the debris object in the radar beam for each radar pulse. From these locations, the motion of the object through the beam can be recreated and used to estimate rough orbital elements. In addition, the signal strength can be augmented by the relative antenna gain determined by the antenna beam-pattern calibration discussed below. Thus, the returned signal strength can be estimated as if the object were at the center of the radar beam. The RCS is determined by applying the absolute radar calibration, antenna beam shape, and the range to the object.

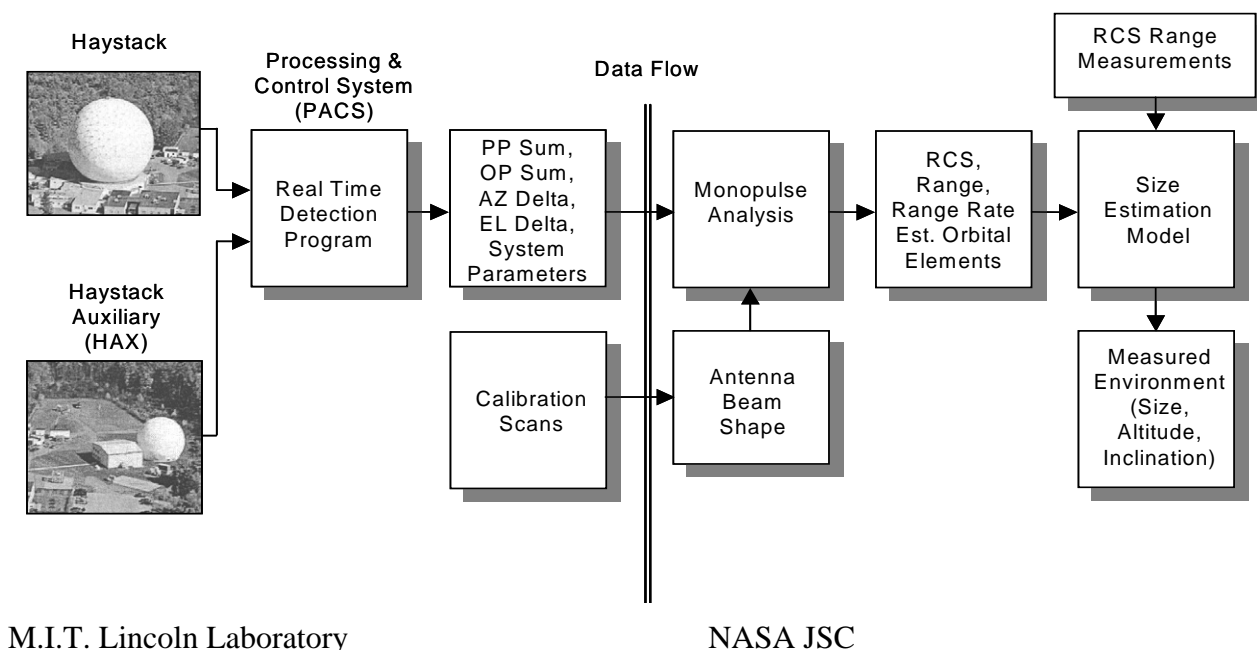


Figure B-1. An overview of the data collection and analysis.

The sensitivity of the antenna pattern is measured by scanning around a calibration sphere as it moves across the sky. This determines both the absolute calibration and the antenna beam

pattern. Spheres return a circularly polarized signal with only a PP component. Test signals injected into the receiver preamplifiers are used to determine the absolute OP calibration.

A simple SNR threshold test is used for object detection. The noise floor varies, however, as a function of Doppler frequency. A “shape factor” representing the noise floor is subtracted from the signal emerging from the intermediate bandwidth filter. This shape factor is determined by averaging a large number of pulse returns that do not contain a valid detection.

Both the HUSIR and HAX radars primarily report Doppler inclination, although the path through the beam is estimated to correct for antenna pattern loss when calculating RCS.

B.3 Campaign Parameters

Table B-3 lists the campaign parameters for the 2015 IADC campaign.

Table B-3 – Campaign Parameters for the HUSIR Radar for the 2015 Campaign

Campaign Parameters		
Campaign Start	8 December 2015 12:16 UT	
Maximum range	2407	km
Minimum range	834	km
Azimuth of line of sight	180	deg
Elevation of line of sight	20	deg
Duration of campaign	24	hrs
Total recorded data	19.2	hrs

B.4 Detection List

Table B-4 provides the list of detections observed by the HUSIR radar during the 2008 campaign. The column showing possible correlations with the U.S. Space Surveillance Network (SSN) catalog of known objects was produced by using U.S. Air Force Space Command provided software.

Table B-4 – HUSIR Detection List for the 2015 Campaign

	Epoch				Slant Range	Range Rate	Radar Cross Section	Altitude	Doppler Inclination	Characteristic Length	Possible Correlation
NO.	doy	hr	min	sec	(km)	(km/sec)	(dBsm)	(km)	(deg)	(m)	Catalog #
1	342	12	16	55.818	1692.8	1.456	-40.19	760.2	147.8	0.007	
2	342	12	18	7.359	1649.9	-6.252	-42.48	736.9	95.7	0.006	
3	342	12	22	26.102	1829.2	5.999	-34.76	835.8	101.6	0.018	31780
4	342	12	25	0.906	1439.8	-6.103	-45.27	625.6	74.1	0.006	
5	342	12	31	19.5	2105	-5.935	-28.53	992.7	95.3	0.041	

	Epoch				Slant Range	Range Rate	Radar Cross Section	Altitude	Doppler Inclination	Characteristic Length	Possible Correlation
6	342	12	31	51.328	1813.6	-5.427	-40.13	826.6	114.7	0.007	
7	342	12	39	19.26	2399.6	5.286	-18.87	1168.9	68.9	0.129	34758
8	342	12	39	27.146	1914.8	5.352	-41.14	883.7	64.9	0.007	
9	342	12	59	53.726	834.3	2.278	-48.38	332.7	140	0.005	
10	342	13	0	12.979	1853.6	6.071	-32.63	849.3	97.9	0.024	32094
11	342	13	2	46.576	1977.4	6.05	-44.67	919.1	87.5	0.006	
12	342	13	7	34.446	1625.2	1.365	-37.02	723.5	147.7	0.011	22552
13	342	13	27	30.685	1716.2	-6.161	-33.73	773.1	81.8	0.021	
14	342	13	28	8.409	2024	-5.326	-43.58	945.8	65.5	0.006	
15	342	13	31	16.818	1909.4	5.315	-40.05	881	64.3	0.007	
16	342	13	55	44.587	1879.5	5.374	-35.58	863.9	65	0.015	
17	342	13	56	34.602	1628.2	6.217	-42.76	725.6	98.5	0.006	
18	342	13	58	33.032	2106.4	-5.901	-34.52	993.7	97.6	0.019	11736
19	342	14	2	55.185	1978.5	-5.362	-39.06	920	65.7	0.008	
20	342	14	8	34.386	1827.5	6.111	-42.1	834.7	96.6	0.007	
21	342	14	9	8.274	1925.9	5.342	-41.03	890.2	115.1	0.007	
22	342	14	11	22.121	2407.3	3.288	-31.62	1173.8	42	0.027	
23	342	14	16	34.359	1789.6	5.377	-43.34	813.4	64.3	0.006	
24	342	14	18	47.78	1513	-6.306	-39.61	664	98	0.008	
25	342	14	37	42.708	1918.7	5.041	-37.13	886	60.2	0.011	
26	342	14	38	26.4	2203.5	-5.741	-38.06	1050.6	101.8	0.009	
27	342	14	39	0.643	1853.3	6.098	-41.12	849.2	83.7	0.007	
28	342	14	40	9.2	2057.6	1.079	-38.7	965.6	28.9	0.009	
29	342	14	56	4.529	1557.4	-5.527	-38.13	687.6	64.8	0.009	
30	342	14	58	29.743	1976.6	5.344	-40.47	918.5	65.4	0.007	
31	342	14	59	58.477	1763.3	6.107	-42.86	798.8	99.2	0.006	
32	342	15	5	53.342	2018.2	5.968	-43.06	942.4	82.8	0.006	
33	342	15	13	8.699	1381.9	-6.747	-41.32	596.1	90.7	0.007	
34	342	15	15	32.048	1730.7	-6.037	-36.5	780.9	102.6	0.013	
35	342	15	15	46.488	1963.7	5.341	-39.21	911.1	65.2	0.008	
36	342	15	30	31.018	1679.9	5.965	-18.12	753.1	74.4	0.14	33936
37	342	15	36	10.466	1854.9	-5.37	-38.09	849.6	64.7	0.009	
38	342	15	36	28.227	1654	6.047	-45.57	739.6	76.2	0.006	
39	342	15	38	44.276	1940.2	5.363	-41.66	897.4	65.3	0.007	
40	342	15	41	15.813	1796.9	6.089	-41.14	817.7	98.9	0.007	
41	342	15	41	28.317	1449.3	-0.998	-33.47	631	32.4	0.022	
42	342	15	41	34.143	1629.9	6.232	-41.77	726.5	97.7	0.007	

	Epoch				Slant Range	Range Rate	Radar Cross Section	Altitude	Doppler Inclination	Characteristic Length	Possible Correlation
43	342	15	43	17.583	2135.9	2.739	-37.93	1011.2	142.5	0.01	
44	342	15	44	28.822	1168.3	-2.96	-51.97	489.2	138.5	0.005	
45	342	15	47	12.383	2035.9	5.247	-38.87	953	64.2	0.008	
46	342	15	49	6.764	1903.9	-6.03	-35.82	877.5	98.2	0.015	
47	342	15	56	41.09	1358.5	-6.487	-43.93	584.3	93.3	0.006	
48	342	15	59	53.904	2088.5	-6.274	-39.46	982.6	152.5	0.008	
49	342	16	5	18.93	1338.8	6.378	-42.31	574	80	0.006	
50	342	16	25	2.452	1986.4	5.327	-38.81	924	114.8	0.008	
51	342	16	28	44.34	2206.9	-5.608	-41.36	1052.4	106	0.007	
52	342	16	40	26.844	1717.3	6.183	-38.66	773.3	97	0.009	
53	342	16	41	21.548	1791.2	6.133	-47.33	814.3	96.9	0.005	
54	342	16	46	30.589	1783.5	-6.13	-35.73	810.3	97.3	0.015	
55	342	16	53	14.474	1828.6	0.59	-35.75	835.3	29.1	0.015	
56	342	16	59	33.494	2045.7	5.902	-34.39	958.5	80.4	0.019	
57	342	17	3	41.793	1879.4	-5.381	-39.68	863.8	65.1	0.008	
58	342	17	8	44.866	1692.3	-3.689	-18.21	759.6	45.3	0.139	
59	342	17	16	45.976	1560.7	-6.116	-44.75	689.4	103.6	0.006	
60	342	17	17	41.888	1798	6.059	-43.58	818.2	79.8	0.006	
61	342	17	20	39.285	1905.9	6.133	-37.11	878.7	102.3	0.011	
62	342	17	27	40.718	1973	-5.377	-40.54	916.9	65.9	0.007	
63	342	17	29	23.163	1754.7	-6.055	-33.37	793.8	101.4	0.022	
64	342	17	31	15.91	2015.9	5.249	-38.85	941.3	64.1	0.008	
65	342	17	32	4.717	1708.5	-6.26	-42.8	768.8	91.2	0.006	
66	342	17	35	9.574	1677.4	5.938	-43.07	752.2	73.7	0.006	
67	342	17	59	32.637	948.8	0.573	-45.03	384.5	35.1	0.006	
68	342	18	8	53.052	1158.9	-4.266	-51.43	484.7	50.1	0.005	
69	342	18	10	51.695	1839.8	-5.343	-39.47	840.9	64.1	0.008	
70	342	18	14	12.679	1570.7	5.988	-48.9	694.5	106.7	0.005	
71	342	18	18	15.791	1893.5	6.03	-40.44	871.8	98.6	0.007	
72	342	18	24	3.481	1275.5	-6.472	-37.12	542.2	98	0.011	
73	342	18	33	23.094	959.8	-5.164	-55.47	389.7	122.2	0.004	
74	342	18	35	39.996	1420	1.905	-22.44	615.9	144.6	0.085	3611
75	342	18	38	0.379	1858.9	6.069	-41.69	852.4	82.2	0.007	
76	342	18	41	39.763	1739.7	-5.457	-37.07	786.1	65.1	0.011	
77	342	18	47	38.109	1946.6	5.371	-41.49	901.6	114.5	0.007	
78	342	19	4	37.448	1915.4	5.33	-39.16	884	115.4	0.008	
79	342	19	6	50.442	1710.4	6.135	-39.87	769.7	99.6	0.008	

	Epoch				Slant Range	Range Rate	Radar Cross Section	Altitude	Doppler Inclination	Characteristic Length	Possible Correlation
80	342	19	8	59.814	1953.2	5.34	-39.74	905.2	65.1	0.008	
81	342	19	13	13.014	1769.3	-6.186	-37.28	802.5	85.9	0.011	
82	342	19	17	0.426	1878.4	5.857	-42.83	863.1	75	0.006	
83	342	19	18	38.183	2067.5	-4.146	-44.83	970.9	130	0.006	
84	342	19	18	53.173	1465	6.41	-47.79	638.9	86.5	0.005	
85	342	19	20	6.846	2092.9	-1.938	-41.81	985.5	32.5	0.007	
86	342	19	21	30.322	2162.6	5.801	-42.61	1026.5	79.5	0.006	
87	342	19	22	41.082	1883.1	-2.937	-38.27	865.7	140.6	0.009	
88	342	19	23	27.687	1849.5	-7.244	-46.76	846.6	58.2	0.005	
89	342	19	24	25.943	1858.5	5.363	-42.33	851.5	64.6	0.006	
90	342	20	1	18.361	1673.3	-6.152	-43.89	750.1	80.1	0.006	
91	342	20	2	37.078	1824.8	-6.099	-36.68	833.1	82.6	0.013	
92	342	20	4	36.148	1580.8	-5.613	-37.71	700.3	66.3	0.01	
93	342	20	5	42.219	1799.1	3.244	-43.87	818.8	41.8	0.006	
94	342	20	17	33.227	1922.8	5.318	-39.35	888.3	115.6	0.008	
95	342	20	18	54.501	1747.7	-5.449	-40.79	790.2	65.1	0.007	
96	342	20	23	50.755	2251	-5.902	-31.82	1078.4	122.7	0.027	
97	342	20	51	52.864	1773.1	-5.407	-41.07	804.8	64.6	0.007	
98	342	20	53	48.523	1064.8	0.038	-57	439.3	34	0.004	
99	342	20	53	53.07	1381.6	-1.476	-52.44	596	34.1	0.004	
100	342	20	54	3.656	2197.5	0.033	-35.62	1047.3	26.3	0.015	
101	342	20	54	41.877	1463.3	-2.806	-45.93	638.2	39.6	0.006	26339
102	342	20	55	5.535	1921.5	-5.375	-41.83	887.3	65.4	0.007	
103	342	20	56	23.47	1440.8	-6.433	-43.15	626.3	92.8	0.006	
104	342	20	57	11.78	1442.5	-6.392	-41.34	627.1	96.1	0.007	
105	342	20	57	31.246	1778.1	-7.265	-39.15	807.4	45.6	0.008	34032
106	342	20	57	41.548	1358.5	-4.963	-15.1	584.2	56.7	0.198	
107	342	20	57	51.565	1402.7	-5.512	-54.3	606.7	63.5	0.004	
108	342	20	57	55.969	1086.3	6.426	-57.82	449.4	103.5	0.003	
109	342	20	57	58.172	1157.2	-5.038	-39.27	484	57	0.008	
110	342	20	58	0.374	1954.7	-5.499	-14.09	906	112.1	0.223	
111	342	20	58	4.921	1212.1	-3.698	-29.83	510.7	45.9	0.034	
112	342	20	58	7.408	2307.3	-4.332	-29.99	1112.5	52.9	0.034	
113	342	20	58	18.988	1597.6	-1.408	-34.5	708.9	147.4	0.019	
114	342	20	58	25.737	2266.4	-6.416	-18.31	1088.6	130.6	0.137	
115	342	20	58	28.223	1515.8	-3.336	-34.92	665.9	42.9	0.018	

	Epoch				Slant Range	Range Rate	Radar Cross Section	Altitude	Doppler Inclination	Characteristic Length	Possible Correlation
116	342	21	0	28.927	1358.5	6.432	-	584.5	82.8	0	
117	342	21	1	39.474	1886.6	-5.39	-40.68	867.6	65.3	0.007	
118	342	21	2	2.563	2236	-2.702	-44.29	1070	142.9	0.006	
119	342	21	2	6.399	1278.4	-0.394	-41.88	543.7	147.4	0.007	
120	342	21	2	11.088	1651.5	-1.896	-46.65	738.2	34.2	0.005	
121	342	21	2	21.958	2388.2	0.994	-31.65	1161	153.1	0.027	
122	342	21	2	30.75	834.3	-6.737	-	332.1	99.3	0	
123	342	21	2	44.266	1043.8	0.684	-58.06	429.2	34.6	0.003	
124	342	21	3	39.041	2140.7	7.113	-26.56	1013.3	29.9	0.052	
125	342	21	3	59.004	1848.9	5.725	-41.01	846.2	108.7	0.007	
126	342	21	5	3.512	2214.1	5.204	-40.63	1057	114.8	0.007	
127	342	21	5	8.024	1978.5	6.437	-40.91	919.9	147	0.007	
128	342	21	5	33.209	2197.7	0.021	-53.11	1046.9	153.7	0.004	
129	342	21	5	35.482	1491.9	2.684	-40.49	653	38.8	0.007	
130	342	21	5	39.247	1968.7	-1.265	-45.97	913.5	30.1	0.006	
131	342	21	5	44.931	1465.3	5.18	-40.22	639.1	120.4	0.007	32148
132	342	21	6	24.289	1902.3	-5.458	-31.22	875.9	113.4	0.029	
133	342	21	6	25.71	2386.9	-6.647	-37.48	1160.5	78.7	0.01	21754
134	342	21	6	35.017	1673.3	3.487	-42.46	749.8	43.8	0.006	
135	342	21	10	20.937	1778.2	6.338	-48.74	806.8	72	0.005	
136	342	21	16	59.778	1499.7	-6.407	-45.57	657.3	51.3	0.006	
137	342	21	17	25.212	1874.2	-3.899	-39.79	860.7	132.8	0.008	
138	342	21	17	52.635	986.5	-5.398	-48.6	402.1	119.8	0.005	
139	342	21	18	1.302	2367.7	-1.521	-35.76	1148.5	150.8	0.015	
140	342	21	18	6.701	2077.5	-3.581	-42.18	977	44.5	0.007	
141	342	21	18	19.489	1826.8	-5.398	-37.15	834.2	64.9	0.011	
142	342	21	18	25.528	1469	5.773	-38.7	641.2	112	0.009	
143	342	21	18	36.185	1603.7	-4.622	-55.39	712.9	126.2	0.004	
144	342	21	18	46.06	868.7	-0.055	-41.68	347.9	35.5	0.007	
145	342	21	33	9.614	2061.5	5.629	-43.53	967.5	107.9	0.006	
146	342	21	37	33.826	1850.5	-6.067	-41.27	847.3	98.2	0.007	
147	342	21	40	29.589	1906.4	-5.326	-38.69	878.6	64.4	0.009	
148	342	21	43	8.23	1916.7	-6.018	9.84	884.7	98.4	3.502	17527
149	342	21	45	43.603	2330.8	-5.574	-30.66	1126.8	104.7	0.031	
150	342	22	2	45.998	1818.3	6.213	-44.21	829.2	149.5	0.006	

	Epoch				Slant Range	Range Rate	Radar Cross Section	Altitude	Doppler Inclination	Characteristic Length	Possible Correlation
151	342	22	9	46.791	1919.3	5.99	-35.98	886.3	80.4	0.014	
152	342	22	11	14.033	1746.7	6.182	-43.6	789.6	95.7	0.006	
153	342	22	18	54.612	1868.2	-6.073	-41.9	857.2	82.8	0.007	
154	342	22	24	32	1815.2	6.054	-40.97	827.4	80.1	0.007	
155	342	22	31	49.417	1749.3	5.94	-43.96	791.1	75	0.006	
156	342	22	34	7.74	1833.2	-5.398	-41.31	837.7	65	0.007	
157	342	22	36	57.606	1896.9	6.19	-39.4	873.7	133.3	0.008	
158	342	22	41	35.53	1868.5	-5.376	-38.11	857.4	64.9	0.009	
159	342	22	43	20.32	2374.5	-5.598	-36.26	1152.7	102.9	0.014	
160	342	22	44	57.224	1838.9	-6.082	-37.79	840.9	97.8	0.01	
161	342	22	45	32.888	1499.6	-6.082	-35.59	657.3	74.5	0.015	
162	342	23	10	34.83	1962.2	-5.351	-35.76	910.7	65.3	0.015	
163	342	23	11	57.17	1679.5	-6.195	-37.02	753.5	97.8	0.011	
164	342	23	18	2.336	1818.7	-6.092	-39.36	829.5	81.9	0.008	
165	343	1	25	32.871	1462.3	-6.304	-45.45	637.4	80.4	0.006	
166	343	1	32	31.96	1164.2	-6.884	-39.75	487.3	77.7	0.008	
167	343	1	40	11.046	1549.4	-6.047	-30.03	683.2	74.4	0.033	35037
168	343	1	47	54.466	1345.6	6.465	-45.27	577.6	95.8	0.006	
169	343	1	48	16.134	1292	-6.554	-43.69	550.5	112.2	0.006	
170	343	2	15	11.837	1659.8	-6.044	-42.94	742.4	103.8	0.006	
171	343	2	19	9.976	1943.6	-5.355	-33.52	899.9	65.2	0.021	
172	343	2	24	31.308	1289.9	3.531	-50.16	549.1	44.6	0.005	
173	343	2	28	5.15	2246.1	5.791	-43.99	1074.9	98.3	0.006	4644
174	343	2	31	25.637	1750.3	-6.147	-38.36	791.7	97.7	0.009	
175	343	2	33	26.838	1193	6.517	-41.65	501	98.5	0.007	
176	343	2	36	50.663	1764.3	6.154	-36.8	799.2	96.8	0.012	
177	343	2	44	54.828	1920.4	5.341	-38.8	887.1	64.8	0.008	
178	343	2	45	14.933	1805.7	-5.397	-38.77	822.4	64.7	0.008	
179	343	2	57	28.32	1841.3	-6.095	-42.67	842.3	83	0.006	
180	343	3	3	19.704	1572.4	-6.043	-43.18	695.5	74.7	0.006	
181	343	3	5	38.453	1784.2	-5.409	-37.27	810.4	64.7	0.011	
182	343	3	9	6.043	1501.5	6.388	-37.51	658.3	93	0.01	
183	343	3	13	13.987	1859.7	5.464	-24.69	853.1	66.3	0.066	
184	343	3	14	18.14	1900.6	-5.373	-41.24	875.8	65.1	0.007	
185	343	3	16	43.851	1826.6	-6.053	-41.32	834.3	99.6	0.007	
186	343	3	21	29.448	1778.2	-6.101	-43.82	807	81	0.006	
187	343	3	23	32.283	1704.9	-6.161	-36.02	766.9	81.4	0.014	

	Epoch				Slant Range	Range Rate	Radar Cross Section	Altitude	Doppler Inclination	Characteristic Length	Possible Correlation
188	343	3	25	18.92	1965.4	5.332	-39.33	912.7	115	0.008	
189	343	3	36	40.658	1663.5	-6.183	-1.78	744.5	98.9	0.92	7228
190	343	3	39	22.923	1595.8	5.561	-43.71	708	65.6	0.006	
191	343	3	54	29.871	1875.5	5.364	-37.02	861.2	64.8	0.011	
192	343	4	4	9.43	1585.6	-6.187	-36.81	702.7	100.8	0.012	
193	343	4	16	53.224	1928.1	-6.006	-37.87	891.1	81.4	0.01	
194	343	4	19	33.428	1189.4	5.726	-47.94	499.5	65.1	0.005	
195	343	4	25	15.15	1592.5	5.494	-41.96	706.2	64.5	0.007	
196	343	4	32	52.745	1673.3	-6.151	-42.13	749.9	80.1	0.007	
197	343	4	33	23.791	2264.8	0.197	-42.64	1087.2	154.1	0.006	
198	343	4	34	20.271	1861.5	1.268	-34.69	853.2	30.6	0.018	
199	343	4	35	26.484	1694	6.164	-57.27	761.4	98.8	0.004	
200	343	4	49	16.704	2318.6	-5.703	-30.72	1119.8	100.2	0.031	
201	343	4	51	0.286	1489.4	-1.186	-24.78	651.8	32.6	0.065	3978
202	343	5	17	33.941	1841.2	-5.771	-44.16	842	107.8	0.006	
203	343	5	21	7.641	1470.8	-6.452	-46.51	642	145.9	0.005	
204	343	5	30	42.316	1693.6	5.96	-36.16	760.1	74.5	0.014	6965
205	343	5	42	58.687	2101	-5.787	-41.19	990.3	102.6	0.007	
206	343	5	55	21.097	1906.4	-1.789	-37.46	878.8	32.5	0.01	
207	343	5	55	36.727	1978	-5.282	-33.33	919.4	64.3	0.022	
208	343	6	1	45.09	1799.2	-6.104	-38.06	818.7	98.1	0.009	
209	343	6	4	28.704	1918.4	-5.965	-38.41	885.4	100.6	0.009	
210	343	6	9	16.006	1962.3	-5.399	-38.64	910.7	113.8	0.009	
211	343	6	22	54.504	1793.8	-5.427	-40.62	815.7	65.1	0.007	
212	343	6	42	23.095	1625.7	-5.945	-49.77	724	106.9	0.005	
213	343	6	58	37.25	1506.3	-6.315	-42.25	660.3	82.2	0.006	
214	343	6	58	39.31	2118.4	5.533	-31.73	1000.8	70.7	0.027	
215	343	7	3	46.575	1763.6	-5.939	-37.69	798.9	75.2	0.01	
216	343	7	5	11.402	1760.6	-5.437	-37.99	797.2	115	0.009	
217	343	7	12	46.368	1673.1	-5.997	-39.99	749.9	104.8	0.007	
218	343	7	30	48.794	1699.7	1.38	-41.97	764	148.1	0.007	
219	343	7	33	56.99	2254.7	-5.863	-21.5	1080.6	99.6	0.095	
220	343	7	53	12.884	1883.1	4.797	-39.87	865.8	123.2	0.008	
221	343	7	57	32.692	1824.8	6.047	-34.18	833	80.1	0.02	
222	343	8	19	10.382	1666.1	-6.197	-45.58	746.1	98.1	0.006	
223	343	8	19	49.35	1148.7	-6.067	-55.99	479.6	110	0.004	
224	343	8	20	2.315	1944.7	5.369	-40.71	900.7	65.5	0.007	

	Epoch				Slant Range	Range Rate	Radar Cross Section	Altitude	Doppler Inclination	Characteristic Length	Possible Correlation
225	343	8	23	46.601	1922.9	5.371	-37.8	887.9	114.7	0.01	
226	343	8	32	3.554	1655.9	5.45	-42.85	740.2	64.4	0.006	34819
227	343	8	36	7.803	2168.2	-5.893	-41.12	1029.7	95.1	0.007	
228	343	8	51	34.856	1558.3	-6.036	-43.86	688.1	74.3	0.006	
229	343	8	52	59.257	2316.1	-5.595	-37.47	1118.1	75.7	0.01	
230	343	9	5	31.613	1634.7	5.952	-43.7	728.8	73.4	0.006	
231	343	9	8	12.953	2245.4	-5.792	-41.28	1075.5	98.3	0.007	
232	343	9	24	9.066	1925.6	-5.959	-36.82	889.5	79.3	0.012	
233	343	9	31	55.114	1920.9	6.024	-26.41	886.9	97.9	0.053	12373
234	343	9	34	5.693	1965.2	5.302	-41.21	912.3	115.5	0.007	
235	343	9	36	20.677	1373.9	6.42	-50.5	592	97.2	0.005	
236	343	9	55	16.741	1857.1	6.041	-38.99	851.2	99.2	0.008	
237	343	10	0	50.506	1701.8	5.436	-40.68	764.9	64.5	0.007	
238	343	10	2	34.799	2367.2	-5.429	-41.13	1149.1	71.9	0.007	
239	343	10	6	39.048	1986.1	-5.946	-36.48	924.1	99.5	0.013	
240	343	10	10	23.263	1985	6.084	-42.17	923.5	102.9	0.007	
241	343	10	13	46.875	1718.5	-6.24	-42.93	774.4	88.5	0.006	
242	343	10	38	8.038	1568.5	-6.328	-40.55	693.4	85.8	0.007	
243	343	10	39	10.414	1980.3	0.611	-23.69	922.2	28.2	0.074	59
244	343	10	43	11.822	2407.3	-4.875	-38.91	1172.7	61.2	0.008	
245	343	10	48	43.668	2032	-5.278	-31.83	950.2	64.7	0.027	
246	343	11	17	15.331	1553.5	6.388	-45.38	685.2	62.8	0.006	
247	343	11	20	23.953	920.3	4.163	-53.19	371.7	49.6	0.004	
248	343	11	20	42.212	1356.9	6.431	-40.28	583.2	97.3	0.007	
249	343	11	29	19.625	1846.7	5.392	-37.33	845.1	65	0.011	
250	343	11	38	28.795	1828.9	6.067	-39.74	835.1	81.1	0.008	30543
251	343	11	42	29.137	1895.8	-6.053	-32.65	872.7	97.3	0.024	

B.5 References

- [1] Stansbery, E. G., Bohannon, G., Pitts, C., Tracy, T., and Stanley, J. "Radar Observations of Small Debris." *Adv. Space Res.* Vol. 13, No. 8, pp. (8)43 - (8)48, 1993.

Appendix C

Goldstone Radar

C.1 Experimental Setup

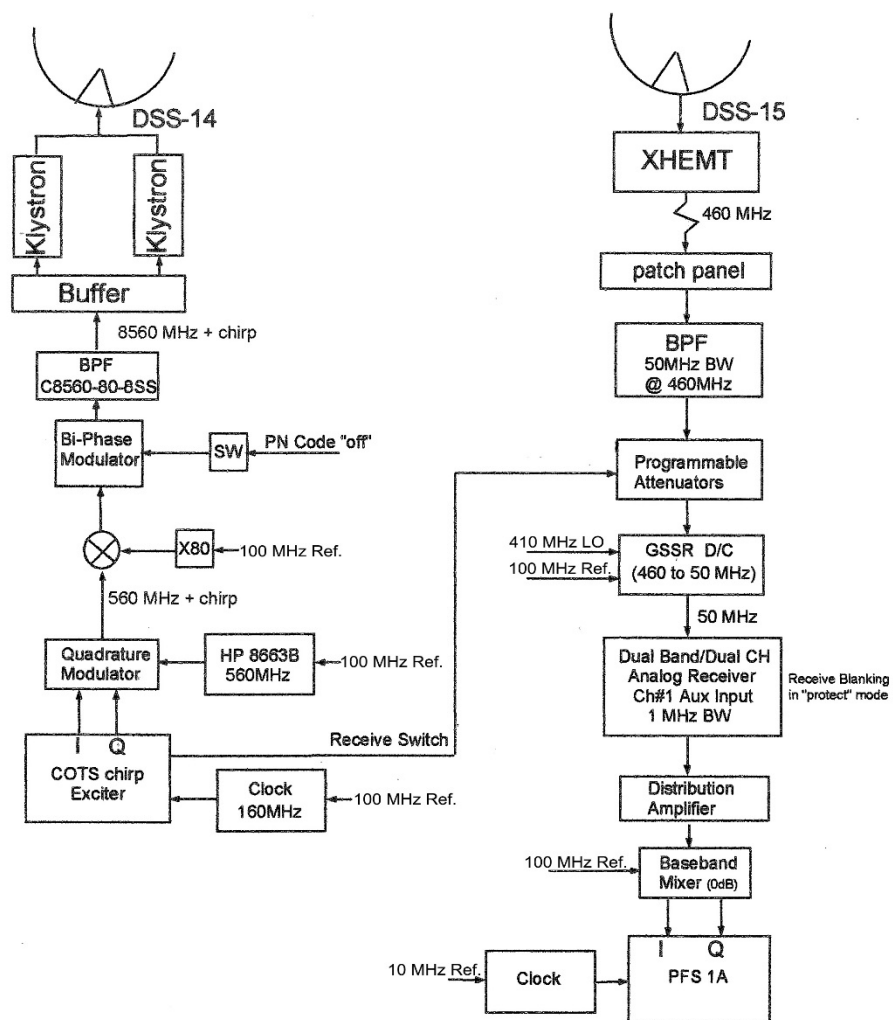
During the 2015 IADC 24-Hour Campaign, approximately 6 hours of Goldstone data was collected with the radar pointing at 25° elevation and at an azimuth of 180°. The data was collected from approximately 02:51 GMT until 08:49 GMT on 8 December 2015.

The Goldstone radar is a high power, X-band radar with very high sensitivity allowing detections of millimeter sized debris. The operating parameters for the Goldstone radar during the 2015 campaign are shown in Table C-1. For Goldstone, the single pulse SNR on a 1-m² target at 1000 km range is 84.7 dB.

**Table C-1 – Instrument Parameters used by the Goldstone Radar
for the 2015 Campaign**

Goldstone Instrument Parameters		
Geocentric latitude of sensor	35.24	deg
Geocentric longitude of sensor	116.16	deg
Geodetic altitude	0.899	km
Wavelength	0.03502	m
Transmit beam width	0.034	deg
Receive beam width	0.069	deg
Transmit antenna gain (DSS-14)	74.24	dB
Receive antenna gain (DSS-15)	68.42	dB
Transmitted power (peak)	430	kW
Pulse period	22.5	msec
Pulse (chirp) duration	2.34	msec
Pulse bandwidth	46.15	kHz
Desired false alarm time (Marcum)	unknown	sec
Number of independent threshold decisions per pulse	29952	

For debris observations, the radar is operated in a bi-static staring, or beam park mode in which the transmit antenna is pointed at a specific elevation and azimuth and the receive antenna is pointed at a slightly offset elevation and azimuth to achieve a desired overlapping range extent. Figure C-1 contains a block diagram illustration of the bi-static setup.



Jet Propulsion Laboratory	
ODR Configuration	
GSSR	03/22/2010
00403	

Figure C-1. Block diagram of the Goldstone Orbital Debris Radar (ODR) bi-static configuration.

C.2 Campaign Parameters

Table C-2 lists the campaign parameters for the 2015 IADC campaign.

Table C-2 – Campaign Parameters for the Goldstone Radar for the 2015 Campaign

Campaign Parameters		
Campaign Start	8 December 2015 02:51 UT	
Maximum range	4013.8	km
Minimum range	183.1	km
Azimuth of line of sight	180	deg
Elevation of line of sight	25	deg
Duration of campaign	6	hrs
Total recorded data	6	hrs

C.3 Detection List

Pw/Av-1: “Pw” is the energy of the reflected signal. “Av” (average noise) can be considered the noise background. Therefore Pw/Av-1 is very similar to SNR, but not a direct comparison [2].

Table C-3 – Goldstone Detection List for the 2015 Campaign

	Epoch				Pw/Av-1	Range	F	Inclination	RCS	Size
NO.	doy	hr	min	sec		(km)	(Hz)		(mm^2)	(mm)
1	343	2	51	42.48	2135.28	2791.9	-241574	nan	24066.07	175.05
2	343	3	4	55.56	24.5	1058.4	122303	146.37	0.34	3.13
3	343	3	18	6.12	24.3	2061.6	103218	135.23	6.58	5.13
4	343	3	21	43.92	17	2086.3	-193842	nan	5.5	4.98
5	343	3	32	26.52	30.35	2637.4	-108165	33.24	22.26	6.28
6	343	3	47	17.16	312.12	3069.2	1033	88.06	1413.19	42.42
7	343	3	54	-4E-13	16.06	2010.8	9323	91.55	1.5	4.01
8	343	3	54	7.92	16.13	547	142257	164.84	0.01	1.58
9	343	3	59	18.24	27.89	1552.5	70820	118.02	1.14	3.83
10	343	4	11	22.92	16.18	1203.1	-267389	nan	1.25	3.89
11	343	4	14	7.44	15.44	1260.1	-43121	69.57	0.14	2.71
12	343	4	17	33.36	54.5	1540.3	140126	165.63	4.5	4.81
13	343	4	24	39.96	16.59	544.4	137788	159	0	1.55
14	343	4	25	10.56	18.14	3043.7	-11583	82.69	11.43	5.62

	Epoch				Pw/Av- 1	Range	F	Inclination	RCS	Size
15	343	4	32	27.6	16.48	1305	79709	122.09	0.31	3.08
16	343	4	45	12.24	15.84	2700.5	-290089	nan	152.18	13.92
17	343	4	52	46.92	17.01	1521.9	-239349	nan	1.79	4.13
18	343	4	58	31.08	15.2	2325.1	86975	126.49	3.67	4.65
19	343	5	0	5.4	16.25	2345.7	-227820	nan	12.09	5.68
20	343	5	41	58.92	18.82	3029.7	-438	87.43	19.92	6.17
21	343	5	43	5.88	17.61	3032	981	88.04	18.16	6.07
22	343	5	43	8.4	18.27	3034.4	2608	88.73	42.25	7.33
23	343	5	44	0.24	17.16	3045.1	-133	87.56	13.96	5.81
24	343	5	45	4.68	17.96	3046.2	-13346	81.93	11.22	5.61
25	343	5	48	34.56	734.74	1646.2	82919	123.91	55.05	8.37
26	343	5	48	41.76	16.33	3033.6	-10083	83.33	8.06	5.3
27	343	6	26	34.08	16.13	3057.8	38077	103.92	11.58	5.64
28	343	6	27	16.2	591.09	2296	-273495	nan	12534.86	126.33
29	343	6	47	18.24	16	1728.6	19319	95.69	0.75	3.57
30	343	6	53	49.56	17.92	879.4	-148295	nan	0.05	2.3
31	343	7	11	12.12	2410.47	557.6	-114103	32.25	1.39	3.96
32	343	7	26	49.56	16.37	3050.2	273255	nan	105.25	11.58
33	343	7	43	29.28	44.76	795.8	37	87.73	0.04	2.21
34	343	8	2	13.56	47.09	3051.1	1489	88.25	161.36	14.33
35	343	8	33	58.68	15.56	1934.6	147874	nan	2.79	4.45
36	343	8	45	5.04	16.28	3141.3	125981	153.25	22.93	6.31
37	343	8	49	58.44	741.72	861	105088	134.99	3.01	4.5

C.4 References

- [1] Slade, Martin. Stanchfield, Kevin. “Solar System Radar Group: Group 332F.” NASA JPL. 15 January 2016. Web. 20 February 2017. <http://gssr.jpl.nasa.gov/>
- [2] Jao, J., “ODR Question.” Message to Christopher Blackwell. 2017 January 24. Email.

Appendix D

COBRA DANE Radar

D.1 Experimental Setup

Cobra Dane is an L-band (23-cm wavelength) phased array radar that first became operational in 1977. The radar generates approximately 15.4 MW of peak RF power (0.92 MW average) from 96 Traveling Wave Tube (TWT) amplifiers arranged in 12 groups of eight. This power is radiated through 15,360 active array elements. The face of the radar is aligned at an azimuth of 319°, true.

The Cobra Dane is different from the pencil-beam radars in that it is an electronically steered, phased array radar. This means that the antenna beam can be instantaneously moved within some angular limits. What is typically done with phased array radars is to rapidly move the beam in a long, narrow pattern to create a virtual fan beam, or fence. If each individual beam position in the fence is revisited often, enough that orbiting objects cannot travel the width of the fence between revisits, then the fence is referred to as a “leak proof” fence. While maintaining the fence, some radar time and transmit power is typically allocated for tracking of objects detected by the fence. The instrument parameters for Cobra Dane used in the 2015 campaign are shown in Table D-1.

Table D-1 – Instrument Parameters for the Cobra Dane Radar used during the 2015 Campaign

Instrument Parameters		
Geocentric latitude of sensor	52.737	deg
Geocentric longitude of sensor	174.091	deg
Geodetic altitude	0.091	km
Wavelength	0.23	m
Beam width (fence)	0.6 x 40	deg
Antenna constant (Gain)	unavailable	
Transmitted power (peak)	15.4	MW
Pulse period	varies	msec
Pulse duration	1.5	msec
Desired false alarm time (Marcum)	unavailable	
Number of independent threshold decisions per pulse	unavailable	
Maximum number of pulses to integrate	unavailable	
Noise equivalent RCS (NRCS)	unavailable	
Transmitted power for NRCS	unavailable	
Pulse duration for NRCS	unavailable	
Range for NRCS	unavailable	

D.2 Data Collection

Cobra Dane operated for 13 hours from ~19:38 GMT on 8 December 2015 to ~08:10 GMT on 9 December 2015. During the campaign, a fence covering an elevation range of 20°-60° and at an azimuth of 319° was erected. The fence was one beamwidth wide, or 0.6°. The radar detected objects crossing this fence at slant ranges from 415 – 3000 km. A 1500 μ sec pulse was used for detection. Objects passing through the fence were checked against known objects in the U.S. SSN catalog (including analyst, or 80,000 series satellites). If the detection was correlated with a known object, then no further tracking was done. In this way, radar resources (time and transmit power) could be conserved for use with uncorrelated targets (UCTs). Campaign parameters for Cobra Dane during the 2015 campaign are shown in Table D-2.

Table D-2 – Campaign Parameters for the Cobra Dane Radar used during the 2015 Campaign

Campaign Parameters		
Campaign Start	8 December 2015 19:38 UT	
Maximum range	2501	km
Minimum range	415	km
Azimuth of line of sight	319	deg
Elevation of line of sight	20-60	deg
Duration of campaign	13	hrs
Total recorded data	13	hrs

D.3 Detection List

Table D-3 provides the list of detections of UNASSO observed by the COBRA DANE radar during the 2015 campaign.

Table D-3 – Cobra Dane Detection List for the 2015 Campaign

NO.	Epoch				Slant Range	Range Rate	Radar Cross Section	Altitude	Inc	ECC	Characteristic Length
	doy	hr	min	sec	(km)	(km/sec)	(dBsm)	(km)	(deg)		(m)
1	15343	0	33	32	1593.5	-1.565	-26.9897	1459.6	66.8	0.00752	0.054893
2	15342	20	48	43	1649.7	-1.4335	-20.45757	1502.4	66.5	0.01071	0.072592
3	15342	22	34	22	2398.8	-4.1223	-16.38272	1952.5	66.5	0.01071	0.13334
4	15342	19	38	13	1604.1	-0.6803	-12.51812	1552.4	66.9	0.00908	0.24474
5	15343	9	58	31	962	4.1395	-16.19789	960	79.9	0.13258	0.13865
6	15343	10	17	19	1499.1	0	-20.9691	1378.1	62.2	0.02223	0.070184

	Epoch				Slant Range	Range Rate	Radar Cross Section	Altitude	Inc	ECC	Characteristic Length
7	15343	10	45	22	1404.6	4.5404	-30	1356.5	62.8	0.074	0.049457
8	15342	22	24	23	1480.5	4.6417	-21.54902	1424.6	65.6	0.06511	0.067551
9	15343	10	53	17	2239.1	5.2125	-18.86057	1831.9	65.7	0.06676	0.083875
10	15342	21	36	12	2094.3	-4.4223	-17.44727	1888.2	99.9	0.02252	0.104
11	15343	0	3	26	1290.3	-1.5222	-17.69551	1272.9	64.9	0.00484	0.099737
12	15343	10	11	45	1395.3	0	-20	1342.6	98.2	0.02099	0.074871
13	15343	0	59	59	1872.3	3.9023	-16.19789	1861.2	101.4	0.00185	0.13865
14	15343	6	36	28	2140.3	-1.7121	-15.85027	1995.6	65.8	0.09129	0.14704
15	15342	23	53	14	1225.2	-1.557	-10.60481	1222.4	83	0.00167	0.31257
16	15343	14	37	53	1308.3	4.4193	-22.21849	1294.2	65.8	0.05404	0.065408
17	15343	10	3	3	1176.9	0	-26.9897	1163.9	103.4	0.05137	0.054893
18	15343	8	36	20	1525.5	-0.9313	-12.36572	1472.3	65.9	0.01214	0.2496
19	15343	13	59	21	2217.6	-3.4538	-10.13228	1883.5	65.8	0.01278	0.33172
20	15343	12	13	35	2237.5	4.0691	-12.59637	2191	102.4	0.011	0.24228
21	15343	5	4	56	1952.7	5.1923	-3.37242	1651.2	98.5	0.00661	0.7653
22	15342	23	39	47	2020.4	-0.6286	-15.08638	1731.9	82.9	0.00173	0.17053
23	15343	5	1	39	1780.6	-3.7385	-11.73925	1675.8	82.8	0.00985	0.27055
24	15343	13	22	47	1314.2	2.699	-17.69551	1289.9	82.9	0.0031	0.099737
25	15343	2	27	34	2036.4	0	-20.9691	1929.6	65.8	0.09121	0.070184
26	15343	11	2	40	2305	0	-19.58607	1846.6	65.7	0.04897	0.077913
27	15343	7	40	27	947.5	-4.3065	-22.21849	928.2	82.5	0.02037	0.065408
28	15343	7	49	12	1284.7	0	-20	1194.4	97.1	0.00728	0.074871
29	15342	21	31	21	1208.5	-1.5916	-7.05534	1189.6	98.7	0.00077	0.49361
30	15343	4	40	47	1522.1	-5.4607	-21.54902	1411.7	71	0.02052	0.067551
31	15342	21	10	14	1315.8	0	-20	1233.1	86.4	0.0002	0.074871
32	15343	12	13	51	1186.9	0	-26.9897	1145.6	108	0.0181	0.054893
33	15343	0	55	45	1523.2	-1.5886	-18.86057	1352	98.4	0.00132	0.083875
34	15343	1	26	45	1374.3	0	-20	1272	86.4	0.00018	0.074871
35	15343	12	49	48	1829.6	1.6913	-19.20819	1588.9	65	0.48234	0.080797
36	15343	10	50	17	1865.8	-0.7788	-15.52842	1582.7	98.9	0.00069	0.1545
37	15343	10	19	45	1571.7	0	-15.22879	1445.5	99.5	0.01463	0.16503
38	15342	23	55	12	1964.7	4.7859	-16.57577	1802.5	100.4	0.00496	0.12801
39	15342	20	55	14	1499.3	-1.4952	-10.86186	1388.8	98.8	0.00062	0.30262
40	15343	6	36	39	1433.2	0	-19.20819	1354.1	99.1	0.00798	0.080797
41	15343	9	48	28	1315.7	-3.8047	-20.45757	1294.4	99.1	0.00651	0.072592
42	15343	6	28	50	1143.8	-3.4877	-30	1084.1	98.8	0.00675	0.049457
43	15343	15	4	49	2185.7	5.0254	-15.08638	1808.7	98.4	0.01396	0.17053

	Epoch				Slant Range	Range Rate	Radar Cross Section	Altitude	Inc	ECC	Characteristic Length
44	15343	5	39	42	974.6	3.3858	-13.09804	967.3	99.1	0.00177	0.22705
45	15342	20	22	35	1304.5	5.654	-19.58607	1133.7	97.9	0.01145	0.077913
46	15343	11	27	7	1375.9	-1.7965	-18.53872	1314.8	98.8	0.05532	0.087246
47	15343	6	2	39	1077.1	-4.6355	-26.9897	1065.3	98.6	0.0001	0.054893
48	15343	10	14	18	1664.2	0	-15.68636	1400.9	98.4	0.01985	0.15079
49	15342	20	10	40	1260.6	-1.7427	-19.58607	1248.7	96.6	0.0319	0.077913
50	15343	1	29	39	1771.5	0	-19.20819	1497.3	74.1	0.0132	0.080797
51	15342	20	34	35	1733.5	3.563	-20	1474.1	74	0.00555	0.074871
52	15343	6	11	7	1090.3	0	-26.9897	1032.2	73.9	0.00765	0.054893
53	15343	2	59	21	1284.1	-4.99	-14.81486	1214.4	74	0.0026	0.17858
54	15343	10	22	19	1601.5	0	-20.45757	1414.5	74	0.01115	0.072592
55	15343	8	14	55	1017.5	5.3609	-16.77781	961.1	98.4	0.01745	0.12259
56	15343	8	10	15	1557.6	4.1682	-20.45757	1546.5	98.8	0.03859	0.072592
57	15342	23	59	12	1161.8	-1.4146	-18.53872	1149.8	86.4	0.02441	0.087246
58	15343	12	58	41	1060.6	-4.8817	-16.9897	1010.8	74	0.00441	0.11575
59	15343	5	14	34	1017.4	4.6188	-21.54902	1002.8	86.4	0.0008	0.067551
60	15343	13	1	36	1416.9	4.667	-23.0103	1352.1	98.7	0.01719	0.063117
61	15343	10	10	10	2787.5	0.823	8.68468	2367.3	100.4	0.00176	3.0668
62	15342	20	36	31	1710.9	-0.9805	-13.76751	1466	99	0.01759	0.20773
63	15343	6	32	4	1926.3	5.2734	-15.22879	1623.9	99	0.01759	0.16503
64	15342	23	26	22	1787.9	-0.9517	-17.44727	1580.8	98.9	0.00484	0.104
65	15342	21	40	12	742.5	-2.8818	-17.69551	740.3	81.1	0.00115	0.099737
66	15343	14	19	11	928.1	5.624	1.43327	859.9	97.5	0.00134	1.3308
67	15343	13	51	55	1280.8	-1.7091	-17.9588	1245.2	98.6	0.00844	0.09537
68	15343	2	35	10	1067.9	5.2699	-25.22879	1027.9	99.4	0.00276	0.057989
69	15343	1	54	31	1262.7	0	-25.22879	1100.8	74	0.00383	0.057989
70	15342	22	52	32	1248.5	3.5456	-19.58607	1184.9	86.4	0.0203	0.077913
71	15343	4	5	16	2249.3	0	-19.58607	1821.8	99	0.00317	0.077913
72	15343	14	50	26	1550.6	5.7188	9.94581	1238	97.4	0.00011	3.5461
73	15343	13	38	21	1801.5	-5.797	-16.77781	1490.4	74	0.00538	0.12259
74	15343	10	35	15	1022	4.4116	-30	997.1	98.2	0.00012	0.049457
75	15343	8	15	23	1166.7	0	-20.9691	1057.6	64.9	0.00179	0.070184
76	15342	23	26	14	777.2	0	-15.85027	769.7	97.2	0.00136	0.14704
77	15343	6	0	6	1929.9	0	-14.81486	1770.5	63.4	0.00932	0.17858
78	15343	8	15	19	1143.7	0	-14.9485	1043.3	82.4	0.00195	0.17467
79	15343	0	37	18	1664.4	-1.3683	-13.0103	1523.3	98.9	0.00564	0.22964
80	15343	9	28	4	1853.5	1.9466	-14.20216	1626.2	81.2	0.0012	0.19573

	Epoch				Slant Range	Range Rate	Radar Cross Section	Altitude	Inc	ECC	Characteristic Length
81	15343	10	9	20	1265	0	-15.52842	1213	65	0.00197	0.1545
82	15343	10	51	39	1271.3	1.2315	-17.69551	1173.6	74.1	0.00722	0.099737
83	15342	19	52	28	1814.7	-0.9106	-13.87216	1598.5	98.8	0.00627	0.20477
84	15342	23	57	2	890.6	-2.9006	-21.54902	828.7	97.3	0.00018	0.067551
85	15343	6	16	35	1846.7	5.2242	-14.55932	1609.5	98.7	0.00416	0.1863
86	15343	0	12	46	1323	-1.5761	-21.54902	1268.6	98.9	0.00048	0.067551
87	15343	10	7	21	1246.1	4.7453	-19.20819	1218	98.9	0.00048	0.080797
88	15343	10	35	43	1799	4.1241	-16.0206	1596	98.9	0.00059	0.14324
89	15343	0	6	14	1270.8	-1.6116	-14.81486	1240.4	98.9	0.00218	0.17858
90	15343	10	40	7	1937.7	0	-20.9691	1708.3	99	0.01723	0.070184
91	15342	23	45	24	1020.6	-1.4534	-12.36572	1019.9	98.9	0.00235	0.2496
92	15343	1	25	4	2200.2	-0.4328	-10.45757	1828.8	98.9	0.00235	0.31842
93	15343	0	27	1	1512.1	0	-25.22879	1412.5	98.9	0.00304	0.057989
94	15342	23	58	29	1171.5	-1.5487	-14.20216	1158.6	98.9	0.0023	0.19573
95	15342	19	53	28	1755.3	-1.8849	-9.87163	1748.5	65.2	0.54705	0.34278
96	15342	23	25	58	876.2	0	-22.21849	847.5	96.7	0.00425	0.065408
97	15343	0	41	32	915.4	0.903	-0.33389	913.7	65	0.5664	1.0858
98	15343	3	18	12	1955.5	-2.6319	-11.67491	1697.5	65.4	0.5516	0.2728
99	15343	4	44	18	2608.3	-3.7183	-3.60514	2281.8	65.2	0.56097	0.74507
100	15343	2	20	45	1589.5	-1.4598	-12.07608	1476.9	64.7	0.55682	0.25908
101	15343	4	36	57	2483.8	-4.3788	-3.16953	2069.8	65.3	0.55253	0.78339
102	15343	1	0	8	1094	-3.9917	-20.45757	1008.1	86.3	0.00218	0.072592
103	15343	3	44	37	2122.7	-4.1835	-11.36677	1759.7	64.7	0.55095	0.28383
104	15343	7	4	7	2517.1	-2.1979	-12.44125	2447.7	65.2	0.56233	0.24719
105	15343	0	14	56	1391.3	-1.8597	-18.53872	1336.2	65.1	0.54536	0.087246
106	15343	7	12	10	665.9	-3.3156	-20.45757	664.2	73.7	0.01262	0.072592
107	15343	10	5	26	1152.9	4.81	-23.0103	1130.3	99.1	0.00431	0.063117
108	15342	23	45	37	1063.1	-1.416	-16.9897	1062.3	98.9	0.00358	0.11575
109	15343	0	26	32	1467.6	-1.5307	-17.9588	1354.7	99	0.00748	0.09537
110	15342	23	53	50	1093.1	-1.5934	-15.68636	1086.1	99	0.00561	0.15079
111	15343	0	25	24	1443.6	-1.6143	-22.21849	1337.5	98.9	0.01635	0.065408
112	15342	19	59	19	1747.9	-1.7947	-17.9588	1746.3	65.5	0.54505	0.09537
113	15343	7	26	47	1327.2	4.6337	-19.58607	1302.4	99.2	0.00794	0.077913
114	15342	22	2	4	1391.7	-1.7833	-21.54902	1265	98.5	0.0043	0.067551
115	15343	6	13	16	1017.6	3.6261	-16.0206	1007.9	123	0.00639	0.14324
116	15343	7	49	45	885.3	3.8518	-20.45757	883.2	123	0.00639	0.072592
117	15343	0	33	31	1594	-1.5076	-23.0103	1458	62.2	0.06977	0.063117

	Epoch				Slant Range	Range Rate	Radar Cross Section	Altitude	Inc	ECC	Characteristic Length
118	15343	14	59	57	1573	-1.137	-14.68521	1570.6	100.3	0.01788	0.18245
119	15343	0	7	27	2161.8	1.8073	-14.20216	2054	82.4	0.03067	0.19573
120	15343	4	20	55	1663.1	-2.8723	-17.9588	1661.9	82.6	0.00271	0.09537
121	15343	11	3	13	1345.3	-0.6641	-19.58607	1279.3	66	0.01147	0.077913
122	15343	6	28	34	1203.5	-4.0611	-19.58607	1124.1	65.9	0.07458	0.077913
123	15343	10	19	30	1482.7	7.2794	-14.31798	1368.4	66.4	0.00102	0.19264
124	15343	6	58	12	1269.8	-0.3013	-17.44727	1258.3	65.8	0.00842	0.104
125	15343	2	33	48	1584	5.158	-17.44727	1477	100	0.00236	0.104
126	15343	6	15	28	1244.6	-2.9457	-23.0103	1216.8	89.7	0.00173	0.063117
127	15343	14	18	56	1456.2	-3.9018	-17.69551	1379.6	83.1	0.00154	0.099737
128	15343	1	54	38	1368.5	4.7605	-17.69551	1339.1	100	0.00054	0.099737
129	15343	4	5	12	1350.7	-2.8171	-20	1085.1	63.3	0.03745	0.074871
130	15343	14	37	31	1219.9	4.2131	-23.0103	1218.2	101.9	0.00327	0.063117
131	15342	23	59	5	1172.3	-1.7214	-18.23909	1157.8	99	0.01458	0.090846
132	15343	6	16	40	1741.1	4.4437	-17.9588	1684.8	99.3	0.01389	0.09537
133	15342	22	13	50	1613.9	5.414	-14.81486	1423.7	98.6	0.01	0.17858
134	15342	21	18	24	1338.1	-1.8803	-20.45757	1282.4	99	0.00301	0.072592
135	15342	21	34	32	1634.4	0	-26.9897	1520.3	83	0.01048	0.054893
136	15343	10	45	27	2032.3	5.2138	-23.0103	1709	99	0.01296	0.063117
137	15343	3	19	4	1183.9	3.9317	-17.21246	1182.3	100	0.00143	0.10946
138	15343	3	53	54	1380.1	3.9704	-19.58607	1372.9	98.7	0.02438	0.077913
139	15343	2	27	40	1841.6	3.0142	-15.22879	1801.6	90.3	0.00288	0.16503
140	15343	12	18	9	1368.5	3.6679	-20.9691	1367	98.4	0.02437	0.070184
141	15343	15	47	28	2911	-1.1996	-6.05548	2882.3	65.1	0.59398	0.56103
142	15342	19	33	59	1823.3	-3.4227	-14.9485	1722.4	65.1	0.49157	0.20185
143	15342	19	51	7	911.1	5.124	-30	888.2	99.2	0.00931	0.03568
144	15342	19	56	37	864.2	-1.4776	-21.54902	859.7	99	0.01395	0.09441
145	15342	19	59	20	1223.5	-4.8534	-16.77781	1201	73.4	0.05155	0.16352
146	15342	19	59	59	1203	-0.9665	-23.9794	1118.5	65.6	0.08408	0.07136
147	15342	20	4	43	1110.4	-1.4079	-14.68521	1101.7	99.3	0.038	0.20806
148	15342	20	6	55	1034.9	-2.4468	-19.20819	1034	56.9	0.28883	0.12361
149	15342	20	46	58	840.5	-3.091	-26.9897	836.9	73.9	0.01228	0.05046
150	15342	20	59	27	1045.9	2.6615	-19.20819	1039.6	81.2	0.04106	0.12361
151	15342	21	0	47	978.2	-0.2032	-26.9897	969	64.7	0.06972	0.05046
152	15342	21	14	54	1840.3	5.4635	-17.21246	1477.2	99.4	0.01735	0.15554
153	15342	21	23	19	1226.9	-1.2772	-23.0103	1222.1	100.1	0.06951	0.07979
154	15342	21	26	18	1815.9	-4.2352	-14.9485	1642.7	82.4	0.05704	0.20185

	Epoch				Slant Range	Range Rate	Radar Cross Section	Altitude	Inc	ECC	Characteristic Length
155	15342	21	55	52	1872.5	-0.4592	-18.53872	1870.8	65.2	0.24296	0.13351
156	15342	22	5	55	878.9	-1.5219	-19.20819	878.1	99.8	0.02774	0.12361
157	15342	22	7	29	2439	4.7126	-10.5061	2082.9	96.9	0.13284	0.33663
158	15342	22	41	29	1396.1	-1.6127	-22.21849	1325.8	99	0.13348	0.0874
159	15342	22	55	3	1249	-0.7826	-17.69551	1246.4	56.7	0.43099	0.14712
160	15342	22	59	20	1316.7	2.8326	-23.0103	1250.6	82.1	0.08117	0.07979
161	15342	22	59	45	1061.9	-1.5478	-20.45757	1059.6	98.7	0.01728	0.10705
162	15342	23	3	45	1652.2	4.1726	-17.21246	1636.9	103.2	0.11239	0.15554
163	15342	23	16	4	769	-1.5468	-19.20819	764.5	98.1	0.01962	0.12361
164	15342	23	17	1	1120.5	2.2688	-19.20819	1119.1	82.9	0.11638	0.12361
165	15342	23	36	34	1823.6	4.2911	-16.38272	1762.9	94.9	0.0981	0.17113
166	15342	23	40	6	1009.1	-1.2943	-20.45757	1002.4	98.8	0.00098	0.10705
167	15342	23	46	26	1033.9	-1.4109	-17.44727	1033.4	99	0.0129	0.15139
168	15342	23	50	49	1079.2	-1.5534	-17.44727	1076.1	98.9	0.03652	0.15139
169	15342	23	52	3	1087.6	-1.5597	-18.86057	1083.4	98.7	0.0046	0.12866
170	15342	23	54	12	1159.6	-1.5233	-18.53872	1154.5	98.9	0.0395	0.13351
171	15342	23	57	11	1134.2	-1.597	-18.86057	1121.8	98.8	0.03002	0.12866
172	15342	23	59	23	1266.5	-0.0907	-11.73925	1260.2	63.8	0.07526	0.29207
173	15343	0	5	59	1248.9	-1.7394	-11.30768	1213.7	99.5	0.02203	0.30695
174	15343	0	6	16	1268	-1.6023	-15.85027	1238.8	98.7	0.01448	0.18195
175	15343	0	7	51	937.5	-1.841	-20.9691	931.7	98.3	0.03288	0.10093
176	15343	0	16	16	1340.3	-1.6529	-11.73925	1268.8	99.2	0.0327	0.29207
177	15343	0	23	15	1460.1	-1.5155	-13.76751	1368.8	99.3	0.06145	0.23125
178	15343	0	49	12	1196.3	-0.5835	-25.22879	1163.6	65.4	0.04281	0.0618
179	15343	0	49	34	1222.3	4.7908	-25.22879	1170.2	97.6	0.09191	0.0618
180	15343	0	56	28	822.5	2.2957	-23.0103	822	80.7	0.02207	0.07979
181	15343	1	1	55	1948.9	-0.9636	-15.85027	1690.3	97.9	0.06374	0.18195
182	15343	1	2	48	1993.9	-0.8199	-10.55517	1745.4	98.4	0.13453	0.33473
183	15343	1	7	12	2018.4	-0.7999	-10.75721	1739.1	98.3	0.05826	0.32704
184	15343	1	20	24	1566.4	-1.3345	-17.21246	1555.3	67.6	0.30129	0.15554
185	15343	1	33	3	952.1	0.8081	-13.66532	924.1	66	0.53145	0.23399
186	15343	1	41	58	925.2	-1.4305	-16.19789	923	98.5	0.00613	0.17481
187	15343	1	52	23	1032.5	-3.3617	-23.0103	1029.1	57	0.24109	0.07979
188	15343	2	8	14	1116.5	-1.1272	-19.58607	1114.9	100.2	0.06218	0.11835
189	15343	2	20	11	1267.5	-1.5386	-21.54902	1091.5	64.9	0.45326	0.09441
190	15343	2	21	15	993.3	3.6045	-18.86057	982.1	122.9	0.04212	0.12866
191	15343	2	49	59	1479.4	-0.3936	-17.44727	1409.9	65.9	0.54193	0.15139

	Epoch				Slant Range	Range Rate	Radar Cross Section	Altitude	Inc	ECC	Characteristic Length
192	15343	2	59	53	906.3	3.7057	-25.22879	904	99.1	0.01714	0.0618
193	15343	3	9	30	1232.2	2.927	-17.44727	1231.2	89.5	0.00366	0.15139
194	15343	3	46	11	1615.7	-1.4718	-18.23909	1355.6	99	0.0643	0.1382
195	15343	3	49	24	1229.3	1.2626	-20.45757	1187.8	74.2	0.02295	0.10705
196	15343	3	56	14	1021.5	-1.4196	-21.54902	1016.6	98.8	0.0563	0.09441
197	15343	4	45	11	1837	-1.0507	-12.83997	1500.9	98.2	0.02798	0.25731
198	15343	5	17	1	1230.1	-3.9812	-22.21849	1139.9	86.7	0.00711	0.0874
199	15343	5	45	40	1440.5	-0.8653	12.29247	1433.2	63.4	0.00982	4.64599
200	15343	5	46	51	1569.2	-3.2931	-17.44727	1367.3	64.8	0.55938	0.15139
201	15343	6	28	37	1193.6	-3.8776	-22.21849	1117.3	86.2	0.02806	0.0874
202	15343	6	50	9	837.4	-1.3703	-26.9897	833	100.5	0.021	0.05046
203	15343	7	10	55	1964.9	-0.4537	-18.53872	1908.7	105.6	0.1707	0.13351
204	15343	7	15	50	1172.7	-1.8561	-22.21849	1092.6	100.4	0.08163	0.0874
205	15343	7	44	30	871.4	-1.7438	-14.9485	866.1	98.7	0.01118	0.20185
206	15343	7	53	15	900.8	0.0146	-18.86057	890.3	65.9	0.01099	0.12866
207	15343	8	10	40	911.2	-1.5055	-18.53872	907.4	99.1	0.02792	0.13351
208	15343	8	12	36	1661.9	4.6391	-15.08638	1570.3	100	0.04205	0.19867
209	15343	8	17	35	1371.4	-0.4811	-19.20819	1369.6	65	0.05376	0.12361
210	15343	8	25	40	1096.1	-1.6024	-13.18759	1090.7	99.7	0.05847	0.24722
211	15343	8	56	9	492.1	-4.605	-14.9485	491.7	62	0.24843	0.20185
212	15343	8	59	48	923.2	4.0805	-23.9794	922.6	102.6	0.05324	0.07136
213	15343	9	10	41	1436.2	0.713	-23.0103	1307.1	74.2	0.0365	0.07979
214	15343	9	12	21	927.7	1.5907	-26.9897	917.7	74.2	0.0392	0.05046
215	15343	9	16	50	990.3	-1.4769	-21.54902	986	98.6	0.04059	0.09441
216	15343	9	57	24	1020.9	3.6988	-11.61151	1020.2	99	0.00116	0.2964
217	15343	9	59	41	1051.5	3.7557	-10.17729	1050.9	99.6	0.06837	0.34962
218	15343	10	6	3	819.9	-1.9358	-20.45757	802.2	99.1	0.00777	0.10705
219	15343	10	12	27	1764.7	-4.1628	-16.38272	1730.6	73.7	0.06702	0.17113
220	15343	10	13	25	1318.5	-1.3223	-18.53872	1314.5	97.4	0.05698	0.13351
221	15343	10	14	47	1516.6	4.9922	-17.69551	1401.4	97.3	0.09549	0.14712
222	15343	10	26	29	1742.1	5.2865	-16.9897	1555	94.1	0.14336	0.15958
223	15343	10	35	18	1032.7	4.6692	-20	1009.7	96.3	0.04355	0.11284
224	15343	10	42	2	1968.1	4.9191	-13.66532	1724.7	98.1	0.13628	0.23399
225	15343	10	42	6	1928.9	5.0029	-10.17729	1679.5	98.8	0.02105	0.34962
226	15343	10	47	29	2028.2	5.0045	-15.68636	1738.1	97.6	0.23133	0.18541
227	15343	10	49	24	2036.5	5.0845	-16.38272	1719.6	97.8	0.04719	0.17113
228	15343	10	50	38	932.4	-2.9451	-25.22879	913.7	57	0.28722	0.0618

	Epoch				Slant Range	Range Rate	Radar Cross Section	Altitude	Inc	ECC	Characteristic Length
229	15343	10	53	28	1342.8	0.95	-18.86057	1231.1	73.5	0.04398	0.12866
230	15343	11	2	36	2341.4	4.723	-13.37242	1953.9	100.5	0.11613	0.24201
231	15343	11	4	9	1092.7	-1.5536	-19.58607	1089.6	100.7	0.05903	0.11835
232	15343	11	10	59	1433.7	0.5131	-20	1432.6	63.4	0.2413	0.11284
233	15343	11	35	15	826.2	-1.7572	-26.9897	821.8	99.3	0.05378	0.05046
234	15343	12	47	15	1111	1.4285	-23.0103	1072.2	74.1	0.03013	0.07979
235	15343	12	51	15	1223.3	2.5108	-22.21849	1213.3	82.5	0.03903	0.0874
236	15343	12	51	30	1134.7	1.4617	-20	1086.8	73.5	0.02687	0.11284
237	15343	13	4	6	964.6	-1.3298	-20.45757	961.7	99.1	0.02843	0.10705
238	15343	13	33	38	890.3	-4.6351	-30	847.4	57	0.36772	0.03568
239	15343	14	14	2	1191.5	-1.7173	-19.20819	1163.8	98.9	0.03088	0.12361
240	15343	14	15	46	1203.6	1.221	-14.55932	1079.5	74	0.01202	0.2111
241	15343	14	32	5	931.4	-3.974	-23.9794	928.8	73.4	0.00754	0.07136
242	15343	14	32	32	1210.9	-0.1768	-23.9794	1203.3	64.7	0.06703	0.07136
243	15343	14	57	33	967	-2.4597	-15.22879	951.6	57	0.2528	0.19544
244	15343	14	57	37	1343.6	0.9448	-23.0103	1180.8	74	0.12323	0.07979
245	15343	15	14	12	1122.6	3.1024	-16.9897	1115.9	98.7	0.03116	0.15958
246	15343	15	22	29	1837.3	5.5522	-20.45757	1604.2	100.8	0.09135	0.10705

Appendix E

NASA's Size Estimation Model

Physical size is estimated from RCS using NASA's SEM. Debris objects were selected from two hypervelocity impacts of simulated satellites. Some artificial debris-like objects were also included in the sample to better represent the postulated orbital debris environment. This included a printed circuit board and a piece of solid rocket motor aluminum oxide (Al_2O_3) slag. The RCS values of these 39 debris objects were measured at a controlled RCS radar range operated by the System Planning Corporation. The RCSs of these objects were measured over 4 radar frequency bands (2.5647-3.9111 GHz, 4.116-7.986 GHz, 8.1544-12.7684 GHz, and 12.924-17.538 GHz) with 8 steps in the band of the lowest frequency and 16 steps in the band for the other three, and with hundreds of source-object orientations. These frequencies, S-, C-, X-, and Ku-band, respectively, were chosen since they represent radar frequencies often used for orbital debris observations.

The characteristic length of an object is defined as the average of the largest dimensions for an object measured along three orthogonal axes. The first axis was chosen to coincide with the largest dimension, the second axis to coincide with the largest dimension in a plane orthogonal to the first axis, and the third axis to be orthogonal to the first two axes. In this report, the characteristic length of an object is often referred to as size or diameter.

Consistent with Maxwell's equations of electromagnetics, radar data from different wavelengths can be compared by normalizing the size by the wavelength of the measuring frequency and the RCS by the wavelength squared. This results in a size parameter $x = \text{size}/\text{wavelength}$ and a RCS parameter $z = \text{RCS}/\text{wavelength}^2$. Figure E-1 shows the relationship between the measured RCS parameter and the object's physical size parameter. Each of the 2072 points on this plot is a weighted average for a single object over hundreds of different orientations at a single frequency. The data was weighted to account for nonuniform sampling of the object orientations as the data was collected.

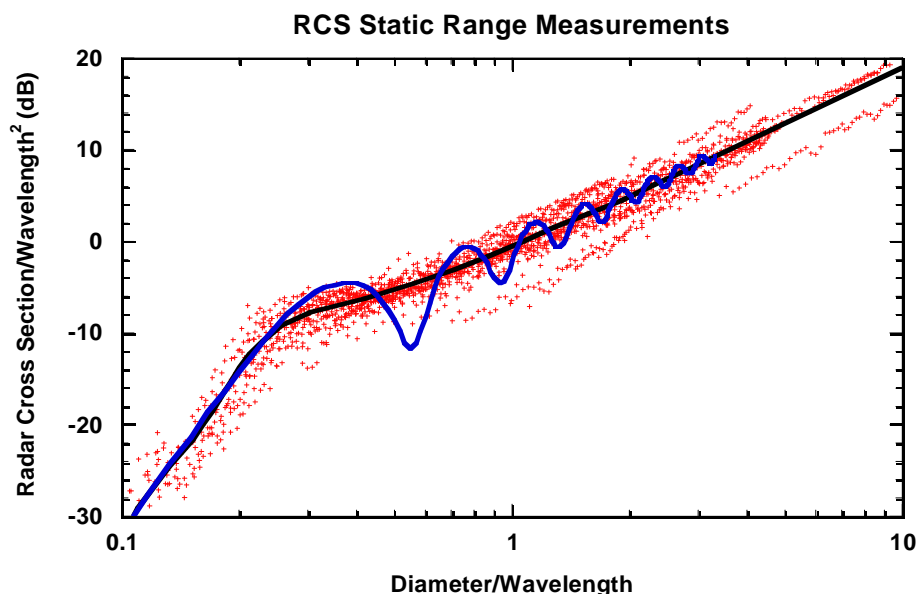


Figure E-1. Results of RCS-to-Physical size measurements on 39 "representative" debris objects over the frequency range 2.0 - 18 GHz (15 - 1.67 cm wavelength). Each point represents an average RCS for a single object measured at a single frequency over many orientations. The oscillating line is the radar cross section for a spherical conductor while the smooth line is the polynomial fit to the data.

From this plot a scaling curve (smooth solid line) was developed that represents the mean of the measured RCS for each size/wavelength. For debris sizes much smaller or larger than the radar wavelength, the scaling curve approaches the Rayleigh or optics region curves, as expected. Between the Rayleigh and optics region curves is the Mie resonance region that results in an enhanced RCS measurement, on average, for a given size. In the resonance region, the scaling curve deviates from the optical curve (not shown) such that for a given RCS, the object is smaller in characteristic length than it would have been interpreted to be by using the optical approximation. The scaling curve may be expressed as:

$$x = \sqrt{\frac{4z}{\pi}}, \text{ for } z > 5, \text{ Optical Regime}$$

$$x = \sqrt[6]{\frac{4z}{9\pi^5}}, \text{ for } z < 0.03, \text{ Rayleigh Regime}$$

$$x = g(z), \text{ in between, Mie Resonance Regime}$$

where $z = \text{RCS}/\lambda$, $x = \text{diameter}/\lambda$, and λ is wavelength. In the above equations, the quantity z is assumed not to be expressed in dB. The smooth function $g(z)$ is expressed by 23 points in Table E-1.

Table E-1 – The NASA SEM Curve $x=g(z)$ in the Mie Resonance Region

$x=\text{diameter}/\lambda$	$z=\text{RCS}/\lambda^2$
0.10997	0.001220
0.11685	0.001735
0.12444	0.002468
0.13302	0.003511
0.14256	0.004993
0.15256	0.007102
0.16220	0.01010
0.17138	0.01437
0.18039	0.02044
0.18982	0.02907
0.20014	0.04135
0.21237	0.05881
0.22902	0.08365
0.25574	0.1190
0.30537	0.1692
0.42028	0.2407
0.56287	0.3424
0.71108	0.4870
0.86714	0.6927
1.0529	0.9852
1.2790	1.401
1.5661	1.993
1.8975	2.835

Note that most of the debris for Haystack is in the Rayleigh region, which allows size estimates that are relatively insensitive to errors in the RCS measurements.

For comparison, the oscillating RCS-to-size curve for a spherical conductor is shown in Figure E-1. The NASA SEM is not applicable to estimate sizes of spherical conductors (such as NaK droplets) in the Mie Resonance region. The oscillations result from constructive and destructive interference of electromagnetically induced waves on the surface of the conducting sphere.

The size-to-RCS curve for a spherical conductor is expressed theoretically as:

$$z = \frac{1}{\pi} \left| \sum_{n=1}^{\infty} (-1)^n \left(n + \frac{1}{2} \right) (b_n - a_n) \right|^2$$

where the coefficients a_n and b_n are

$$a_n = \frac{j_n(2\pi x)}{h_n^{(2)}(2\pi x)}$$

$$b_n = \frac{2\pi x \cdot j_{n-1}(2\pi x) - n \cdot j_n(2\pi x)}{2\pi x \cdot h_{n-1}^{(2)}(2\pi x) - n \cdot h_n^{(2)}(2\pi x)}$$

where $h_n^{(2)}(x) = j_n(x) - i \cdot y_n(x)$, in which $j_n(x)$ and $y_n(x)$ are the spherical Bessel functions of the first and second kinds, respectively.

Appendix F

World Map of Participating Radar Locations



Figure F-1. Map of radar locations for 2015 campaign.